

Stimela Model descriptions

From Wswiki

Contents

- 1 Introduction
 - 1.1 Basic differential equations for drinking water treatment processes
 - 1.1.1 Transport of a compound through a reactor in water phase
 - 1.1.2 Equilibrium of dissolved compounds between water and gas or solid phase
 - 1.1.3 Transfer of compounds to and from gas or solid phase
 - 1.1.4 Reactions of compounds in water
 - 1.1.5 Overall equation for fate of compound in water
 - 1.1.6 Mass balance between water and gas or solid phase
 - 1.2 References
- 2 Aeration and Degassing
 - 2.1 Gas Transfer in General
 - 2.1.1 Introduction
 - 2.1.2 General theory
 - 2.1.3 General model equations
 - 2.2 Weir/Cascade Aeration
 - 2.2.1 Process
 - 2.2.2 Model
 - 2.2.2.1 Options for Usage
 - 2.2.2.2 Model Calibration
 - 2.2.2.3 Input and Output
 - 2.3 Plate Aeration (INKA aerator)
 - 2.3.1 Process
 - 2.3.2 Model
 - 2.3.2.1 Options for Usage
 - 2.3.2.2 Model Calibration
 - 2.3.2.3 Input and Output
 - 2.4 Tower/Column Aeration
 - 2.4.1 Process
 - 2.4.2 Model
 - 2.4.2.1 Options for Usage
 - 2.4.2.2 Model Calibration
 - 2.4.2.3 Input and Output
 - 2.5 Vacuum Degassing
 - 2.5.1 Process
 - 2.5.2 Model
 - 2.5.2.1 Options for Usage
 - 2.5.2.2 Model Calibration
 - 2.5.2.3 Input and Output
 - 2.6 References
- 3 Filtration
 - 3.1 Filtration in General
 - 3.2 Single and Dual Media Filter (removal of suspended solids)
 - 3.2.1 Process
 - 3.2.2 Theory
 - 3.2.3 Model
 - 3.2.3.1 Options for Usage
 - 3.2.3.2 Model Equations
 - 3.2.3.3 Model Calibration
 - 3.2.3.4 Input and Output
 - 3.3 Biological Filter
 - 3.3.1 Process
 - 3.3.2 Theory
 - 3.3.3 Model
 - 3.3.3.1 Options for Usage
 - 3.3.3.2 Model Equations
 - 3.3.3.3 Model Calibration
 - 3.3.3.4 Input and Output
 - 3.4 Iron Filter
 - 3.4.1 Process

- 3.4.2 Theory
- 3.4.3 Model
 - 3.4.3.1 Options for Usage
 - 3.4.3.2 Model Equations
 - 3.4.3.3 Model Calibration
 - 3.4.3.4 Input and Output
- 3.5 Nitrification
 - 3.5.1 Process
 - 3.5.2 Theory
 - 3.5.3 Model
 - 3.5.3.1 Options for Usage
 - 3.5.3.2 Model Equations
 - 3.5.3.3 Model Calibration
 - 3.5.3.4 Input and Output
- 3.6 Activated Carbon Filter
 - 3.6.1 Process
 - 3.6.2 Theory
 - 3.6.3 Model
 - 3.6.3.1 Options for Usage
 - 3.6.3.2 Model Equations
 - 3.6.3.3 Model Calibration
 - 3.6.3.4 Input and Output
- 3.7 References
- 4 Oxidation and Disinfection
 - 4.1 Disinfection in General
 - 4.2 Disinfection with Ozone
 - 4.2.1 Process
 - 4.2.2 Theory
 - 4.2.3 Model
 - 4.2.3.1 Options for Usage
 - 4.2.3.2 Model Equations
 - 4.2.3.3 Model Calibration
 - 4.2.3.4 Input and Output
 - 4.3 References
- 5 Softening
 - 5.1 Pellet Softening Reactor
 - 5.1.1 Process
 - 5.1.2 Theory
 - 5.1.3 Model
 - 5.1.3.1 Options for Usage
 - 5.1.3.2 Model Equations
 - 5.1.3.3 Model Calibration
 - 5.1.3.4 Input and Output
 - 5.2 References
- 6 Coagulation and Flocculation
 - 6.1 Coagulation
 - 6.1.1 Process
 - 6.1.2 Theory
 - 6.1.3 Model
 - 6.1.3.1 Options for Usage
 - 6.1.3.2 Model Equations
 - 6.1.3.3 Model Calibration
 - 6.1.3.4 Input and Output
 - 6.2 Flocculation
 - 6.2.1 Process
 - 6.2.2 Theory
 - 6.2.3 Model
 - 6.2.3.1 Options for Usage
 - 6.2.3.2 Model Equations
 - 6.2.3.3 Model Calibration
 - 6.2.3.4 Input and Output
 - 6.3 References
- 7 pH adjustment
 - 7.1 Model description
 - 7.2 Model Calibration
 - 7.3 References

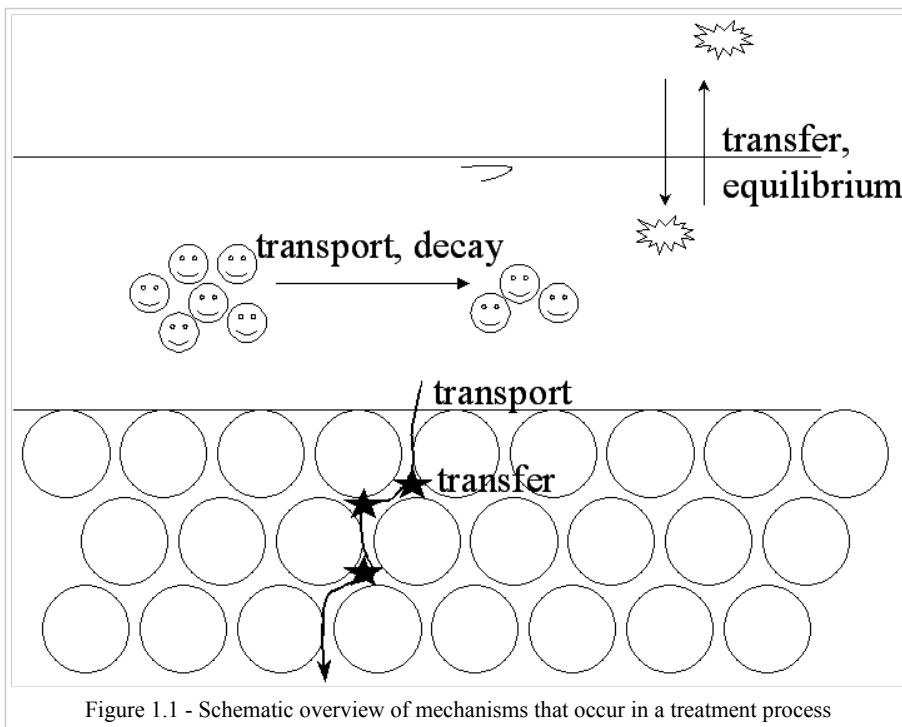
1 Introduction

Water quality models attempt to simulate changes in the concentration of pollutants as they move through the environment or a reactor. Most reactions of importance in water treatment occur in more than a single phase, i.e. multiphase reactions. One example is that a gas is mixed with water to achieve the transformation of some undesired constituents. In other cases, a solid precipitate is formed, which removes the contaminant. Various types of reactors can be used to carry out multiphase reactions. Examples characteristic of water treatment problems include stirred tanks, venturi mixers, several tanks in series, packed columns, spray towers, filters, fluidised bed reactors. Normally, they operate on a continuous basis (in contrast to batch reactors) because of the large volumes of water processed.

There are some pollutants that are sufficiently inert for their concentration to be regarded as unchanging, except by physical transport phenomena like advection and dispersion. These are referred to as conservative substances and are often useful as tracers in the calibration of water quality models. Superimposed upon these mass transport mechanisms are physical, chemical and biological processes, which also cause changes in concentration. The fate of pollutants is the result of interactions between mass transfer and kinetic processes (James, 1993).

A treatment process consists of the following mechanisms (see figure 1.1):

- Flow of water containing compounds through the reactor
- Equilibrium between water and gas or solid phase
- Transfer of compounds to gas or solid phase
- Decay in the water and/or solid phase
- Mass balance between water and gas and solid phase (continuity law)



The processes in drinking water treatment have similar mechanisms and can be described with similar partial differential equations, based on the advection-dispersion model. It is the purpose of this chapter to give an overview of the basic partial differential equations for reactors in drinking water treatment. Examples are given for some of the “conventional” treatment processes for surface and groundwater:

- Aeration and gas transfer
- Floc formation and floc removal
- Rapid filtration

All the next chapters will deal with the modelling of the different treatment steps in more detail.

1.1 Basic differential equations for drinking water treatment processes

1.1.1 Transport of a compound through a reactor in water phase

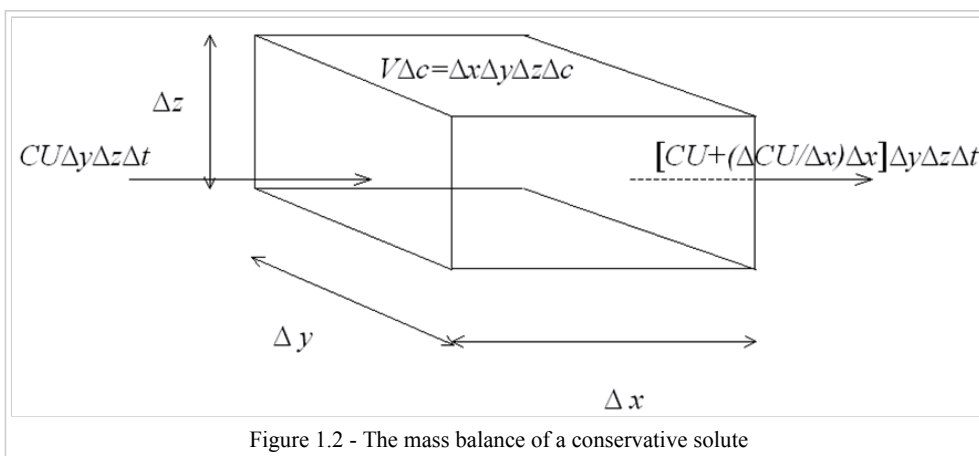
Fluid behaviour in reactors is complex and difficult to describe mathematically. Two extreme, ideal flow conditions in a reactor, i.e. complete mixing and plug flow, can be distinguished. In a continuous stirred tank reactor (CSTR), the concentration of reactants and products is assumed to be uniform in all points in the reactor. In a plug flow reactor each fluid element has the same residence time. Often flow behaviour deviates substantially from the assumptions of ideal flow. There are three principal types of non-ideal fluid behaviour in processing equipment: short-circuiting and dispersion. To evaluate the effects of deviations from the ideal models the distribution of residence times must be estimated. Two (one-parameter) models are widely used in water treatment applications, the advection-dispersion model and the tank-in-series model. The advection-dispersion model draws on the analogy of diffusional mixing in plug flow reactors. The tank-in-series model assumes that the residence time distribution from any reactor can be simulated by a series of equal volume CSTR's (Montgomery, 1985). The tank-in-series model can be used whenever the dispersion model is used and for not too large a deviation from plug flow both models give identical results, for all practical purposes (Armirtharajah et al., 1991, Levenspiel, 1999). For the description of the processes, in this chapter, the advection-dispersion model is used.

In the advection-dispersion model, there are three basic mechanisms distinguished that are responsible for the transport of dissolved and suspended solids in natural waters (James, 1993):

- Advection refers to transport due to the bulk movement of the water
- Diffusion is the transport due to migration of a solute in response to a concentration gradient as a result of Brownian motion
- Dispersion is the transport due to turbulence of the fluid and velocity shear

The molecular diffusion can, however, generally be neglected related to the large scale mixing due to turbulence. If uncertainty exists on the flow pattern, computational fluid dynamics calculations can be performed to describe it. Schematization towards the ideal flow schemes can subsequently be made to be incorporated in the water quality modelling. A mass balance for a system with defined boundaries can generally be expressed as (see figure 2.2):

accumulation of mass in system = (net transport into system) - (net transport out of system)



For a one-dimensional turbulent flow through a reactor the dissolved compounds with a concentration $C(x,y,z,t)$ can be calculated with:

$$\begin{aligned} V\Delta C &= \Delta x \Delta y \Delta z \Delta C = CU\Delta y \Delta z \Delta t - (CU\Delta y \Delta z \Delta t + \frac{\Delta CU}{\Delta x}\Delta x \Delta y \Delta z \Delta t) \\ &\Rightarrow \frac{\Delta C}{\Delta t} + \frac{\Delta CU}{\Delta x} = 0 \end{aligned}$$

The instantaneous velocity component U (m/s) and concentration C (g/m^3) can be expressed as:

$$U = u + u'$$

$$C = c + c'$$

Where u and c are time-averaged components and u' and c' are turbulent components.

These expressions can be substituted into the equation, each term averaged, and with dimensions of the unit element (m) Δx , Δy , $\Delta z \rightarrow 0$ and the unit time step (s) $\Delta t \rightarrow 0$, the equation results in:

$$\frac{\partial c}{\partial t} + \frac{\partial c u}{\partial x} + \frac{\partial c' u'}{\partial x} = 0$$

Assuming that the turbulent dispersion can be described with Fick's law for molecular diffusion, the uniform flow in x-direction, with a constant dispersion coefficient D_x (m^2/s) can be written as:

$$\frac{\partial c}{\partial t} - D_x \frac{\partial^2 c}{\partial x^2} + u \frac{\partial c}{\partial x} = 0$$

1.1.2 Equilibrium of dissolved compounds between water and gas or solid phase

If water is exposed to a gas or gas mixture, a continuous exchange of gas molecules takes place from the water into the gaseous phase and vice versa. As soon as the equilibrium concentration in the water is reached both gas streams will be of equal magnitude such that no overall change of the gas concentrations in both phases occurs. This dynamic equilibrium is generally referred to as the solubility or the saturation concentration of the gas in water. The higher the gas concentration in the gaseous phase, the greater the saturation concentration in the water will be.

The relation between the saturation concentration and gas concentration in the gas phase is linear (Mueller et al., 2002):

$$c_e = K_D c_g$$

Where:

c_e = equilibrium concentration of compound in water (g/m^3)

c_g = concentration of compound in gas phase (g/m^3)

K_D = distribution coefficient (-)

In adsorption to a solid phase, saturation is determined by the adsorption capacity (q_{max} in g/kg). The adsorption capacity is determined empirically for different water concentrations. When the results are plotted on logarithmic scale a straight line is found for the relation between the water concentration and the adsorption capacity. This relation can be written by the Freundlich isotherm (Sontheimer, 1988):

$$q_{max} = K c_e^{1/n}$$

Where:

K = Freundlich constant ($(g/kg).(g/m^3)^n$)

$1/n$ = Freundlich constant

If q_{max} is expressed in concentration c_s ($c_s = q_{max} \rho_p$), the Freundlich isotherm can also be written as:

$$c_e = \left(\frac{c_s}{K \rho_p} \right)^n$$

Where:

c_s = concentration of compound in solid phase (g/m^3)

ρ_p = particle density (kg/m^3)

If $n=1$ the Freundlich isotherm is linear and becomes similar to the Henry's law describing transfer of gases. Linear isotherms are typically observed for the absorption of hydrophobic substances on organic or organically coated particles (Stumm and Morgan, 1996). The general equilibrium concentration for the gas and the solid phase can thus be expressed as:

$$c_e = K_D c_{g,s}^n$$

Where:

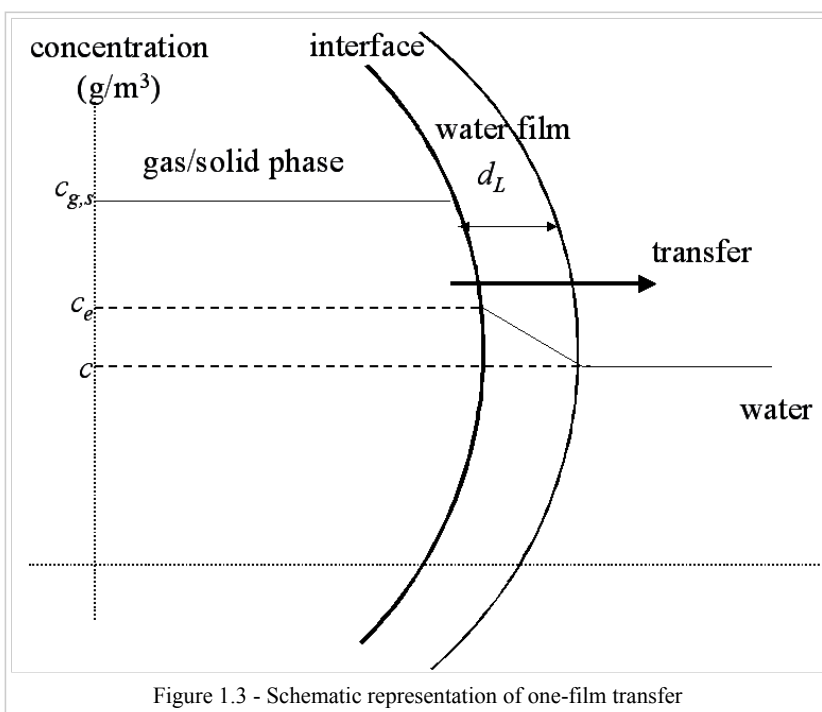
$c_{g,s}$ = concentration of compound in gas or solid phase (g/m^3)

K_D = distribution coefficient (g/m^3) $^{1-n}$

n = constant (-)

1.1.3 Transfer of compounds to and from gas or solid phase

To count for the velocity of transfer from the water to the solid or gas phase, a kinetic equation is necessary. The rate of mass transfer of a substance across a water-solid/gas boundary has been described in terms of a diffusion film model (see Figure 1.3). In general, it is necessary to consider two diffusion films, one in the water and one in the gas or solid phase.



Assuming that diffusion through the water film is limiting, from Fick's first law it is concluded that the flux F through the water film is given by (Stumm and Morgan, 1996, Schroeder, 1977):

$$F = -D_{Br} \frac{\partial c}{\partial x}$$

The transfer by diffusion from the bulk water to the interface will thus be:

$$\frac{\partial c}{\partial t} = \frac{F A_I}{V} = - \frac{D_{Br} A}{V} \frac{\partial c}{\partial x}$$

Where:

A_I = interfacial area (m^2)

V = volume of water (m^3)

D_{Br} = diffusion coefficient (m^2/s)

$$F = \text{flux (g/m}^2.\text{s)}$$

Through a gross simplification, linear concentration profiles are used in the water film with a sharp discontinuity between the film and the bulk phase concentration gradient, where the water concentration in the bulk water is uniform (due to turbulence). The water film coefficient is given as a function of a characteristic water film thickness d_L , resulting in (Mueller et al., 2002):

$$\frac{dc}{dt} = -D_{Br} \frac{A_f}{V} \frac{c_e - c}{d_L} = -k_L a(c_e - c) = -k_2(c_e - c) = f_2(c, c_{g,s})$$

Where:

k_L = transfer coefficient (m/s)

a = specific surface area (m^{-1})

k_2 = overall transfer coefficient (s^{-1})

d_L = thickness of water film (m)

f_2 = transfer function

1.1.4 Reactions of compounds in water

Reaction kinetics describe the rates at which molecules are transferred into new compounds. The rate of transformation of any i th reactant or product is defined as the quantity of material changing per unit time per unit volume, given as:

$$\frac{dc_i}{dt} = -f_{1,i}$$

Where:

$f_{1,i}$ = decay function of i^{th} reactant ($\text{g}/\text{m}^3.\text{s}$)

Simple reactions can be described by an expression for f_i . Complex reactions consist of numerous reaction paths and require multiple reaction rate expressions to describe the overall reaction rate. Finally, reactions that proceed in one direction are designated irreversible. Reactions occurring in both forward and reverse directions are known as reversible. Often, irreversible homogeneous reactions with unknown mechanisms can be modelled with an γ -order rate expression:

$$\frac{dc_i}{dt} = -f_{1,i} = -k_1 c_i^\gamma$$

(Montgomery, 1985)

Where:

k_1 = reaction rate ($(\text{g}/\text{m}^3)^{1-\gamma} \cdot \text{s}^{-1}$)

γ = order of reaction (-)

Assuming a first order decay, the equation can be written as:

$$\frac{dc_i}{dt} + k_1 c_i = 0$$

Resulting in the following analytical solution:

$$c_i = c_{i0} e^{-k_1 t}$$

where k_1 is the decay rate (s^{-1}) and c_{i0} is the initial concentration (g/m^3).

1.1.5 Overall equation for fate of compound in water

The dissolved or suspended compound in water is subject to transport, transfer and degradation, the overall equation for a one-dimensional flow is therefore:

$$\frac{\partial c}{\partial t} - D_x \frac{\partial^2 c}{\partial x^2} + u \frac{\partial c}{\partial x} + f_1(c) + f_2(c, c_{g,s}) = 0$$

Where:

u = velocity of water through reactor (m/s)

c = concentration of compound in water (g/m³)

D_x = dispersion coefficient in water (m²/s)

f_1 = decay function in water

f_2 = transfer function of compound from water

The first term on the left side is the change of concentration in time. When $dc/dt=0$, there is a stationary situation and the concentration on a certain location is independent of time. The second term is the turbulent dispersion of the gradient type (following Fick's law). The third term indicates the transport of the concentration through the reactor by advection. The fourth term indicates a function for the decay of the compound. The last term indicates a function for the transfer of the compound from the water to the solid or gas phase.

1.1.6 Mass balance between water and gas or solid phase

The gas or solid phase can be fixed in the reactor, but can also be transported through the reactor. Flow of gas normally occurs in aerators. Flow of the solid phase can be observed in continuous sand filters or fluidised bed reactors. The equation for this transport is:

$$\frac{\partial c_{g,s}}{\partial t} - D_{x,g,s} \frac{\partial^2 c_{g,s}}{\partial x^2} + u_{g,s} \frac{\partial c_{g,s}}{\partial x} + f_{1,g,s}(c_{g,s}) + f_{2,g,s}(c, c_{g,s}) = 0$$

Where:

$u_{g,s}$ = velocity of gas or solid phase through reactor (m/s)

$c_{g,s}$ = concentration of compound in gas or solid phase (g/m³)

$D_{x,g,s}$ = dispersion coefficient in gas or solid phase (m²/s)

$f_{1,g,s}$ = decay function in gas or solid phase

$f_{2,g,s}$ = transfer function of compound into gas or solid phase

The equation is similar to the equation of transport in water. The decay function (fourth term) is normally only present in the solid phase. For example, the concentration of the compound can be changed by (bio)-degradation. The last term indicates the function for transfer from the water to the solid or gas phase. The sign is opposite to the sign in water. The compounds that are taken from the water are stored in the solid or gas phase and vice versa.

The mass balance between the water phase and solid or gas phase can be expressed as follows (see figure 1.4):

$$\begin{aligned} V \Delta C + V_{g,s} \Delta C_{g,s} &= \Delta x \Delta y \Delta z \Delta C + \Delta x \Delta y \Delta z_{g,s} \Delta C_{g,s} = \\ CU \Delta y \Delta z \Delta t - (CU \Delta y \Delta z \Delta t + \frac{\Delta C U}{\Delta x} \Delta x \Delta y \Delta z \Delta t) + \\ C_{g,s} U_{g,s} \Delta y \Delta z_{g,s} \Delta t - (C_{g,s} U_{g,s} \Delta y \Delta z_{g,s} \Delta t + \frac{\Delta C_{g,s} U_{g,s}}{\Delta x} \Delta x \Delta y \Delta z_{g,s} \Delta t) \end{aligned}$$

with $\Delta x, \Delta y, \Delta z, \Delta z_{g,s}, \Delta t \rightarrow 0$

$$\Rightarrow V \frac{\partial C}{\partial t} + \frac{\partial CU}{\partial x} dx dy dz + V_{g,s} \frac{\partial C_{g,s} U_{g,s}}{\partial x} dx dy dz_{g,s} = 0$$

In case dispersion is neglected ($C=c$, $C_{g,s}=c_{g,s}$, $U=u$ and $U_{g,s}=u_{g,s}$), the equation can also be written as:

$$\frac{\partial c}{\partial t} + \frac{\partial cu}{\partial x} = - \frac{V_{g,s}}{V} \left(\frac{\partial c_{g,s}}{\partial t} + \frac{\partial c_{g,s} u_{g,s}}{\partial x} \right)$$

Where:

V = volume of water (m^3)

$V_{g,s}$ = volume of gas or solid (m^3)

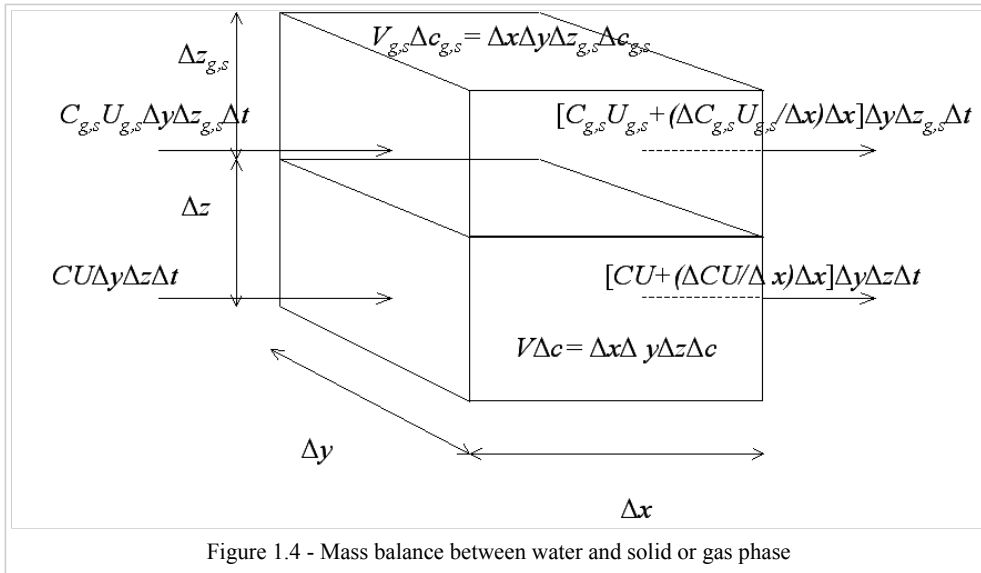


Figure 1.4 - Mass balance between water and solid or gas phase

1.2 References

- Armirtharajah, A., Clark, M.M., and Trussel, R.R., Mixing in coagulation and flocculation, AWWARF, 1991
- Armirtharajah, A., Some theoretical and conceptual views of filtration, Journal of the American Water Works Association, Vol.80, No.12, pp. 36-46, 1988
- James, A., An introduction to water quality modelling, John Wiley and sons Ltd., Chichester, West Sussex, 1993
- Levenspiel, O., Chemical reaction engineering, 3rd edition, Wiley & Sons, 1999
- Montgomery, J.M., Consulting Engineers, Inc., Water treatment principles & design, Wiley & Sons, 1985
- Mueller, J.A., Boyle, W.C., Pöpel, H. J., Aeration, principles and practice, Water quality management library, CRC Press, 2002
- Schroeder, E.D, Water and wastewater treatment, McGraw-Hill book company, 1977
- Sontheimer, H., Crittenden, J.C. and Summers, R.S., Activated carbon for water treatment, AWWA Research foundation, Denver, 1988
- Stumm, W. and Morgan, J.J., Aquatic Chemistry, chemical equilibria and rates in natural water, third edition, John Wiley & Sons, 1996

2 Aeration and Degassing

2.1 Gas Transfer in General

2.1.1 Introduction

Aeration (gas addition) and gas stripping (gas removal) are normally the first treatment steps during the production of drinking water from groundwater or riverbank water. This artificially induced gas transfer aims at the addition of oxygen (O_2) and the removal of carbon dioxide (CO_2), methane (CH_4), hydrogen sulfide (H_2S), and other volatile organic compounds, for example 1,2 Dichloropropane (1,2 DCP), Trichloroethene (TCE), Tetrachloroethene (PER) and Trichloromethane (chloroform). Gas transfer is seldom applied in the treatment of surface water because surface water has been in contact with air for a prolonged period. Consequently, surface water contains sufficient oxygen, while other gases, like methane and hydrogen sulfide, are absent.

The addition of oxygen is required for the oxidation of bivalent iron (Fe^{2+}), manganese (Mn^{2+}) and ammonium (NH_4^+). These substances are present in dissolved form in groundwater. Due to chemical and biological oxidation, the substances can be removed by following a filtration step. Reducing the carbon dioxide concentration leads to a rise in pH. A higher pH lowers the metal dissolving capacity of the water.

Methane should be removed because it influences the following filtration treatment processes. Hydrogen sulfide has the odour of rotting eggs and therefore needs to be removed from the water. Volatile organic compounds are usually toxic; some of them are even carcinogenic. Obviously, these compounds are not allowed in drinking water.

2.1.2 General theory

A model consists of three elements: equilibrium, kinetics and mass balance.

Equilibrium, Henry's law

Water contains dissolved gases. In a closed vessel containing both gas (e.g., air) and water, the concentration of a volatile component in the gas phase will be in equilibrium with the concentration in the water phase, according to Henry's law. The equilibrium concentration can be calculated using the following form of Henry's law:

$$c_w = k_H c_g$$

Where:

c_w = the equilibrium concentration of a gas in water [g/m^3]

k_H = the Henry's constant or distribution coefficient [-]

c_g = the concentration of the gas in air [g/m^3]

The distribution coefficient k_H depends on the type of gas, and the temperature. In addition, pollution and impurities in the water influence the equilibrium concentration. This issue will not be discussed here.

Often partial pressure is used instead of the gas concentration in air, and/or molar concentration in the water instead of weight concentration. Consequently this results in a different unit for the distribution coefficient, or Henry's law constant (i.e. [$\text{mol}/(m^3 \text{ Pa})$] or [$\text{mol}/l/\text{atm}$]). For gas stripping, often the volatility is given instead of the solubility of a gas. In this case, the distribution coefficient is inverted (gas/water, instead of water/gas).

In Table 2.1 for a number of gases a list of values is given of the distribution coefficient at different water temperatures, (intermediate values can be obtained with linear interpolation). In the table it is shown that nitrogen, oxygen and methane have low k_H -values. This means that these gases hardly dissolve in water and they can, therefore, be easily removed. The other gases have high k_H -values and dissolve easily, which makes it difficult to remove them from the water or easy to add them to water.

Gas	Distribution coefficient (k_H)			Molecular weight (MW) [g/mol]
	T = 0 °C	T = 10 °C	T = 20 °C	
Nitrogen (N ₂)	0.023	0.019	0.016	28
Oxygen (O ₂)	0.049	0.041	0.033	32
Methane (CH ₄)	0.055	0.043	0.034	16
Carbon dioxide (CO ₂)	1.71	1.23	0.942	44
Hydrogen sulfide (H ₂ S)	4.69	3.65	2.87	34
Tetrachloroethylene (C ₂ HCl ₄)	-1	3.20	1.21	167
Tetrachloroethene (C ₂ HCl ₃)	-1	3.90	2.43	131.5
Chloroform (CHCl ₃)	-1	9.0	7.87	119.5
Ammonia (NH ₃)	-	0.94	0.76	17

¹ These substances are still in the liquid phase at a temperature of 0°C and therefore the k_H is not known

Table 2.1 - The mass balance of a conservative solute

The gas concentration in the air c_g must be known before the equilibrium (or saturation) concentration can be calculated. This concentration can be determined using the universal gas law:

$$PV = nRT$$

Where:

p = the partial pressure of gas in gas phase [Pa]

V = the total gas volume [m³]

n = the number of moles of a gas [mol]

R = the universal gas constant = 8,3142 [J/(K.mol)]

T = the (air) temperature [K]

The gas concentration can be calculated by multiplying the molar gas concentration in air [mol/m³] with the molecule weight of the considered gas:

$$c_g = \frac{n}{V} MW = \frac{P}{RT} MW$$

Where MW is the molecular weight of a gas [g/mol]

The partial pressure of a certain gas is proportional to the volume fraction of that gas in air:

$$p = p_0 V_f$$

Where:

p_0 = the standard pressure at sea level (=101,325) [Pa]

V_f = the volume fraction [-]

In Table 2.2 the volume fractions of different gases that occur in air are given. These values are valid for dry air with a standard pressure of 101,325 Pa. With these volume fractions the partial pressures of all gases in air can be calculated. Gases that do not occur in air have a partial pressure equal to zero and thus a c_g equal to zero and also a c_w equal to zero (for example, methane).

Gas	Volume fraction ¹ [%]	Saturation concentration ² c_w [g/m ³]
Nitrogen (N ₂)	78.084	17.9
Oxygen (O ₂)	20.948	11.3
Argon (Ar)	0.934	-
Carbon dioxide (CO ₂)	0.032	0.79
Other gases	0.02	-

¹ In dry air at a standard pressure of 101,325 Pa

² Water and air temperature of 10 °C

Table 2.2 - The volume fraction of gases

In Figure 2.1 the equilibrium (saturation) concentration of oxygen is given as a function of water temperature. With an increase in water temperature, the saturation concentration decreases because less oxygen can be dissolved in warm water.

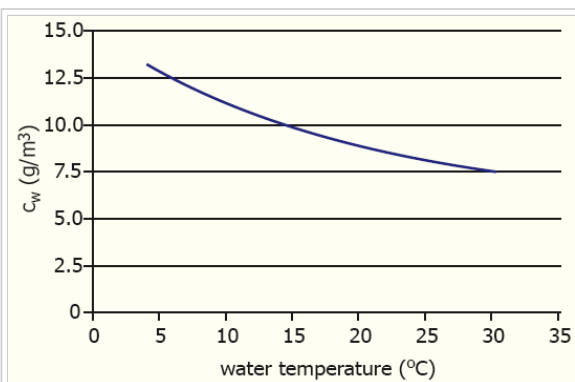


Figure 2.1 - The saturation concentration of oxygen as a function of the temperature of the water

The saturation concentration c_w is linearly dependent on pressure. The saturation concentration for oxygen at the standard pressure of 101,325 Pa is 11.3 g/m³. At a height of 8,000 meters (for example, Mount Everest), the air pressure is only 10,000 Pa which means that the saturation concentration for oxygen is 1.1 g/m³. In the sea at a depth of 100 meters below sea level, the pressure is 1,100,000 Pa. This results in a saturation concentration for oxygen of 113 g/m³.

Kinetics

As soon as water and air are in contact, gas molecules will be exchanged continuously. The direction of the net gas transport depends on the gas concentration in the water (c_w) and the equilibrium concentration c_e . The velocity of gas transfer is determined by the kinetic equation:

$$\frac{dc_w}{dt} = k_2(c_s - c_w)$$

Where:

c_w = the concentration of a gas in water [g/m³] and

k_2 = the gas transfer coefficient [s⁻¹]

The time dependent gas concentration in water is represented by the term dc_w/dt . The changes in concentration are determined by the magnitude of the gas transfer coefficient k_2 and the driving force ($c_s - c_w$). The gas transfer coefficient k_2 is a device-dependent parameter. The larger the contact surface area between air and water and the renewal of this surface area, the better the gas transfer and the higher the gas transfer coefficient.

For a batch reactor the differential equation can be solved by integration, with $c_w = c_{w0}$ at time $t=0$, taking into account that

c_s is constant:

$$c_s = (c_s - c_{w,0})e^{-k_2 t}$$

or:

$$\frac{c_s - c_{w,t}}{c_s - c_{w,0}} = e^{-k_2 t}$$

Mass balance

For situations in which the gas concentration changes in air are important, a mass balance needs to be formulated. For the gas transfer system, the law of continuity is valid: the total amount of gas that enters and leaves the system must be equal and a mass balance can be set up:

$$Q_w c_{w,0} + Q_a c_{a,0} = Q_w c_{w,e} + Q_a c_{a,e}$$

Using the mass balance RQ (relationship between the air flow and the water flow) can be defined as follows:

$$RQ = \frac{Q_a}{Q_w} = \frac{c_{w,e} - c_{w,0}}{c_{a,0} - c_{a,e}}$$

2.1.3 General model equations

Previous theory on equilibrium, kinetics and mass balance can be combined to form the following partial differential equations:

$$\frac{\partial c_l}{\partial t} = v_{lx} \frac{\partial c_l}{\partial x} + k_2 (k_D \cdot c_g - c_l) - r_l$$

$$\frac{\partial c_g}{\partial t} = v_{lx} \frac{\partial c_g}{\partial x} - \frac{k_2}{RQ} (k_D \cdot c_g - c_l) - r_g$$

If the partial differential equation for the concentration of a gas in water needs to be applied to a flow of water modelled in a numerical model, it changes to the following equation which needs to be solved for each modelling step:

$$\frac{dc_l}{dt} = v_{lx} \frac{dc_l}{dx} + k_2 (k_D \cdot c_g - c_l) - r_l$$

The amount of steps (and therefore the magnitude of each step) determines the degree to which the numerical calculation approaches the partial differential equation.

When T is the amount of time that a drop of water stays in the same step, the equation becomes:

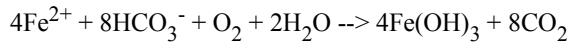
$$\frac{dc_l}{dt} = \frac{dc_l}{T} + k_2 (k_D \cdot c_g - c_l) - r_l$$

In the same way the model equation for the gas phase becomes:

$$\frac{dc_g}{dt} = \frac{dc_g}{T} + \frac{k_2}{RQ} (k_D \cdot c_g - c_l) - r_g$$

Model equations for the oxygen concentration in water and air

The oxygen concentration in water changes due to convection, gas transfer between water and air and by oxidation of Fe^{2+} in water. The corresponding chemical equation is:



This implies that 0.25 mmol/l of oxygen is used to convert 1 mmol/l of iron, which gives the following equation for the oxygen concentration:

$$f_{\text{O}_2} = -0.25 \cdot \frac{d[\text{K}_{\text{Fe}^{2+}} \cdot \text{Fe}^{2+}]}{dT}$$

In which:

$\text{K}_{\text{Fe}^{2+}}$ = the percentage of Fe^{2+} that oxidizes during the period of gas transfer.

The complete model equation for the oxygen concentration will become:

$$\frac{d[\text{O}_2]_t}{dt} = \frac{d[\text{O}_2]_t}{dT} + k_{2,\text{O}_2} (k_{D,\text{O}_2} \cdot [\text{O}_2]_g - [\text{O}_2]_t) - 0.25 \cdot \frac{d[\text{K}_{\text{Fe}^{2+}} \cdot \text{Fe}^{2+}]}{dT}$$

In the same way the model equation for oxygen in air becomes:

$$\frac{d[\text{O}_2]_g}{dt} = \frac{d[\text{O}_2]_g}{T} + \frac{k_{2,\text{O}_2}}{RQ} (k_{D,\text{O}_2} \cdot [\text{O}_2]_g - [\text{O}_2]_t)$$

A similar method is applied on methane, carbon dioxide, bicarbonate, iron and calcium. The difference for the latter two being that they are not influenced by gas transfer, but just by the chemical reactions. For more information on the aeration and gas transfer modelling equations, please refer to the MSc thesis by Alex van der Helm.

pH calculation

The pH is calculated with the bicarbonate and carbon dioxide concentration in water as follows:

$$pH = pK_1 - \log([\text{CO}_2]) + \log([\text{HCO}_3^-] \cdot f(\text{HCO}_3^-))$$

In which:

$f(\text{HCO}_3^-)$ = activity coefficient of bicarbonate [-]

2.2 Weir/Cascade Aeration

2.2.1 Process

To achieve gas transfer a number of systems have been developed over the years. One of the oldest systems is the cascade.



Figure 2.2 - A cascade aerator in a treatment plant

The water falls in several steps. In each step, the water falls over a weir into a lower placed trough. When the falling stream enters the water body, air is entrapped in the form of bubbles, providing a mixture of water and air in which gas transfer will occur. The efficiency of the cascade or weir aerator is limited, due to the fact that only a little amount of air is dragged into the next trench. From practice it is learned that a cascade aerator has an RQ of about 0.4. The cascade aerator is often applied because of its simplicity, its lack of pollution, high applicable discharge and visual attractiveness.

2.2.2 Model

2.2.2.1 Options for Usage

The model for cascade aeration can be used for the calculation of gas removal efficiencies for methane, carbon monoxide, nitrogen and hydrogen sulphide and the gas transfer efficiency of oxygen from air to water. By using the block "graphical output cascade" the progress of degassing and aeration of the previously mentioned gasses across the cascade can be seen.

2.2.2.2 Model Calibration

2.2.2.3 Input and Output

The input of the model can be water quality data from a previous model/treatment step or the raw water input block. On top of that the model parameters have to be entered into the cascade/weir aerator model block. The output are the new water quality parameters that have been calculated by the model, which can be displayed as time series in graphs.

Model Parameters

When in Stimela a new project including a weir aerator is created, the model displayed in Figure 2.x will pop up. In the window are included: a raw water input block, a graphical output block and a cascade/weir aerator block. For the last one, the model parameters have to be changed for each different situation. In Figure 2.x the model parameters for the block are shown. The model parameter window pops up when the block is double clicked.

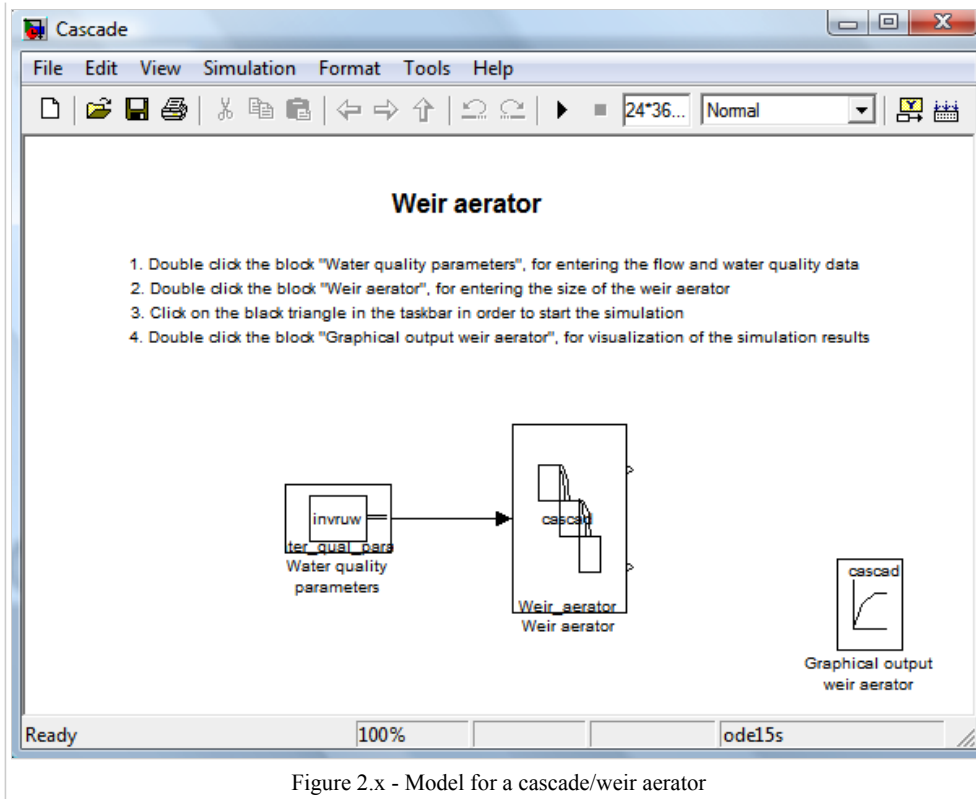


Figure 2.x - Model for a cascade/weir aerator

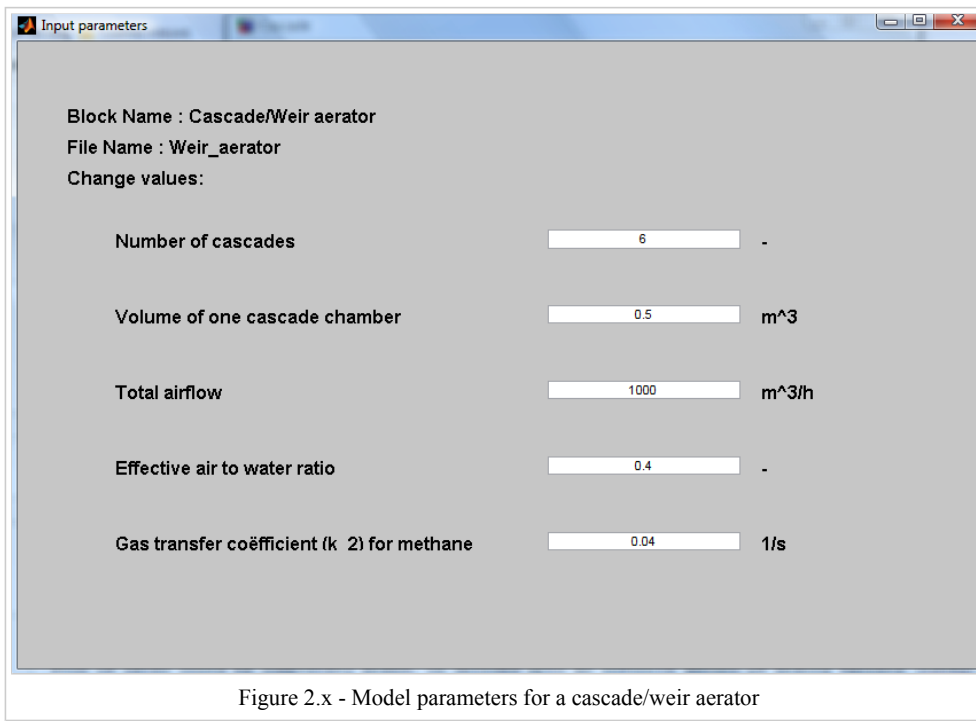


Figure 2.x - Model parameters for a cascade/weir aerator

For an explanation of the input parameters needs to be referred to the previous section on model equations.

Graphs

When double clicked, the block "Graphical output weir aerator" will produce in 5 graphs for oxygen, methane, carbon monoxide, nitrogen and hydrogen sulphide the change in gas concentration over the different cascade chambers. The curve for the gas saturation concentration is given as well for all 5 gasses. The gas saturation concentration is the gas concentration in air multiplied by the distribution coefficient k_D (see Section 2.1).

Apart from the 5 graphs, there is a list of the input parameters and the start and end pH displayed. The results shown in Figure 2.x are acquired by entering the default parameters shown in Figure 2.x.

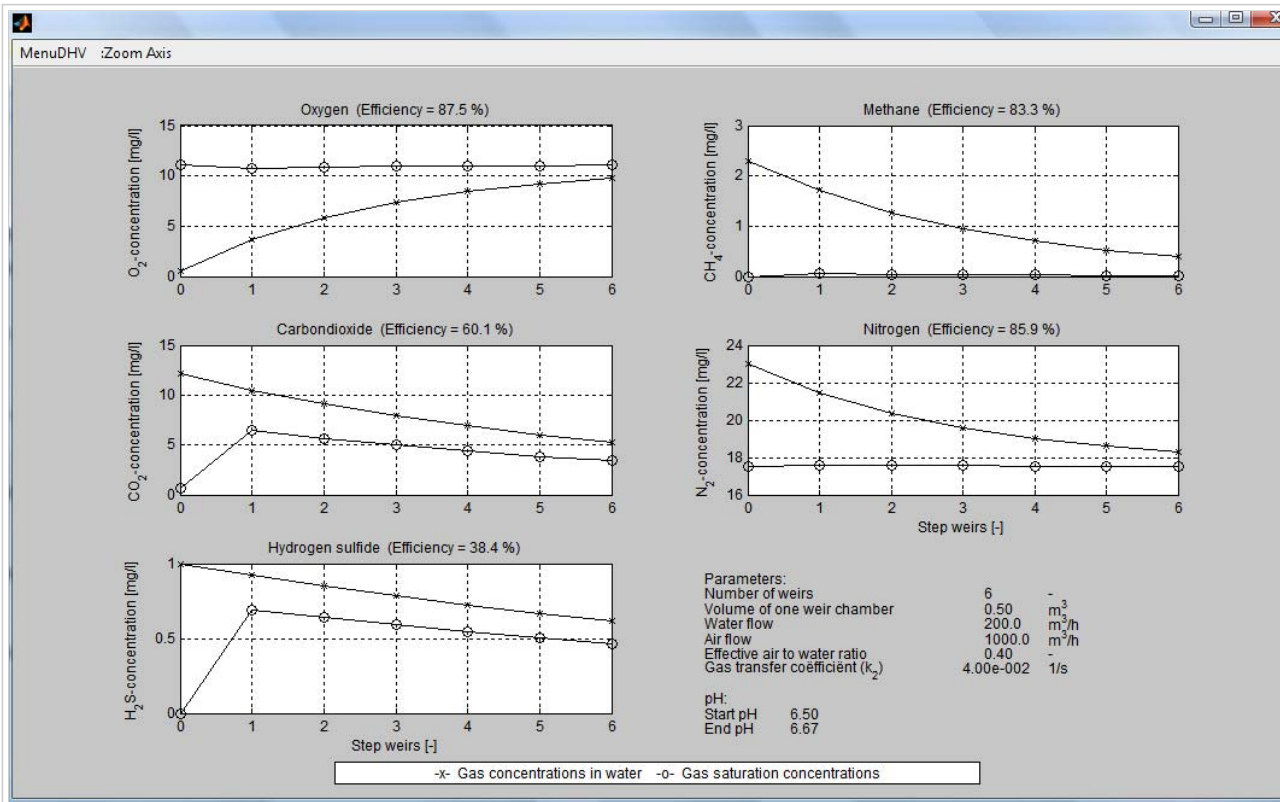


Figure 2.x - Graphical output for a cascade/weir aerator

2.3 Plate Aeration (INKA aerator)

2.3.1 Process

With a plate aerator the water flows horizontally over a perforated plate, through which air is pumped in upward direction, thereby creating a bed of air bubbles (see Figure 2.x). This creates extensive contact between water and air. The combination of a horizontal flow of water and a vertical flow of air is called cross flow aeration. The height of the bubble bed is determined by the adjustment of a weir at the end of the plate. The diameter of the holes in the perforated plate is usually about 1-1.5 mm. The open surface varies with plate aerators from 1.5 to 3%

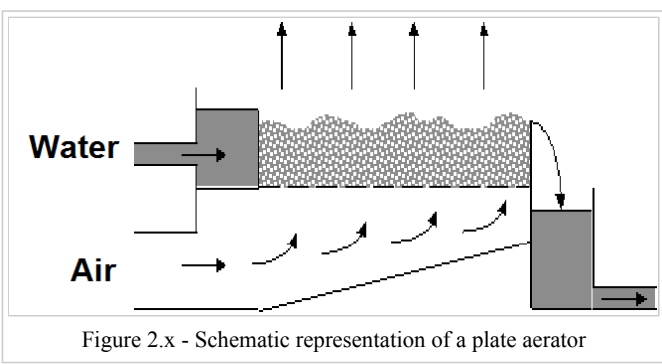


Figure 2.x - Schematic representation of a plate aerator

Because of the limited construction height and head of the discharge that is necessary for a well functioning plate aerator, it offers good possibilities for applying it in an existing treatment station. In some cases it's even possible to apply them just above the pre-filters.

2.3.2 Model

2.3.2.1 Options for Usage

The model for plate aeration can be used for the calculation of gas removal efficiencies for methane, carbon monoxide, nitrogen and hydrogen sulphide and the gas transfer efficiency of oxygen from air to water. By using the block "graphical output plate aerator" the progress of degassing and aeration of the previously mentioned gasses across the plate can be seen.

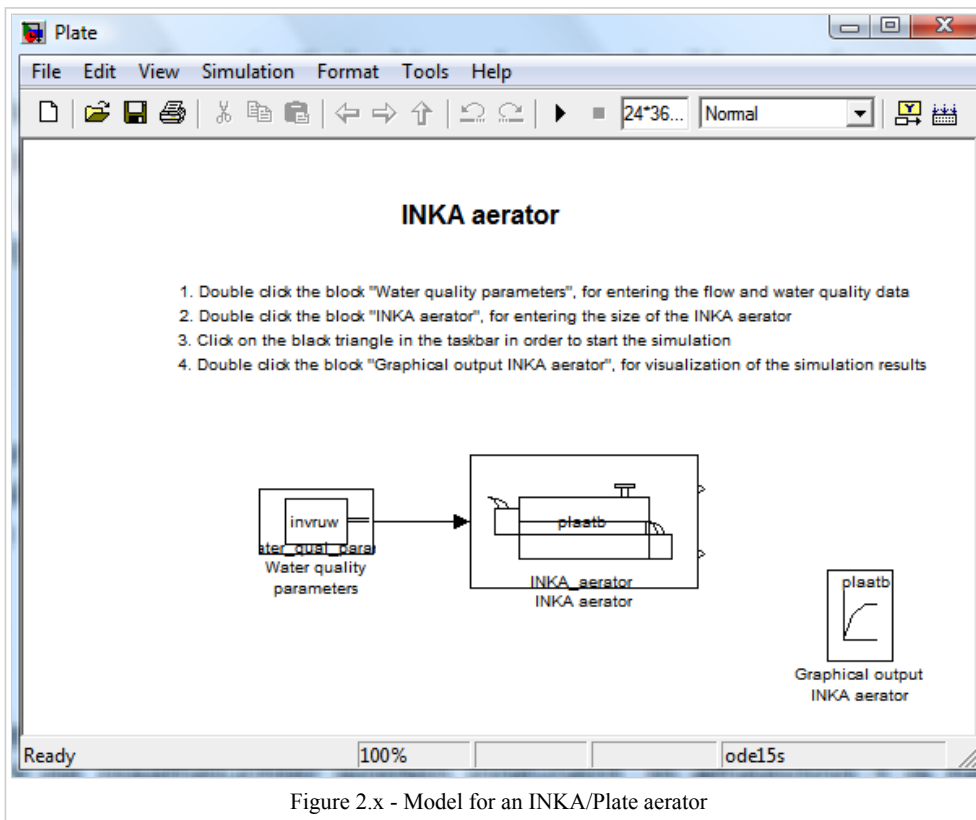
2.3.2.2 Model Calibration

2.3.2.3 Input and Output

The input of the model can be water quality data from a previous model/treatment step or the raw water input block. On top of that the model parameters have to be entered into the INKA aerator model block. The output are the new water quality parameters that have been calculated by the model, which can be displayed as time series in graphs.

Model Parameters

When in Stimela a new project including an INKA aerator is created, the model displayed in Figure 2.x will pop up. In the window are included: a raw water input block, a graphical output block and an INKA aerator block. For the last one, the model parameters have to be changed for each different situation. In Figure 2.x the model parameters for the block are shown. The model parameter window pops up when the block is double clicked.



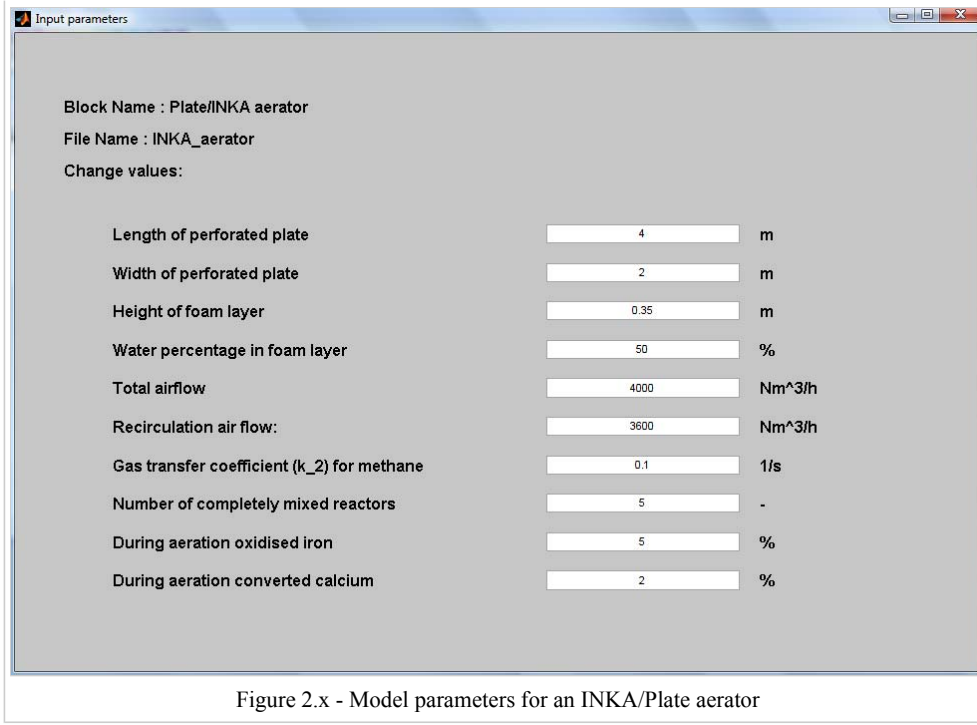
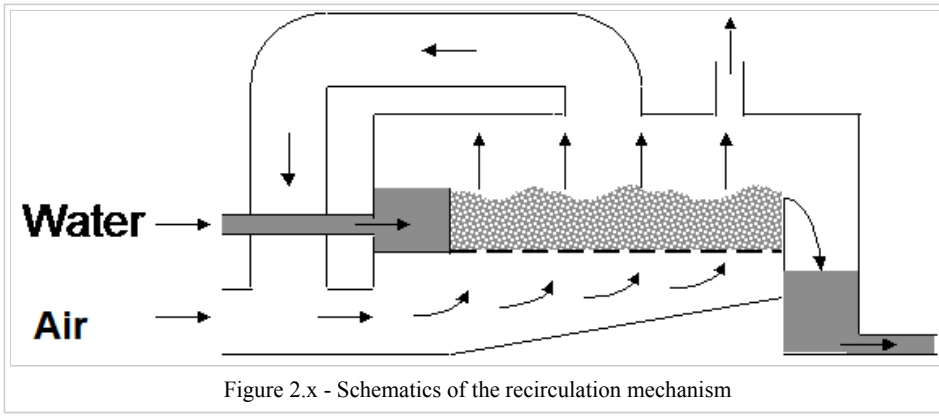


Figure 2.x - Model parameters for an INKA/Plate aerator

For an explanation of the input parameters needs to be referred to the previous section on model equations. The ones that haven't been discussed yet are:

Air recirculation flow: The flow of air that is tapped off the outgoing air flow and is added to the ingoing fresh air supply (see Figure 2.x).

Number of CSTRs between sampling: The number of CSTRs determines the rate of plug flow through the plate aerator. In the most extreme case, a flow of water could be completely mixed, or divided into an infinite amount of mixing barrels (CSTRs). When a number like 100 is filled in here, the flow will be almost perfect plug flow. This is not very probable, because there is always horizontal and vertical mixing going on. The improvement of gas transfer due to the improvement of the plug flow is negligible when the stream is divided into more than 20 completely mixed barrels.



Graphs

When double clicked, the block "Graphical output INKA aerator" will produce in 5 graphs for oxygen, methane, carbon monoxide, nitrogen and hydrogen sulphide the change in gas concentration over the plate aerator. The curve for the gas saturation concentration is given as well for all 5 gasses. The gas saturation concentration is the gas concentration in air multiplied by the distribution coefficient k_D (see Section 2.1).

Apart from the 5 graphs, there is a list of the input parameters, the iron and calcium consumption and the start and end pH displayed. The results shown in Figure 2.x are acquired by entering the default parameters shown in Figure 2.x.

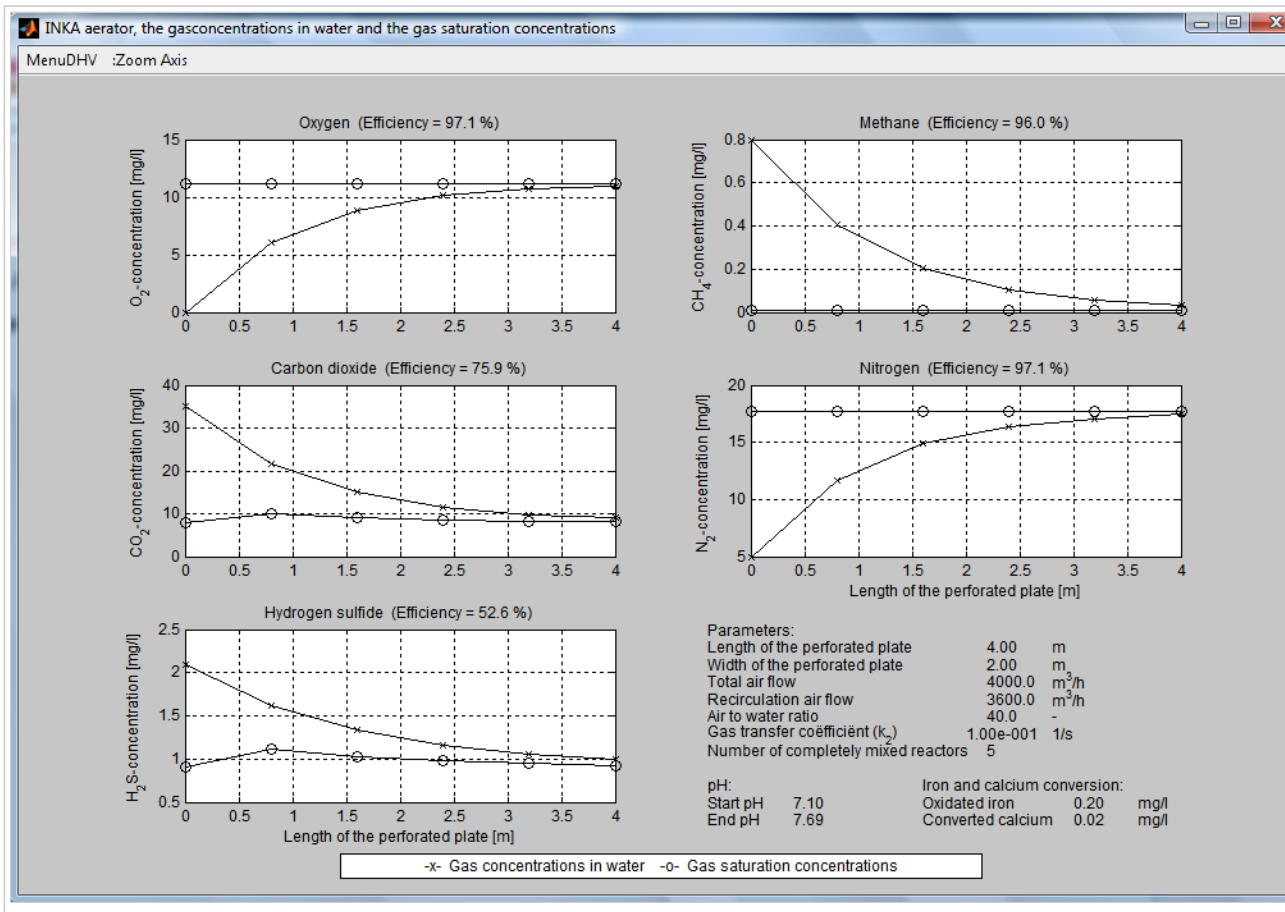


Figure 2.x - Graphical output for an INKA/Plate aerator

2.4 Tower/Column Aeration

2.4.1 Process

A tower aerator consists of a steel or plastic cylinder, which is filled with packing material. This packing material can consist of piled up wooden bars or tubes, or of specially designed packing material like the Pall-ring or the Berl-saddle. In the top of the tower, the water is divided over the packing, after which it flows over and falls onto the packing surface until it reaches the bottom. Because of the flow of water over the packing surface, there is a big contact surface area between air and water for the transfer of gasses. Furthermore, the water keeps falling from one surface to the other, thereby creating smaller and smaller drops of water, continuously renewing the gas transfer surface area.

The air can be supplied through natural ventilation or with the help of a fan. In case a fan is used, the air can be sent through the tower in co-current or counter-current (see Figure 2.x). Counter-current gives higher efficiencies than co-current, but still co-current is applied as well. Reasons to do so can be:

- The carbon monoxide removal cannot be too big, due to calcium deposits or large increases in pH. With co-current with low RQs, the transfer of oxygen and removal of methane is sufficient, while the carbon monoxide removal will not be that big. When applying counter-current, the carbon monoxide removal will increase.
- There are extremely high surface loadings being applied. With counter-current, this can cause flooding. This means that a layer of water is formed within the column by upward pressure of the air. It might even happen that the tower is completely filled up with water.

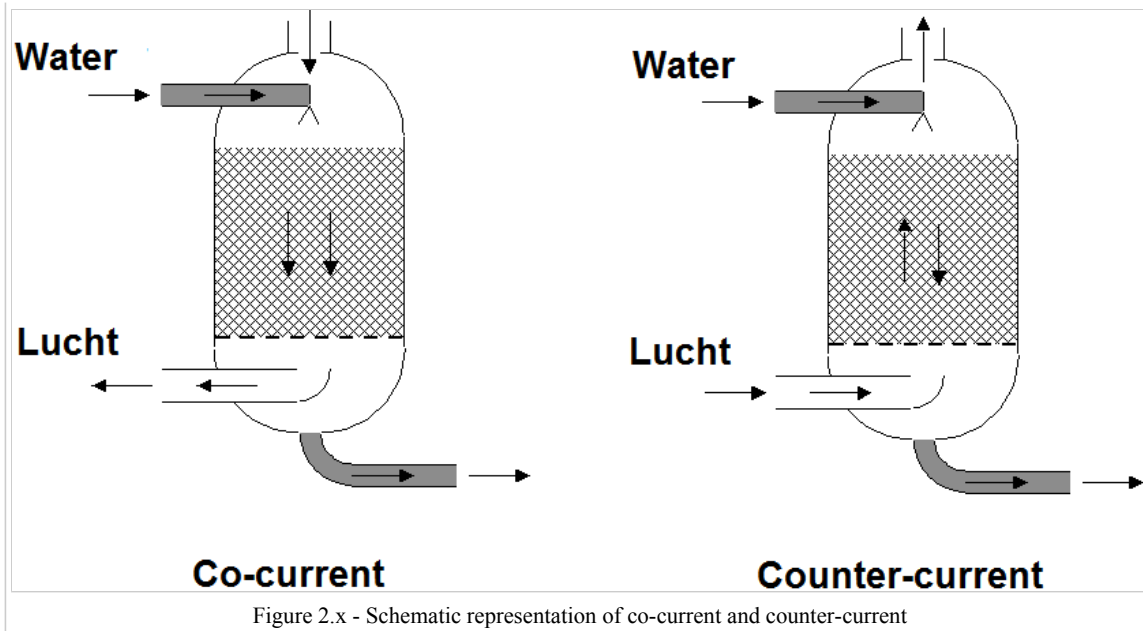


Figure 2.x - Schematic representation of co-current and counter-current

In afbeelding 2 zijn verschillende soorten pakkingmateriaal weergegeven. Deze pakkingen kunnen worden vervaardigd uit kunststof, metaal, koolstof of keramische materialen, de grootte kan variëren van 6 mm tot 75 mm. In praktijk installaties voor de zuivering van drinkwater worden met name kunststoffen pakkingen gebruikt met een grootte van 25-50 mm.

In Figure 2.x different packing materials are shown. These packings can be made out of plastic, metal, carbon or ceramic material. The size of the packing can differ from 6 to 75 mm. In practice packing materials are usually made out of plastic and 25-50 mm in size.



Figure 2.x - Different packing materials

2.4.2 Model

2.4.2.1 Options for Usage

The model for tower aerator can be used for the calculation of gas removal efficiencies for methane, carbon monoxide, nitrogen and hydrogen sulphide and the gas transfer efficiency of oxygen from air to water. By using the block "graphical output tower aerator" the progress of degassing and aeration of the previously mentioned gasses across the tower can be seen.

2.4.2.2 Model Calibration

2.4.2.3 Input and Output

The input of the model can be water quality data from a previous model/treatment step or the raw water input block. On top of that the model parameters have to be entered into the packed column aerator model block. The output are the new water quality parameters that have been calculated by the model, which can be displayed as time series in graphs.

Model Parameters

When in Stimela a new project including a column aerator is created, the model displayed in Figure 2.x will pop up. In the window are included: a raw water input block, a graphical output block and a packed column aerator block. For the last one, the model parameters have to be changed for each different situation. In Figure 2.x the model parameters for the block are shown. The model parameter window pops up when the block is double clicked.

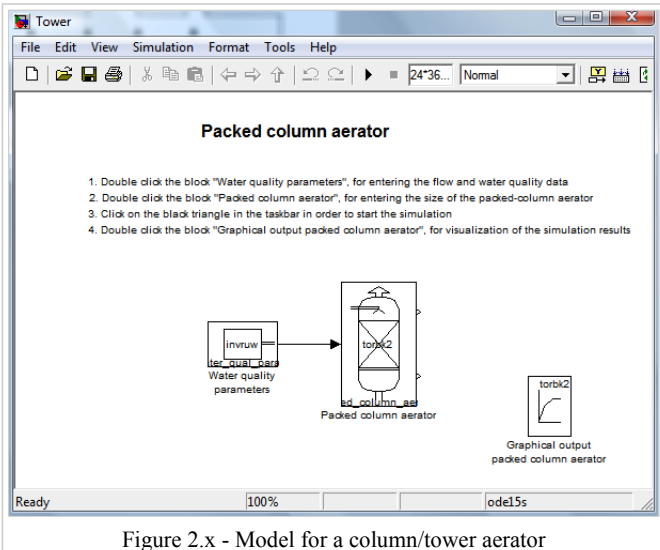


Figure 2.x - Model for a column/tower aerator

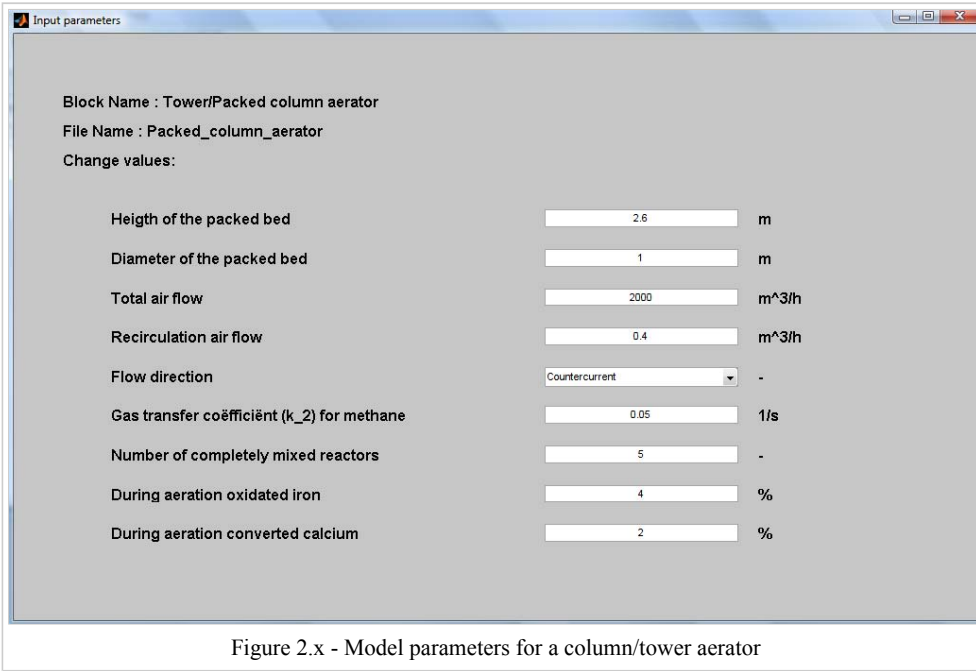
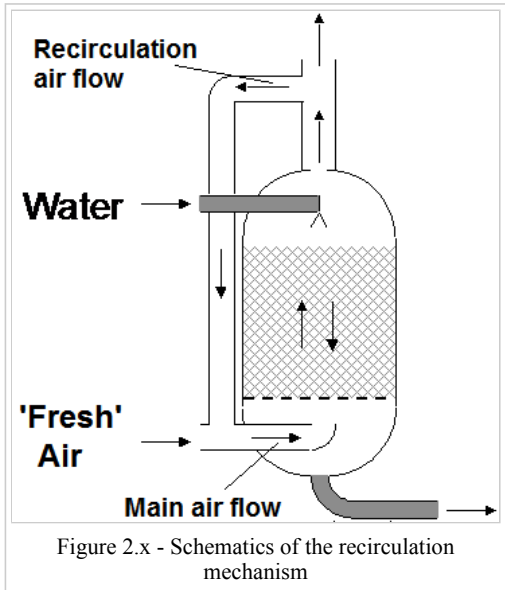


Figure 2.x - Model parameters for a column/tower aerator

For an explanation of the input parameters needs to be referred to the previous section on model equations or Section 2.1. The ones that haven't been discussed yet are:

Air recirculation flow: The flow of air that is tapped off the outgoing air flow and is added to the ingoing fresh air supply (see Figure 2.x).

Number of CSTRs between sampling: The number of CSTRs determines the rate of plug flow through the column aerator. In the most extreme case, a flow of water could be completely mixed, or divided into an infinite amount of mixing barrels (CSTRs). When a number like 100 is filled in here, the flow will be almost perfect plug flow. This is not very probable, because there is always horizontal and vertical mixing going on. The improvement of gas transfer due to the improvement of the plug flow is negligible when the stream is divided into more than 20 completely mixed barrels.



Graphs

When double clicked, the block "Graphical output packed column aerator" will produce in 5 graphs for oxygen, methane, carbon monoxide, nitrogen and hydrogen sulphide the change in gas concentration across the packing material. The curve for the gas saturation concentration is given as well for all 5 gasses. The gas saturation concentration is the gas concentration in air multiplied by the distribution coefficient k_D (see Section 2.1).

Apart from the 5 graphs, there is a list of the input parameters, the iron and calcium consumption and the start and end pH displayed. The results shown in Figure 2.x are acquired by entering the default parameters shown in Figure 2.x.

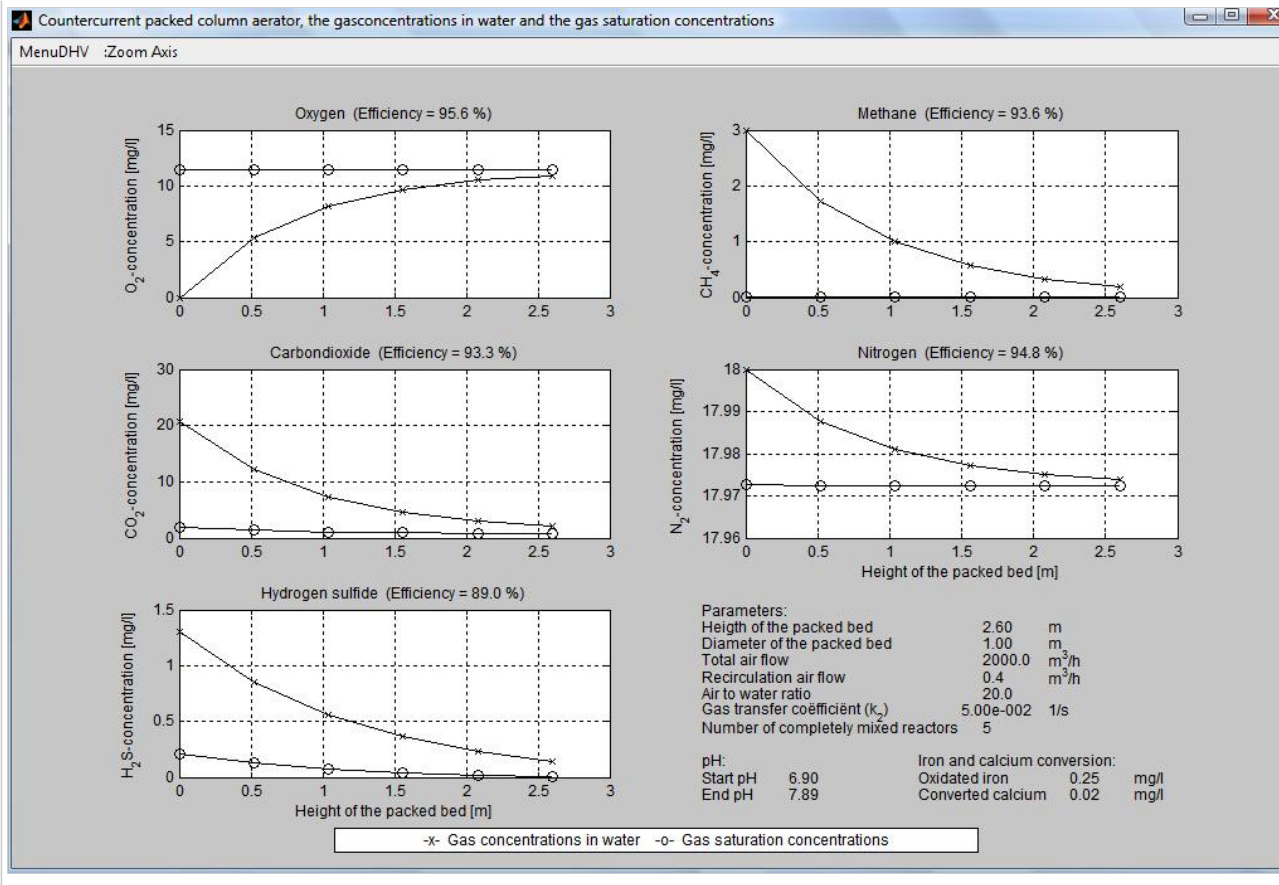


Figure 2.x - Graphical output for a column/tower aerator

2.5 Vacuum Degassing

2.5.1 Process

A vacuum degasser is usually made in the form of an aeration and degassing tower filled with packing material in which the pressure is lowered with a vacuum pump. The vacuum pump removes gasses from the tower, thereby lowering the gas concentrations which causes the pressure to drop. Because the gas concentrations in the tower are lower than in the atmosphere, the gas saturation concentrations will be lower as well. The lower gas saturation concentrations enable the gasses to be removed from the water to a further extent than would be possible under atmospheric conditions. This implies that a vacuum degasser can be used to remove nitrogen and oxygen from water, until the concentrations are under the equilibrium concentration at atmospheric conditions. This can be used for denitrification. The vacuum degasser is the only gas transfer system that is suitable for this. Figure 2.x shows a schematic representation of the vacuum degasser.

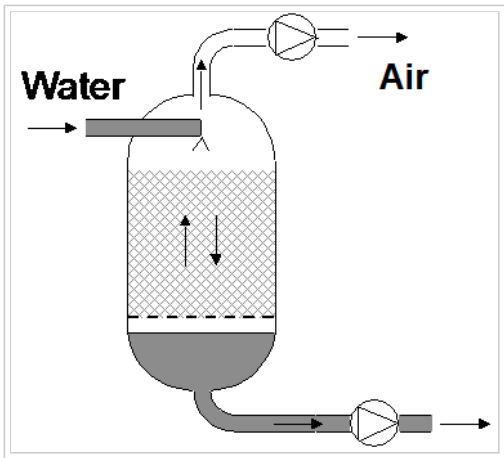


Figure 2.x - Schematic overview of a vacuum degasser

There are different ways at which the vacuum in a vacuum degasser can be maintained:

- With a continuous vacuum pump without drag air
- With a continuous vacuum pump with drag air
- With a discontinuous vacuum pump without drag air

When using a continuous vacuum pump, the vacuum in the tower is kept at a constant pressure by a continuously operative pump. With a discontinuous vacuum pump the pressure will vary between a certain maximum and minimum value. The pump will be turned on when the pressure in the tower reaches the maximum value and is turned off again when the minimum value is reached. Drag air is a small flow of air that gets into the tower through a small vent. When using a discontinuous vacuum pump drag air cannot be applied.

2.5.2 Model

To be able to do calculations with all three ways to maintain the vacuum, two different models have been made for the vacuum degasser. One for the discontinuous and one for the continuous vacuum pump. In the model with the continuous vacuum pump there is an option for the appliance of drag air. Both models can be found in the projects of Stimela as aeration models.

2.5.2.1 Options for Usage

The model for vacuum degassing can be used for the calculation of gas removal efficiencies for methane, carbon monoxide, nitrogen, hydrogen sulphide and oxygen. By using the block "graphical output vacuum degasser" the progress of degassing of the previously mentioned gasses across the vacuum degasser can be seen.

2.5.2.2 Model Calibration

2.5.2.3 Input and Output

The input of the model can be water quality data from a previous model/treatment step or the raw water input block. On top of that the model parameters have to be entered into the packed vacuum degasser model block. The output are the new water quality parameters that have been calculated by the model, which can be displayed as time series in graphs.

Model Parameters

When in Stimela a new project including a vacuum degasser is created, the model displayed in Figure 2.x will pop up. In this case the vacuum degasser with a continuous vacuum pumped is chosen. In the window are included: a raw water input block, a graphical output block and a vacuum degasser block. For the last one, the model parameters have to be changed for each different situation. In Figure 2.x the model parameters for the block are shown. The model parameter window pops up when the block is double clicked.

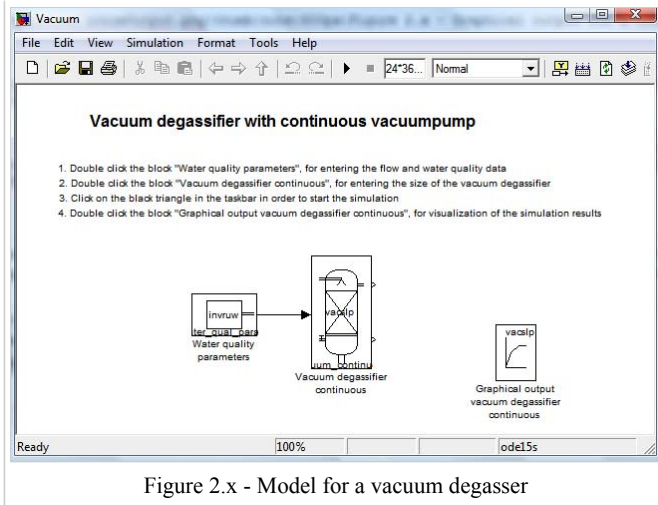


Figure 2.x - Model for a vacuum degasser

Block Name : Vacuum/Vacuum degassifier continuous
File Name : Vacuum_continuous

Change values:

Heighth of the packed bed:	<input type="text" value="2"/>	m
Diameter of the packed bed:	<input type="text" value="1"/>	m
Total air flow:	<input type="text" value="40"/>	m^3/h
Drag air flow:	<input type="text" value="0.5"/>	m^3/h
Recirculation air flow:	<input type="text" value="0"/>	m^3/h
Gas transfer coëfficiënt (k_2) for methane:	<input type="text" value="0.05"/>	1/s
Number of completely mixed reactors:	<input type="text" value="4"/>	-

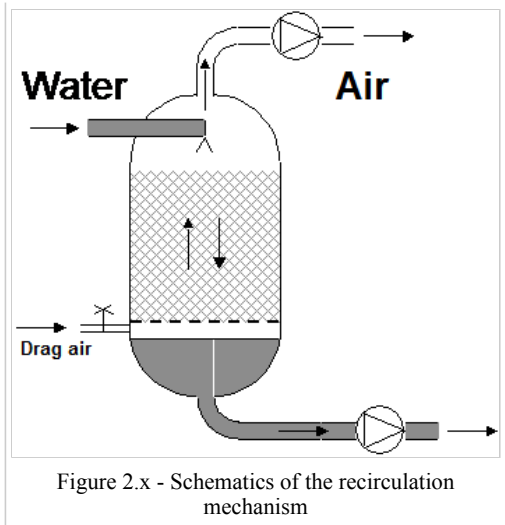
Figure 2.x - Model parameters for a vacuum degasser

For an explanation of the input parameters needs to be referred to the previous section on model equations or Section 2.1. The ones that haven't been discussed yet are:

Drag air flow: The amount of air released from the small drag air vent. If no drag air is required, simply fill in 0. The principle of drag air is shown in Figure 2.x.

Air recirculation flow: The flow of air that is tapped off the outgoing air flow and is added to the ingoing fresh air supply.

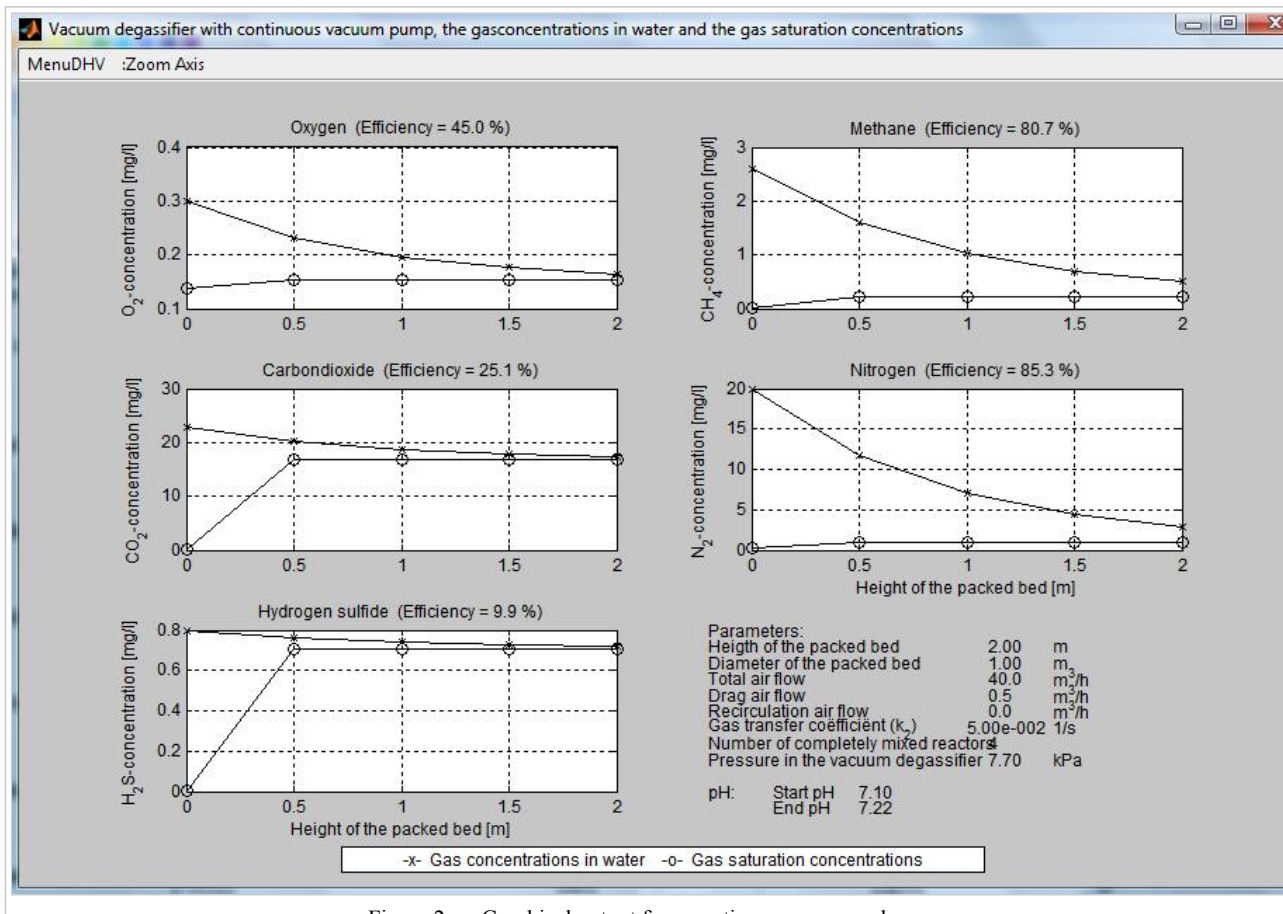
Number of CSTRs between sampling: The number of CSTRs determines the rate of plug flow through the column aerator. In the most extreme case, a flow of water could be completely mixed, or divided into an infinite amount of mixing barrels (CSTRs). When a number like 100 is filled in here, the flow will be almost perfect plug flow. This is not very probable, because there is always horizontal and vertical mixing going on. The improvement of gas transfer due to the improvement of the plug flow is negligible when the stream is divided into more than 20 completely mixed barrels.



Graphs

When double clicked, the block "Graphical output packed column aerator" will produce in 5 graphs for oxygen, methane, carbon monoxide, nitrogen and hydrogen sulphide the change in gas concentration across the vacuum degasser. The curve for the gas saturation concentration is given as well for all 5 gasses. The gas saturation concentration is the gas concentration in air multiplied by the distribution coefficient k_D (see Section 2.1).

Apart from the 5 graphs, there is a list of the input parameters, the iron and calcium consumption and the start and end pH displayed. The results shown in Figure 2.x are acquired by entering the default parameters shown in Figure 2.x.



In vacuum degasser model it is assumed that the air in the vacuum degasser is completely mixed. This can be seen in Figure 2.x because the gas saturation concentration curve is a straight line along the height of the column.

In Figure 2.x it seems as if the gas saturation concentration isn't constant below 0.33 meter. In the calculation however, this is not the case. In the calculation the gas concentration in the air is the same across the entire stream of water, so the saturation concentration is constant as well. That this is not properly expressed in Figure 2.x is due to the fact that the influent gas saturation concentration is displayed at a height of 0 meter.

As mentioned before, a vacuum degasser can function with a discontinuous vacuum pump as well. Most figures and parameters will stay pretty much the same when choosing this option, except for the fact that there is no drag air flow and that the graphical output is quite different:

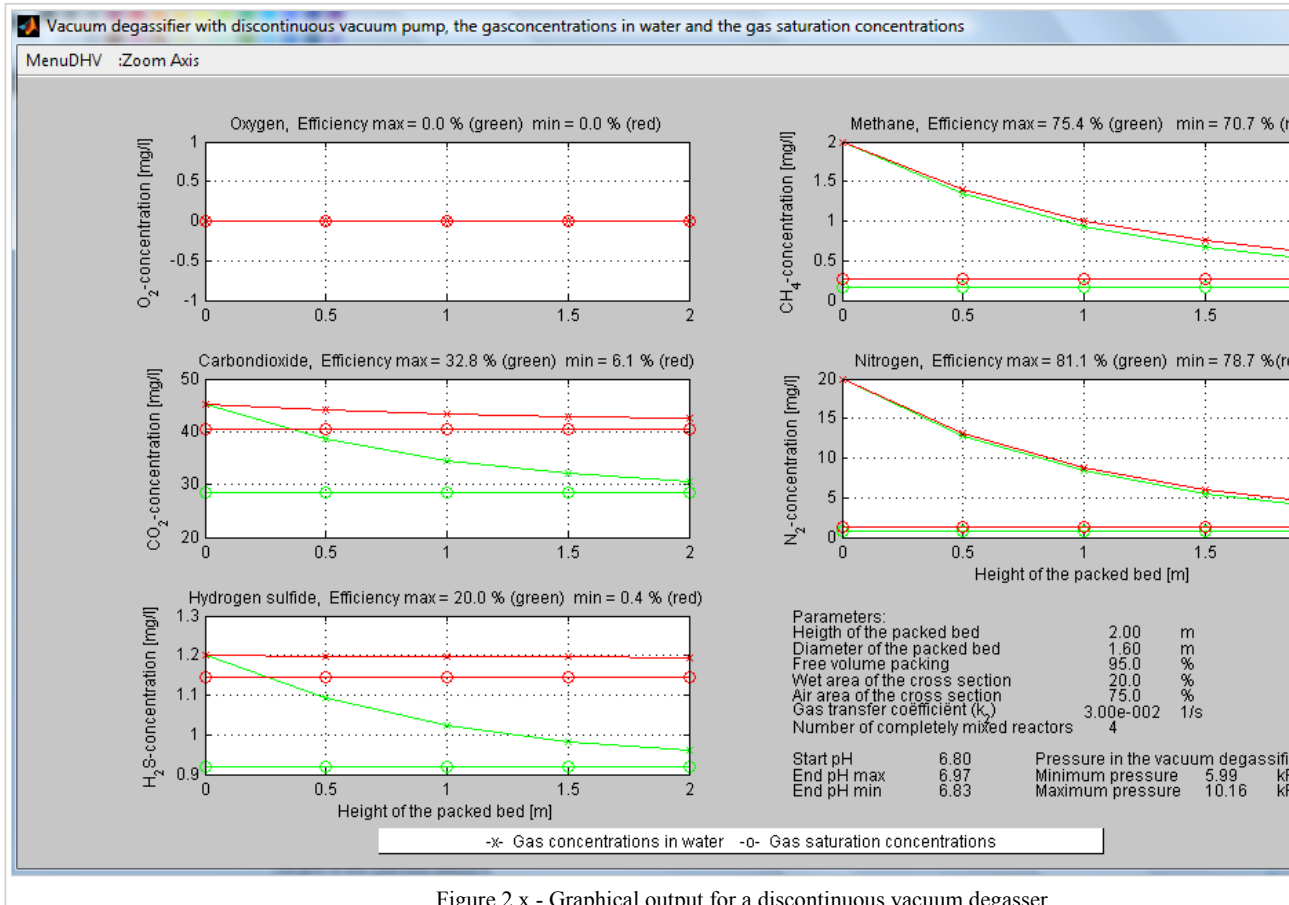


Figure 2.x - Graphical output for a discontinuous vacuum degasser

For every gas the change in gas concentration in water and the gas saturation concentration are shown for the moment at which the pressure is at its lowest (highest efficiency, green line) and when it's at its maximum (lowest efficiency, red line).

2.6 References

van der Helm, A.W.C. (1998), Modellering van intensieve gasuitwisselingssystemen, MSc Thesis, TU Delft

3 Filtration

3.1 Filtration in General

Filtration is a process where water flows through a porous media (often sand) while suspended solids (sand, clay, iron and aluminium flocs) are retained, substances are bio- chemically decomposed and pathogenic micro-organisms (bacteria,

viruses, protozoa) are removed (see Figure 3.1).

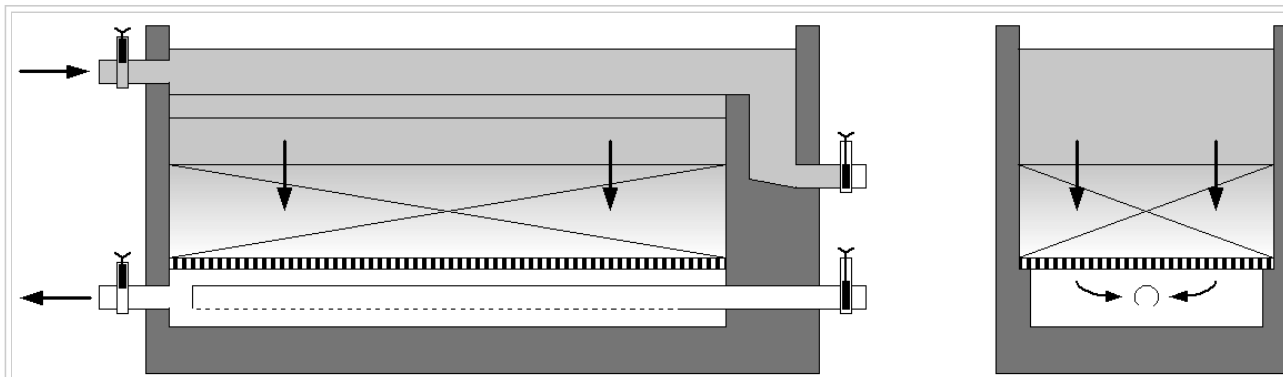


Figure 3.1 - Schematic overview of a filter

The suspended solids slowly fill the pores, resulting in an increase in hydraulic resistance. The suspended solids are removed by periodically cleaning the filter beds. Cleaning the filter beds is done by backwashing, which basically means sending clean water through the filter bed at high velocity, thereby expanding the bed (see Figure 3.2). The dirty water is drained by backwash gutters. The backwash frequency is in the order of days. This prevents the resistance from becoming too high or break through of suspended solids from occurring.

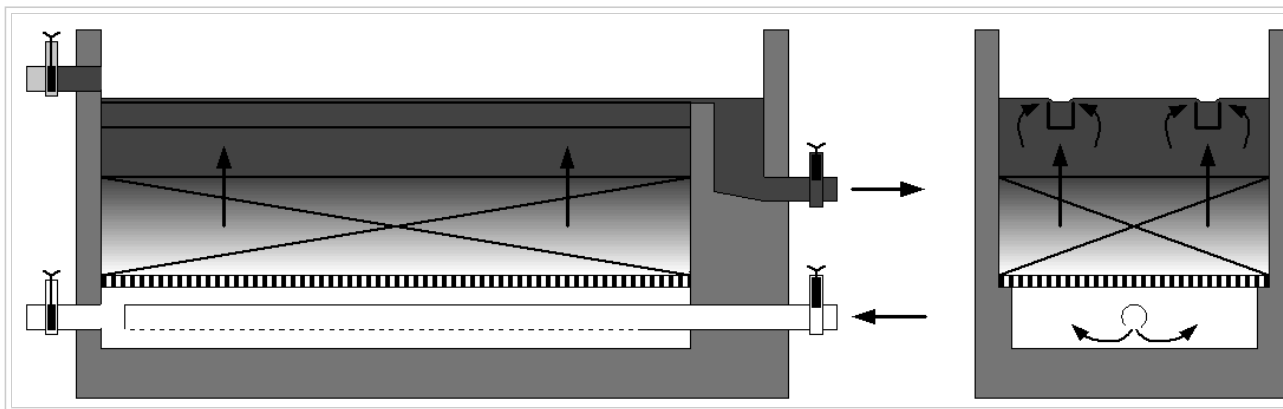


Figure 3.2 - Schematic overview of backwashing a filter

Filters are also used as chemical and biological reactor. This is mainly of importance for the treatment of ground water where the oxidation of iron, manganese, ammonium and, in case of poor aeration, methane takes place. The removal of pathogenic micro-organisms is of importance for surface water treatment and the efficiency is approximately 90 to 99%. The removal of pathogenic micro-organisms occurs by decay and retention on the (sand) grains.

The most common application of filtration is the rapid sand filtration. The characteristics of rapid sand filtration are a bed with a coarse granular media (0.8-1.2 mm) with supernatant water. The filtration velocities (between 5 and 20 m/h) are controlled by varying the supernatant water level (inlet-controlled) or by operating a valve at the outlet pipe (outlet-controlled).

Rapid sand filters are present in nearly every treatment plant. Surface water treatment uses the filters after floc formation and removal to remove the remaining flocs and pathogens and to decompose ammonium. In groundwater treatment the filters are usually placed after aeration to remove iron flocs, manganese and ammonium. Extra filters are frequently placed after pellet reactors to remove the 'carry-over' to avoid contamination of the transport main and the piped network.

When dealing with filtration, the filter material isn't always sand. For the removal of colour, odour, taste and pesticides activated carbon is used. More on this technique can be found in section 3.6.

This chapter deals with the following different forms of filtration (all of which are models included in Stimela):

1. Filtration of suspended solids (Single and Dual Media Filters)
2. Filtration of iron
3. Biological filtration
4. Removal of ammonia through nitrification
5. Granular Activated Carbon filtration

3.2 Single and Dual Media Filter (removal of suspended solids)

3.2.1 Process

Physical filtration is normally installed after floc formation, aeration and/or softening to remove the remaining particles and flocs formed during these processes. Water flows through a (sand) bed while the grains capture the particles and flocs. During the filtration process solids accumulate in the bed and the filtration efficiency is reduced until the filter is clogged (resulting in a too high resistance or inferior product quality). Then the filter is cleaned up by backwashing and the process can be started-up again.

3.2.2 Theory

Single and dual media filters are discussed in the same section because they have the same theoretical background. The difference between a single media and a dual media filter is that in a dual media filter two different filter materials are applied. The materials (often sand and anthracite) are different in particle size and density. The top layer consists of the larger, but less dense, anthracite grains. The bottom layer consists of sand grains with a smaller diameter and a larger density. Because of the double layer, larger particles get stuck in the top layer while smaller particles get caught in the bottom layer. A dual layer filter is less sensitive to clogging than a single media filter. Because the less dense material is on top, there will be no stratification during backwashing which would happen if ordinary large sand grains were used instead of anthracite.

3.2.3 Model

This model only calculates the amount of suspended solids caught by the filter. The finite difference model is a fundamental model that solves the partial differential equations describing the filtration process. The model works by splitting the filter bed into a number of different steps and solving the mass balance, i.e. the amount of solids deposited on the surface of the filtration media and the change in solids concentration of the water within the voids of the bed, for each of these steps.

3.2.3.1 Options for Usage

The models for single and dual layer filtration can be used for the calculation of removal efficiencies of suspended matter, the Lindquist diagram and the variation of the total filter resistance over time.

3.2.3.2 Model Equations

For the removal of solids from the water phase, neglecting dispersion, decay and advection in the solid phase and considering the water velocity in the pores, the overall equations for transport of solids

$$\frac{\partial c}{\partial t} - D_x \frac{\partial^2 c}{\partial x^2} + u \frac{\partial c}{\partial x} + f_1(c) + f_2(c, c_s) = 0$$

$$\frac{\partial c_s}{\partial t} - D_{x,s} \frac{\partial^2 c_s}{\partial x^2} + u_s \frac{\partial c_s}{\partial x} + f_{1,s}(c_s) + f_{2,g}(c, c_s) = 0$$

are reduced to:

$$\frac{\partial c}{\partial t} + \frac{u}{e} \frac{\partial c}{\partial x} + f_2(c, c_s) = 0$$

$$\frac{\partial c_s}{\partial t} + f_{2,s}(c, c_s) = 0$$

For a stationary flow, the mass balance can be written as:

$$\frac{u}{\epsilon} \frac{\partial c}{\partial x} = -f_2(c, c_s)$$

$$\frac{\partial c_s}{\partial t} = -f_{2,s}(c, c_s) = -u \frac{\partial c}{\partial x}$$

$$f_{2,s}(c, c_s) = -\epsilon f_2(c, c_s)$$

Where:

$$f_{2,s}(c, c_s) = -\frac{u}{\epsilon} k_2 c$$

The concentration of the compound in the solid phase is given as mass per volume reactor, whereas water flows with pore velocity u/ϵ (m/s). The transfer rate to the solid phase is therefore lower than the transfer rate from the water. The difference is calculated by multiplication with the porosity ϵ (-).

The filtration rate k_2 is dependent on the clean bed filtration coefficient λ_0 and the concentration of removed solids. Several authors have tried to determine the clean bed filtration rate λ_0 in an empirical way for different circumstances.

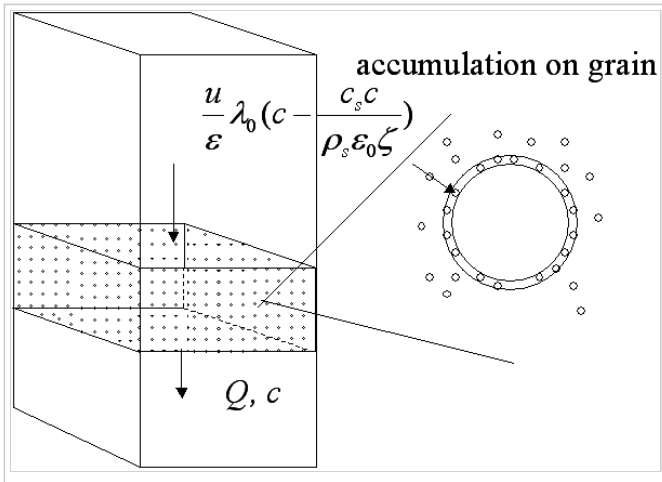


Figure 3.3 - Schematic impression of rapid filter and accumulation

A more scientific approach was first adapted by Yao (1971), who used the theory of floc formation of Von Smoluchowski as a basis to determine λ_0 . Many of the relations between the clean bed filtration rate and the accumulated solids, can be derived from a general equation proposed by Ives (Ives, 1968, Ives, 1975, Amirharajah, 1988):

$$k_2 = \frac{u}{\epsilon} \lambda_0 \left(1 + \frac{c_s}{1 - \epsilon_0} \right)^{b_1} \left(1 - \frac{c_s}{\epsilon_0} \right)^{b_2} \left(1 - \frac{c_s}{c_{s,u}} \right)^{b_3}$$

Where:

$c_{s,u}$ = saturation concentration of solids in filter (g/m^3)

$b_{1,2,3}$ = constants (-)

One of the most commonly used elaborations on this equation is given by Ives (...):

$$k_2 = \frac{u}{e} \lambda_0 \left(1 + n_1 \frac{e_s}{\rho} - \frac{n_2}{e} \left(\frac{e_s}{\rho} \right)^2 \right)$$

Adin and Rebhun found experimentally that the filter headloss could be related to the headloss across a clean filter by the following relationship:

$$H = \frac{H_0}{\left(1 - \sqrt{\sigma/\bar{F}} \right)^3}$$

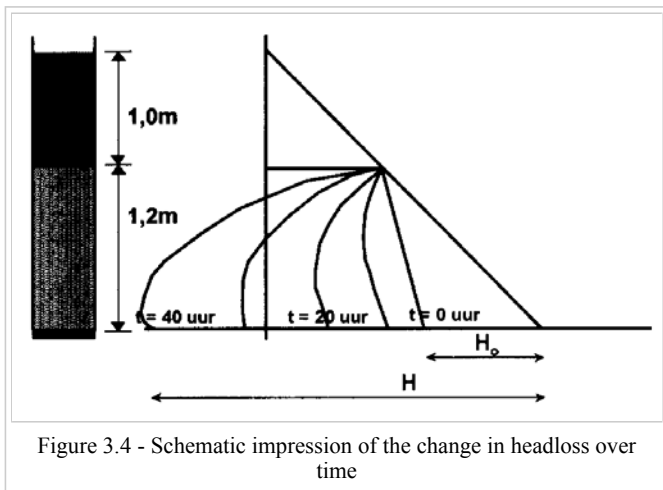
Alternatively the model of Huisman can be used (used in this model):

$$H = H_0 \left(\frac{p_0}{p_0 - \frac{c_0}{\rho}} \right)^2$$

Where:

H_0 = clean bed headloss (m)

In figure 3.4 the progress of the headloss over a clogging bed is shown for time steps of 10 hours.



The clean bed headloss can be estimated from the Carman-Kozeny equation:

$$H_0 = - \frac{v^2 (1 - \epsilon) L}{\Phi 2.16 \cdot 10^6 g d_e e^3} [5 Re_1^{-1} + 0.4 Re_1^{-0.1}]$$

Where:

Re_1 = particle Reynolds number, given by:

$$Re_1 = \frac{v d_e \rho_l \Phi}{21600 (1 - \epsilon) \mu}$$

Where:

d_e = media diameter (m)

g = gravitational constant ($9,81 \text{ m/s}^2$)

H_0 = clean bed headloss (m)

ϵ = voidage (-)

μ = water viscosity (Ns/m^2)

ρ_1 = water density (kg/m^3)

Φ = sphericity of filtration media (-)

v = filtration rate (m/h)

For laminar flow (which is normally present during filtration) the equation can be written as:

$$H_0 = 180 \frac{\mu}{\rho_1 g} \frac{(1 - \epsilon_0)^2}{\epsilon_0^3} \frac{v}{d_e^2} L$$

3.2.3.3 Model Calibration

3.2.3.4 Input and Output

The input of the model can be water quality data from a previous model/treatment step or the raw water input block. On top of that the model parameters have to be entered into the filtration model blocks. The output are the new water quality parameters that have been calculated by the model, which can be displayed as time series in graphs.

Model Parameters

When in Stimela a new project including a dual media filter is created, the model displayed in Figure 3.5 will pop up. In the window are included: a raw water input block, a graphical output block, a dual media filter block and a backwash block. For the latter two, the model parameters have to be changed for each different situation. In Figure 3.6 and 3.7 the model parameters for the two blocks are shown. The model parameter windows pop up when each block is double clicked.

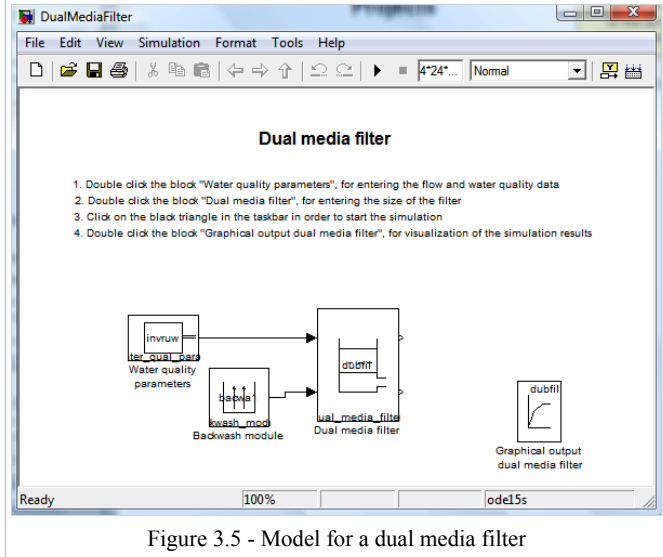


Figure 3.5 - Model for a dual media filter

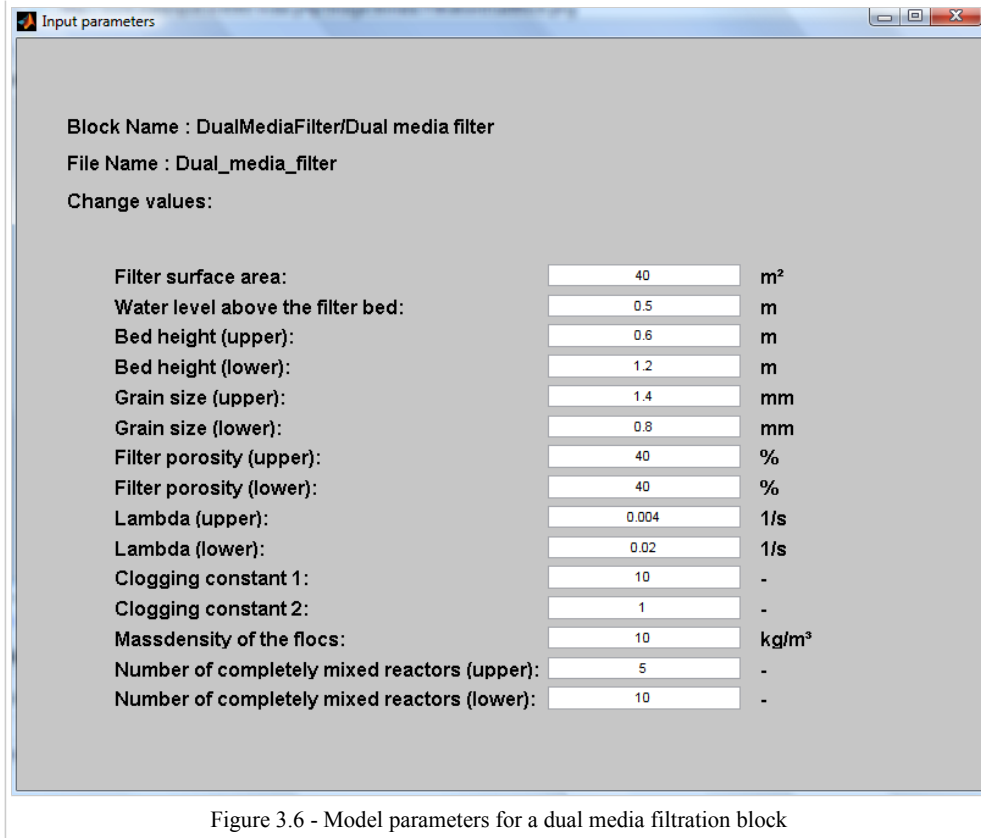


Figure 3.6 - Model parameters for a dual media filtration block

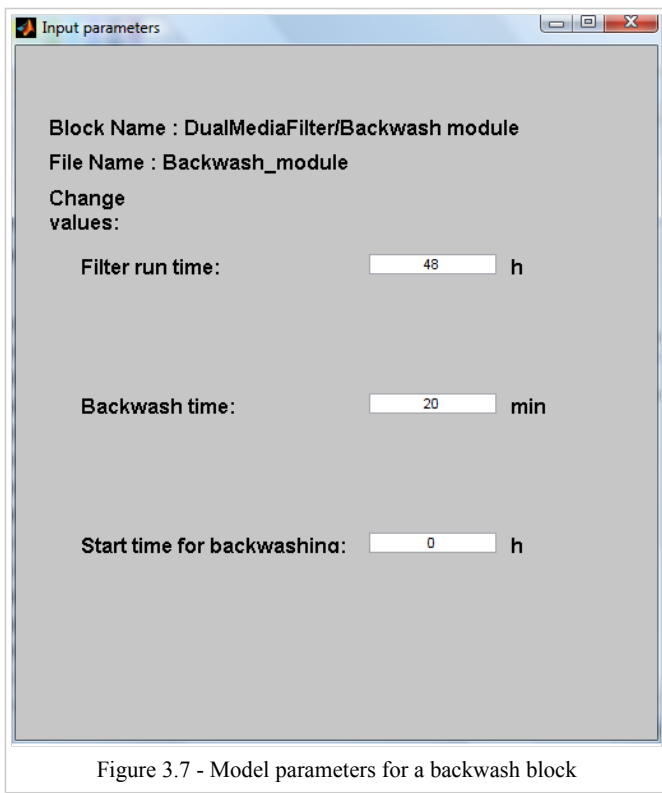


Figure 3.7 - Model parameters for a backwash block

For an explanation of most of the input parameters needs to be referred to the previous section. The ones that haven't been discussed yet are:

Number of CSTRs between sampling: The number of CSTRs determines the rate of plug flow through the filter. In the most extreme case, a flow of water could be completely mixed, or divided into an infinite amount of mixing barrels (CSTRs). When a number like 100 is filled in here, the flow will be almost perfect plug flow. This is not very probable, because there

is always horizontal and vertical mixing going on. The improvement of gas transfer due to the improvement of the plug flow is negligible when the stream is divided into more than 20 completely mixed barrels.

Graphs

When the block for graphical output is clicked, Stimela will first ask for the parameter file of the physical filter for which the output needs to be calculated. Then it will ask for the parameter file of the appropriate backwash module. This is important when there are multiple filters in a project en these have different run times.

The block 'Graphical output dual media filter' will give an output screen with three graphs (see Figure 3.8). On the upper left the graph for the total resistance over time is shown, with underneath it the outgoing concentration of suspended matter over time and on the upper right the Lindquist diagram for the filter. On the bottom right the input parameters are displayed.

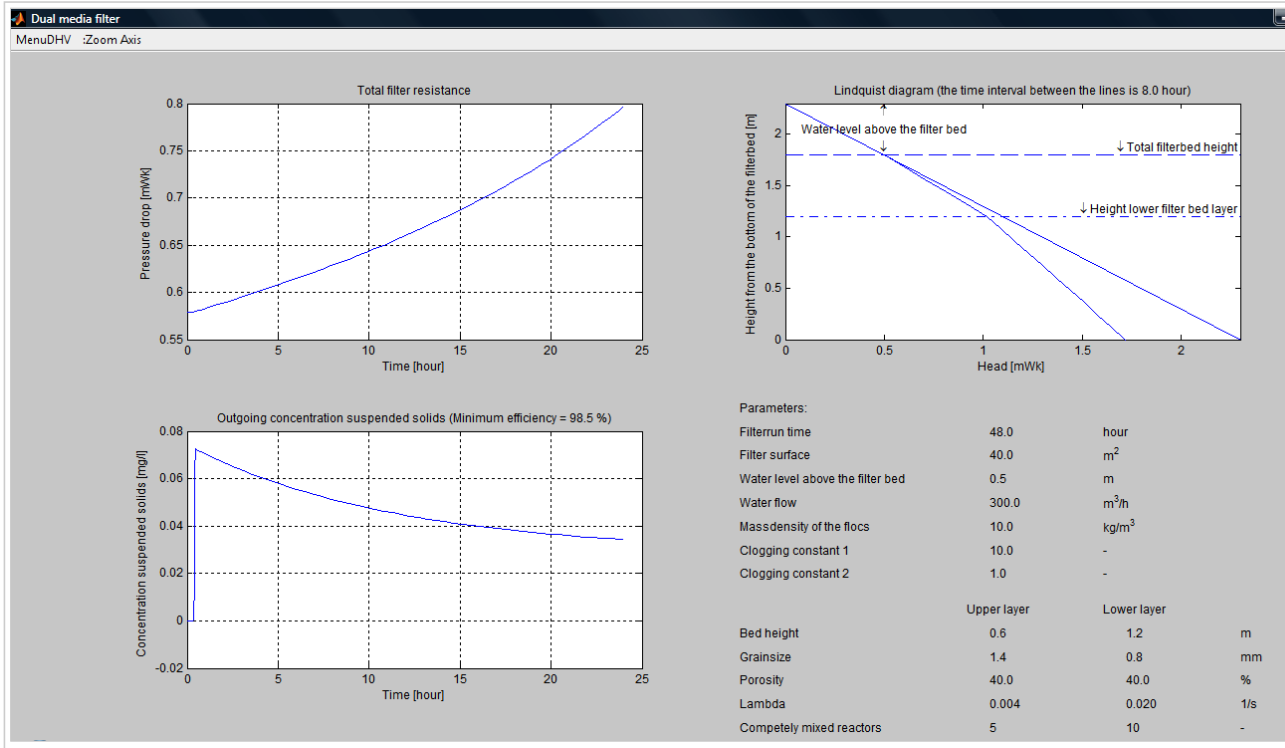


Figure 3.8 - Graphical output for a dual media filter

The block 'Graphical output for single media filter' will give the same kind of output screen as in the case of a dual media filter (see Figure 3.9). In Figure 3.9 it can be seen that the Lindquist diagram and the input parameters are different for the single media filter.

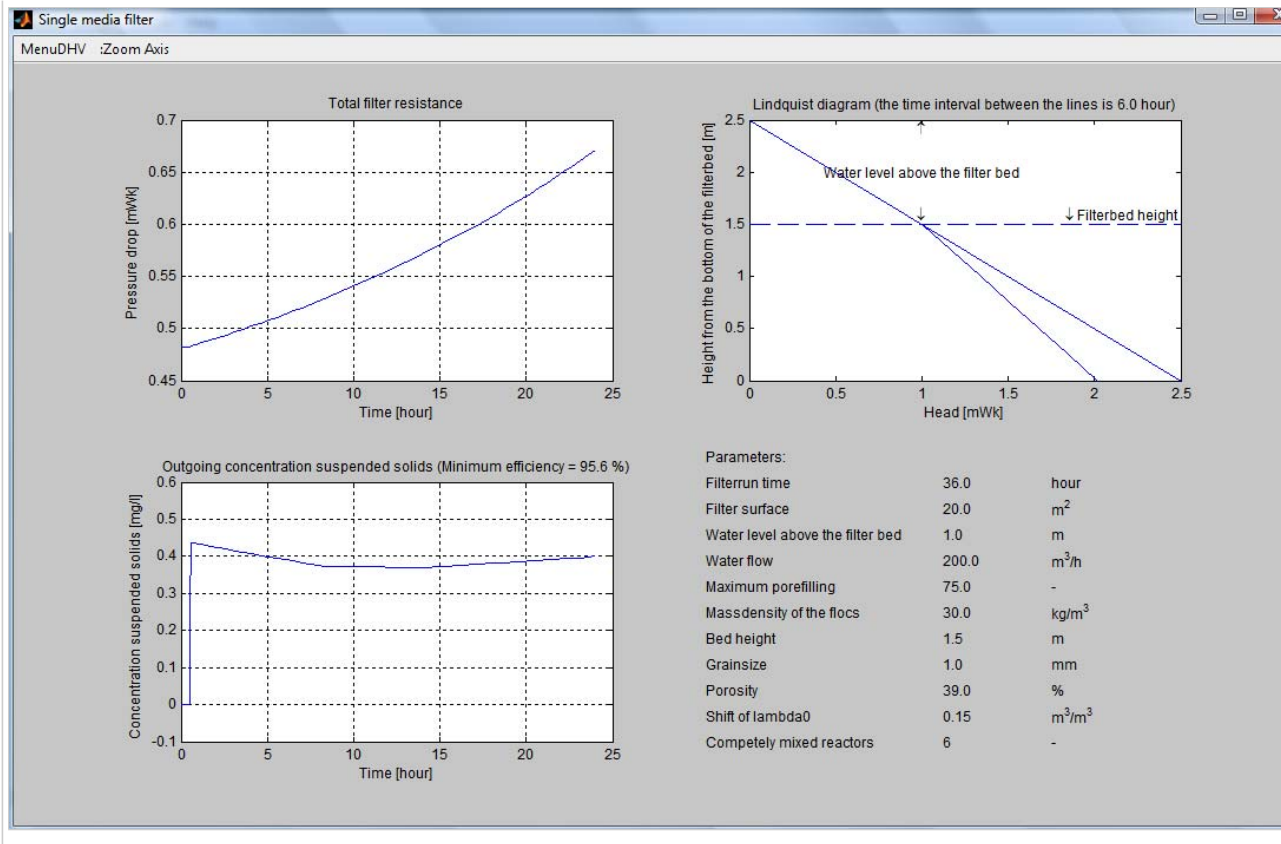


Figure 3.9 - Graphical output for a single media filter

3.3 Biological Filter

3.3.1 Process

Pre-oxidation prior to filtration enhances biological activity resulting in biological filtration. Biodegradation in biofilters removes part of the biodegradable dissolved organic matter (BDOC). This paragraph describes the development of biomass in biofilters, and the corresponding BDOC removal. A biofiltration model was developed for simulation of biomass development and biodegradation of DOC.

3.3.2 Theory

Bacteria fix on the outer surface of the filter material, for example sand and activated carbon grains. Substrate is taken up directly from the water phase and used for growth according to Monod kinetics and for maintenance. The maximum growth rate is a function of temperature and pH. The specific growth rate is a function of maximum growth rate and Monod kinetics depending on the local substrate concentrations in water. Biomass maintenance is linear to the amount of fixed biomass (Schlegel, 1992). Biomass also may release soluble microbial products, which may be a source for biomass development in subsequent layers (Billen et al., 1992, Rittmann et al., 2002).

Biomass increases due to growth and attachment of biomass from the water phase. Especially at low substrate concentrations found in drinking water no true biofilm will develop (Rittmann et al., 1981) and attachment/detachment processes become relevant (Uhl, 2000). From different biological filters used for drinking water production bacteria species have been isolated and studied by Magic-Knezev. Different Polaromonas types were determined as the dominant cultivable species (Magic-Knezev et al., 2006).

3.3.3 Model

In the model the biofilter is divided into a number of completely stirred tank reactors (CSTR's) in series.

Raw water including substrates – biodegradable and non biodegradable dissolved organic carbon (BDOC and NBDOC),

oxygen and phosphate – is led into the biofilter. Through convection and dispersion the substrates are transported through the pores of the filter bed. The flow in the pores is turbulent. The carbon grains are surrounded by a laminar liquid film. Diffusion causes mass transfer through this film from the bulk liquid towards the surface of the grain (Sonneheimer et al., 1988).

Biomass is located on the outer surface of the carbon grain. BDOC, oxygen and phosphate are biodegraded according to Monod kinetics based on the ‘visible’ substrate concentration for the biomass. Suspended biomass, attachment and detachment are neglected. Biomass death rate is linear to the amount of fixed biomass. Dead biomass is assumed to be washed out during backwashing. Biomass maintenance is neglected; all substrate taken up by biomass is converted into biomass.

3.3.3.1 Options for Usage

The model for biological filtration can be used for the calculation of the oxygen demand and the concentration of bacteria (Nitrosomas and Nitrobacter) in the filter layer.

3.3.3.2 Model Equations

Essential in the model is the calculation of the concentration of the substrates at the outer surface of the carbon grain. This is the location of the biomass, and the substrate concentration in the surface layer is the ‘visible’ concentration for the biomass. The dynamically modelled variables are:

$$\frac{\partial c}{\partial t} = -\frac{v}{\epsilon} \frac{\partial c}{\partial x} - \frac{1-\epsilon}{\epsilon} \frac{6}{d_{part}} \frac{D_f}{\delta_f} (c - c_s)$$

$$\frac{dc_s}{dt} = \frac{1}{\delta_s} \frac{D_f}{\delta_f} (c - c_s) - \frac{\mu_{spec}}{Y_{max}} X_s \frac{\rho_{filt} d_{part}}{6\delta_s(1-\epsilon)}$$

$$\frac{dX_s}{dt} = (\mu_{spec} - b) X_s$$

$$\mu_{spec} = \min \left(\left(\frac{c_{s,1}}{K_{M,c1} + c_{s,1}} \alpha_T \mu_{max,15^\circ C} \right) \left(\frac{c_{s,2}}{K_{M,c2} + c_{s,2}} \alpha_T \mu_{max,15^\circ C} \right), etc. \right)$$

Where:

α_T = temperature correction factor [-]

b = death rate biomass [s^{-1}]

c = concentration substrate in bulk liquid [$g C \cdot m^{-3}$]

c_s = concentration substrate in surface liquid film [$g C \cdot m^{-3}$]

d_{part} = particle diameter carbon grains [m]

D_f = diffusion coefficient laminar liquid film [$m^2 \cdot s^{-1}$]

ϵ = filter bed porosity, the ratio of interparticle pore volume to total volume [-]

δ_f = thickness laminar liquid film [m]

δ_s = thickness surface layer[m]

$K_{M,c}$ = Monod constant for substrate c [$g C \cdot m^{-3}$]

μ_{spec} = specific growth rate biomass [s^{-1}]

$\mu_{max,15^\circ C}$ = maximum growth rate biomass at $15^\circ C$ [s^{-1}]

ρ_{filt} = filter density activated carbon [$g \text{ carbon} \cdot m^{-3} \text{ filter}$]

t = time [s]

v = flow velocity, surface load [$\text{m} \cdot \text{s}^{-1}$]

X_s = concentration fixed biomass in surface liquid film [ng ATP•(g carbon) $^{-1}$]

Y_{\max} = maximum yield [ng ATP•(g substrate) $^{-1}$]

In Table 3.1 applied values for some of the above mentioned parameters are summarized along with the references used.

	Applied value	Reference values	Reference
D_f [$\text{m}^2 \cdot \text{s}^{-1}$]	$4.9 \cdot 10^{-10}$	$4 \cdot 10^{-10} - 10 \cdot 10^{-10}$ $12 \cdot 10^{-10}$	Lier, 1989 Hozalski, 1996
K_F [g C•(g carbon) $^{-1}$ •(m 2 •(g C) $^{-1}$) a]	15.6	0 - 80	Sontheimer et al., 1988
n_F [-]	0.78	0.10 - 0.80	Sontheimer et al., 1988
$\mu_{\max,20^\circ\text{C}}$ [s $^{-1}$]	-	$8 \cdot 10^{-5}$	Billen, 1992
$\mu_{\max,15^\circ\text{C}}$ [s $^{-1}$]	$1.9 \cdot 10^{-5}$	$1.9 \cdot 10^{-5}$	Magic-Knezev, 2006
K_{MBDOC} [g C•m $^{-3}$]	$1.5 \cdot 10^{-3}$	$1.5 \cdot 10^{-3}$ $50 \cdot 10^{-3}$	Magic-Knezev, 2006
b [s $^{-1}$]	$0.16 \cdot 10^{-5}$	$2.9 \cdot 10^{-5}$ $0.28 \cdot 10^{-5} - 2.2 \cdot 10^{-5}$	Billen, 1992 Hozalski, 1996
α_T [-]	1.07	-	Billen, 1992
Y_{BDOC} [ng ATP•(g C) $^{-1}$]	$0.8 \cdot 10^{-6}$	-	Magic-Knezev, 2006

Table 3.1 - Model parameter values

Clogging due to biological growth can be modelled in the same way as suspended solids removal. Where c_s is determined by the biological degradable organic matter removal and the overall density of the biomass (which can be far lower than the density of the individual cells).

3.3.3.3 Model Calibration

3.3.3.4 Input and Output

The input of the model can be water quality data from a previous model/treatment step or the raw water input block. On top of that the model parameters have to be entered into the filtration model blocks. The output are the new water quality parameters that have been calculated by the model, which can be displayed as time series in graphs.

Model Parameters

When in Stimela a new project including a biological filter is created, the model displayed in Figure 3.x will pop up. In the window are included: a raw water input block, a graphical output block, a biological filter block and a backwash block. For the latter two, the model parameters have to be changed for each different situation. In Figure 3.x and 3.x the model parameters for the two blocks are shown. The model parameter windows pop up when each block is double clicked.

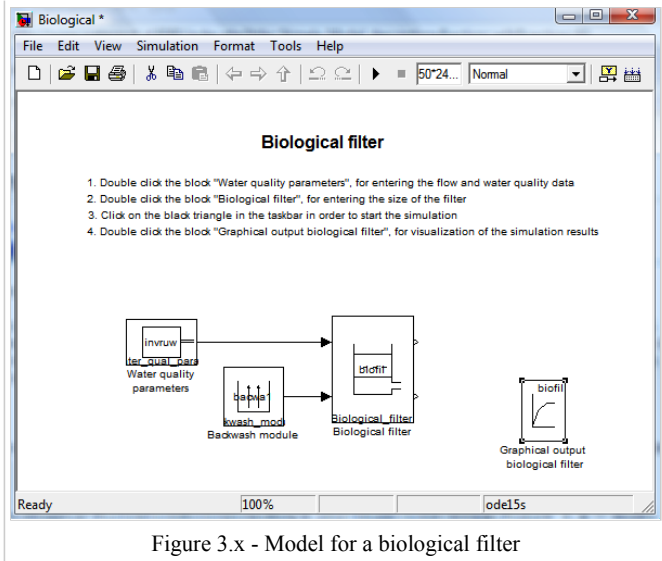


Figure 3.x - Model for a biological filter

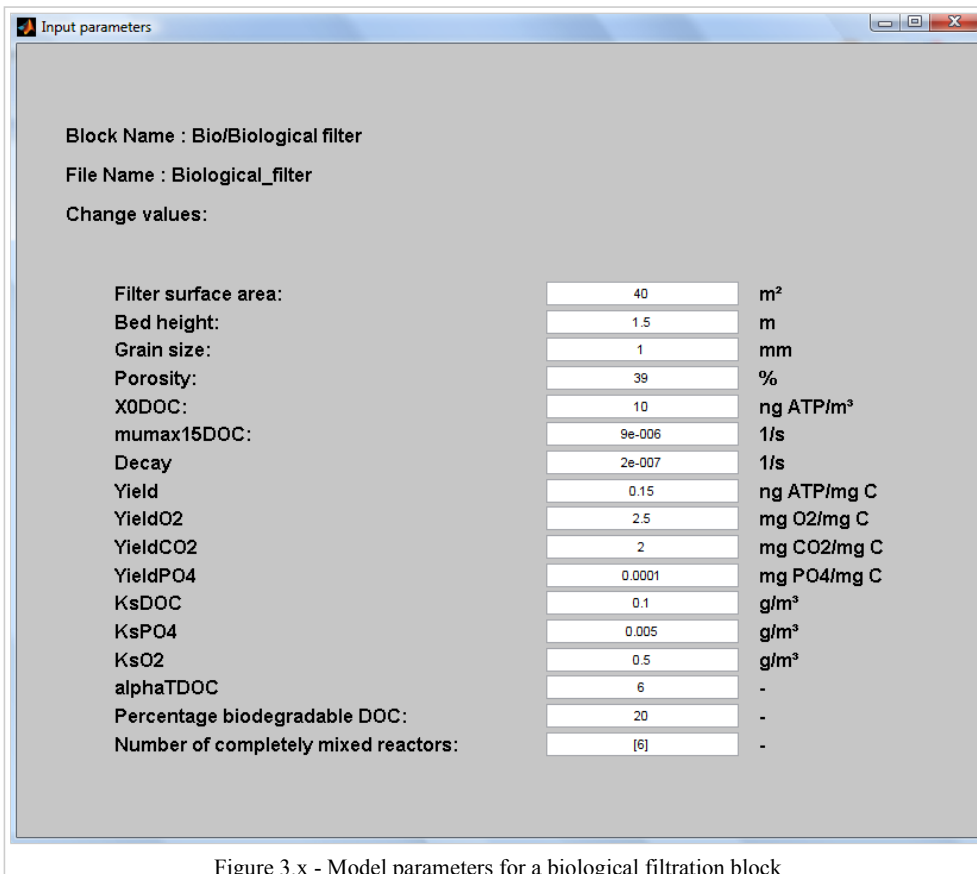


Figure 3.x - Model parameters for a biological filtration block

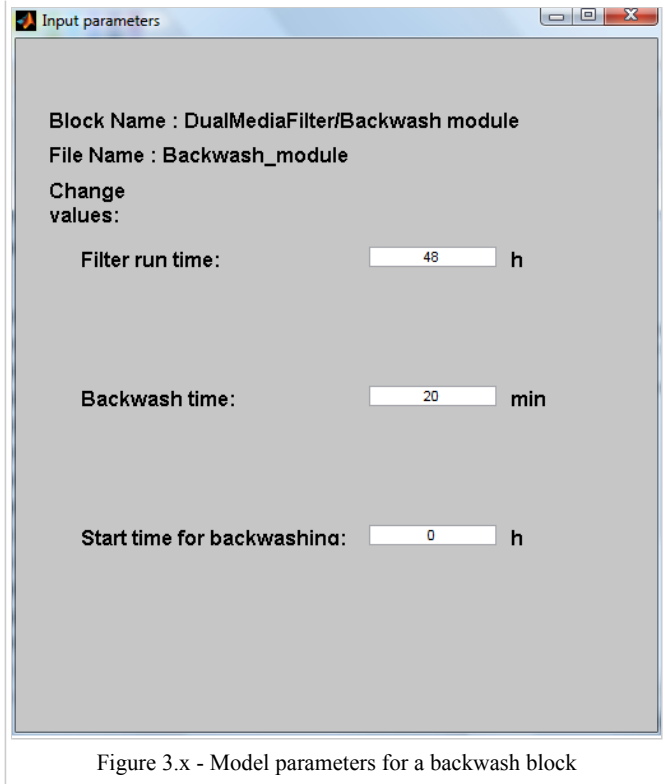


Figure 3.x - Model parameters for a backwash block

For an explanation of most of the input parameters needs to be referred to the previous section on the model equations. The one that hasn't been discussed yet is:

Number of CSTRs between sampling: The number of CSTRs determines the rate of plug flow through the biological filter. In the most extreme case, a flow of water could be completely mixed, or divided into an infinite amount of mixing barrels (CSTRs). When a number like 100 is filled in here, the flow will be almost perfect plug flow. This is not very probable, because there is always horizontal and vertical mixing going on. The improvement of gas transfer due to the improvement of the plug flow is negligible when the stream is divided into more than 20 completely mixed barrels.

Graphs

The block 'Graphical output biological filter' will give an output screen with three graphs (see Figure 3.x). On the upper left the graph for the influent and effluent ammonia and nitrate concentration is shown over time (this model doesn't do anything with these substances), with underneath it the concentration of bacteria in the first filter layer and on the upper right the concentration of the influent and effluent. On the bottom right the input parameters are displayed.

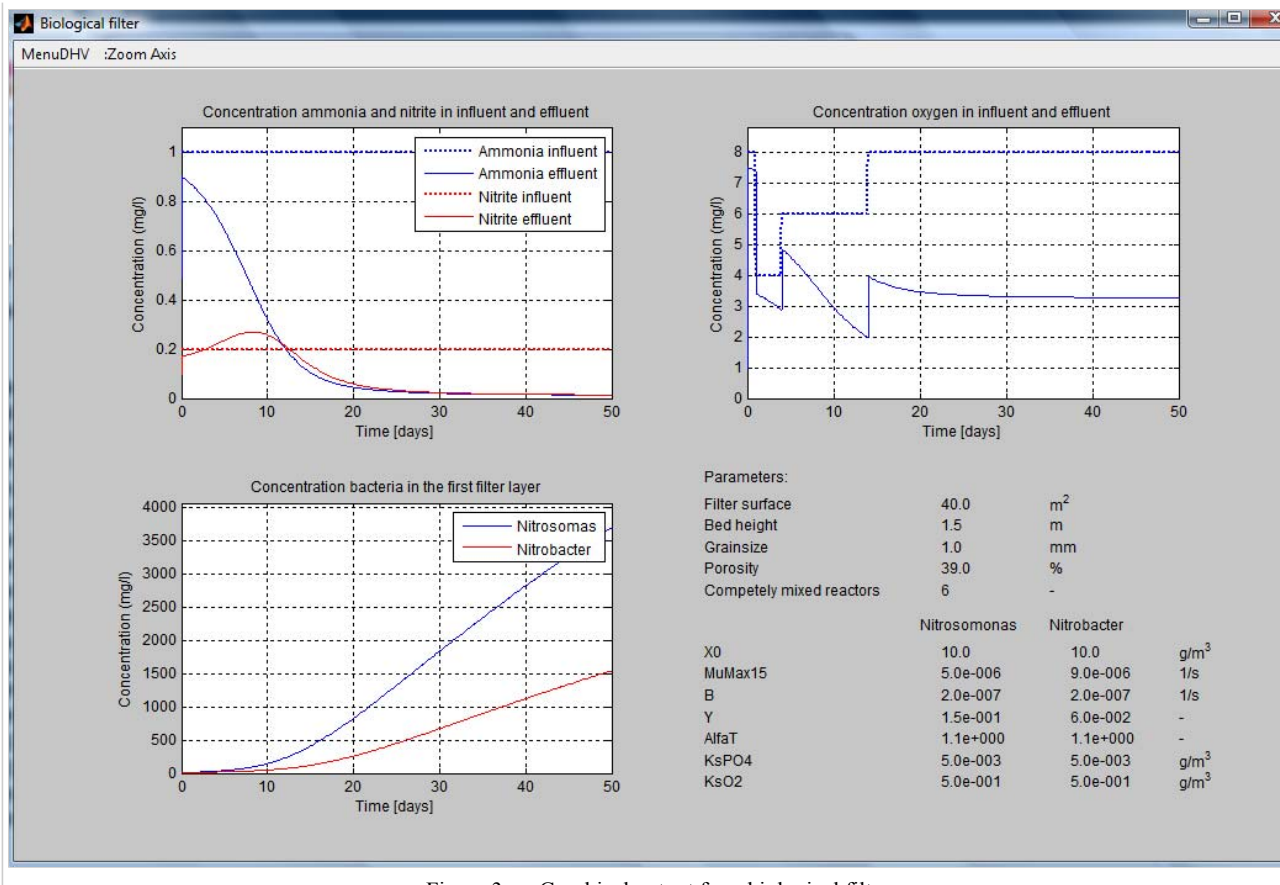


Figure 3.x - Graphical output for a biological filter

3.4 Iron Filter

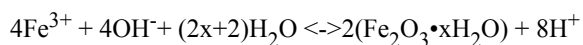
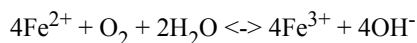
3.4.1 Process

Rapid filtration is also used for the removal of iron. During and before the filtration process iron(II) is oxidized to iron(III) and iron(III)hydroxide flocs are formed. Water flows through a (sand) bed while the grains adsorb iron(II) and capture iron (III) flocs. The solids accumulate in the bed and the filtration efficiency is reduced until the filter is clogged (resulting in a too high resistance or inferior product quality). Then the filter is cleaned up by backwashing and the process can be started-up again. In addition, the adsorbed iron(II) is transformed into iron(III) and an irreversible coating is formed on the grains.

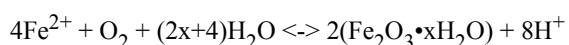
3.4.2 Theory

In the treatment of groundwater with high iron concentrations oxygen is added through aeration, thereby oxidizing Fe^{2+} into Fe^{3+} which is less soluble in water. When H^+ ions are formed hydrolysis occurs, letting the Fe^{3+} form iron hydroxide.

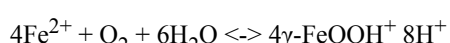
The oxidation and hydrolysis reaction are respectively given by (Lerk 1965):



The overall reaction becomes:



or for the formation of the primary crystal Lepidocrite:



3.4.3 Model

The finite difference model is a fundamental model that solves the partial differential equations describing the iron removal process. The model works by splitting the filter bed into a number of different steps and solving the mass balance, i.e. the amount of iron adsorbed and deposited on the surface of the filtration media and the change in iron concentration of the water within the voids of the bed, for each of these steps.

3.4.3.1 Options for Usage

3.4.3.2 Model Equations

For the removal of iron from the water phase, neglecting dispersion, decay and advection in the solid phase and considering the water velocity in the pores, the overall equations for transport, transformation and accumulation of iron:

$$\begin{aligned} \frac{\partial c_{Fe(II)}}{\partial t} + \frac{u}{\epsilon} \frac{\partial c_{Fe(II)}}{\partial x} + \frac{\rho_{Fe}}{\epsilon} \frac{\partial q_{Fe(II)}}{\partial t} + K_{Fe} \left(\frac{c_{Fe}}{56} \right)^2 \frac{c_{O_2}}{32} \dots &= 0 \\ \frac{\partial q_{Fe(II)}}{\partial t} - k(Kc^n - q) &= 0 \\ \frac{\partial c_{Fe(III)}}{\partial t} + \frac{u}{\epsilon} \frac{\partial c_{Fe(III)}}{\partial x} + \frac{u}{\epsilon} \lambda_0 \left(1 - \frac{\sigma}{\epsilon_0 \rho_s \xi} \right) c_{Fe(III)} - K_{Fe} \left(\frac{c_{Fe}}{56} \right)^2 \frac{c_{O_2}}{32} \dots &= 0 \\ \frac{\partial \sigma}{\partial t} - u \lambda_0 \left(1 - \frac{\sigma}{\epsilon_0 \rho_s \xi} \right) c_{Fe(III)} &= 0 \\ \frac{\partial c_{O_2}}{\partial t} + \frac{u}{\epsilon} \frac{\partial c_{O_2}}{\partial x} + \frac{32}{224} K_{Fe} \left(\frac{c_{Fe}}{56} \right)^2 \frac{c_{O_2}}{32} \dots &= 0 \\ \frac{\partial c_{HCO_3}}{\partial t} + \frac{u}{\epsilon} \frac{\partial c_{HCO_3}}{\partial x} + \frac{8 * 61}{224} K_{Fe} \left(\frac{c_{Fe}}{56} \right)^2 \frac{c_{O_2}}{32} \dots &= 0 \\ \frac{\partial c_{CO_2}}{\partial t} + \frac{u}{\epsilon} \frac{\partial c_{CO_2}}{\partial x} + \frac{8 * 61}{224} K_{Fe} \left(\frac{c_{Fe}}{56} \right)^2 \frac{c_{O_2}}{32} \dots &= 0 \end{aligned}$$

The transformation of iron(II) to iron(III) is depending on the rate constant, the concentration of iron(II) and oxygen and the pH. During the transformation oxygen and bicarbonate are consumed and carbon dioxide is produced. The filtration rate of iron(III) is depending on the clean bed filtration coefficient λ_0 and the concentration of removed iron flocs. In addition, the other parameters, such as adsorption rate, equilibrium constants, floc density, and maximum pore filling have to be determined. Floc formation as such is not part of the present model.

The model of Huisman can be used for the determination of the head loss due to accumulation of iron flocs:

$$H = H_0 \left(\frac{p_0}{p_0 - \frac{c_s}{\rho}} \right)$$

Where:

H_0 = clean bed loss (m)

The clean bed headloss can be estimated from the Carman-Kozeny equation:

$$H_0 = - \frac{v^2 (1 - e) L}{\Phi 2.16 \cdot 10^6 g d_c \epsilon^3} [5 Re_1^{-1} + 0.4 Re_1^{-0.1}]$$

Where:

Re_1 = particle Reynolds number, given by:

$$Re_1 = \frac{vd_e\rho_l\Phi}{21600(1-\epsilon)\mu}$$

Where:

d_e = media diameter (m)

g = gravitational constant (9,81 m/s²)

H_0 = clean bed headloss (m)

ϵ = voidage (-)

μ = water viscosity (Ns/m²)

ρ_1 = water density (kg/m³)

Φ = sphericity of filtration media (-)

v = filtration rate (m/h)

To be able to determine the growth grains due to irreversible adsorption of iron the following equation can be used:

$$N = \frac{6V(1-\epsilon)}{\pi d_0^3}$$

$$V_{Fe} = \frac{q\rho_g}{\rho_{Fe}} = N \frac{\pi}{6} (d^3 - d_0^3) = V(1-\epsilon) \left(\frac{d^3}{d_0^3} - 1 \right)$$

$$d = \sqrt[3]{d_0^3 \left(\frac{q\rho_g}{V(1-\epsilon)\rho_{Fe}} + 1 \right)}$$

3.4.3.3 Model Calibration

3.4.3.4 Input and Output

The input of the model can be water quality data from a previous model/treatment step or the raw water input block. On top of that the model parameters have to be entered into the filtration model blocks. The output are the new water quality parameters that have been calculated by the model, which can be displayed as time series in graphs.

Model Parameters

When in Stimela a new project including an iron filter is created, the model displayed in Figure 3.x will pop up. In the window are included: a raw water input block, a graphical output block, two iron filter blocks and a backwash block. For the latter three, the model parameters have to be changed for each different situation. There are two iron filter blocks, because one is used as a contact chamber for the transition of iron(II) to iron(III) and floc formation. Therefore the porosity in the first iron filter block is 100%. What needs to be changed in the first filter are the Lambda, the transformation coefficient and the Freundlich constants for iron(II). In Figure 3.x and 3.x the model parameters for the backwash and iron filter blocks are shown. The model parameter windows pop up when each block is double clicked.

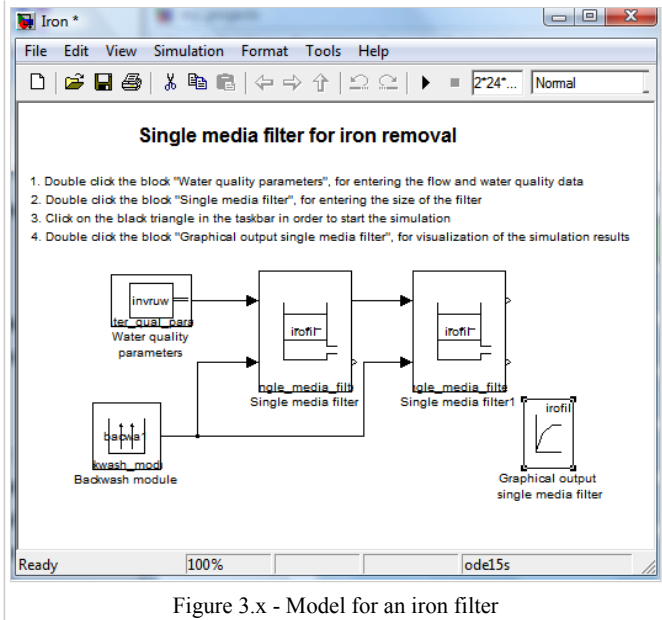


Figure 3.x - Model for an iron filter

Block Name : Iron/Single media filter
File Name : Single_media_filter
Change values:

Filter surface area:	[20]	m ²
Water level above the filter bed:	[0]	m
Bed height:	[1.5]	m
Grainsize:	[10]	mm
Filter porosity:	[100]	%
Maximum porefilling:	[75]	%
Massdensity of the flocs:	[30]	kg/m ³
Number of completely mixed reactors:	[6]	-
Lambda Iron3:	[0.01]	m ⁻¹
Transformation coefficient iron:	[5e-15]	-
Freundlich constant Iron2 K:	[0]	-
Freundlich constant Iron2 n:	[1]	-
Kinetic constant adsorption Iron2:	[1]	-
Massdensity of the filter grains:	[500]	kg/m ³

Figure 3.x - Model parameters for an iron filtration block

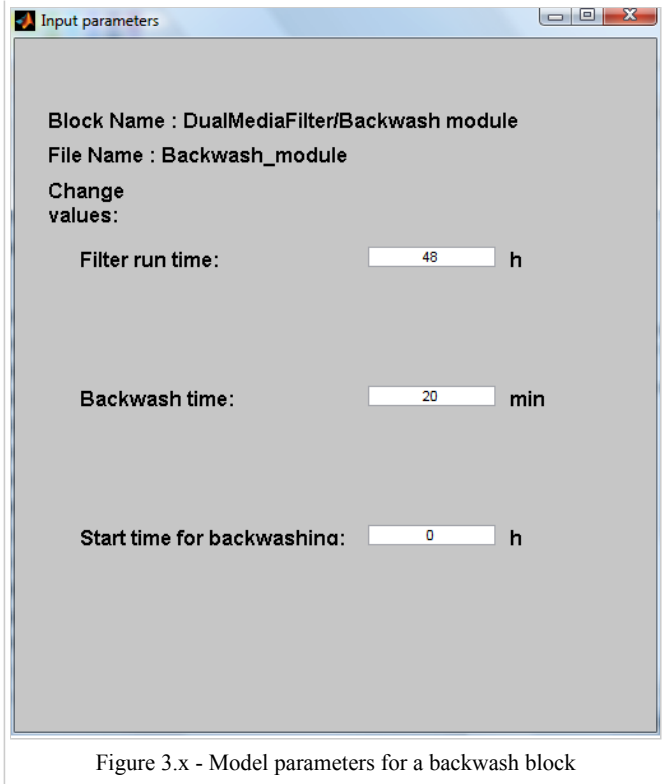


Figure 3.x - Model parameters for a backwash block

For an explanation of most of the input parameters needs to be referred to the previous section on the model equations. The one that hasn't been discussed yet is:

Number of CSTRs between sampling: The number of CSTRs determines the rate of plug flow through the iron filter. In the most extreme case, a flow of water could be completely mixed, or divided into an infinite amount of mixing barrels (CSTRs). When a number like 100 is filled in here, the flow will be almost perfect plug flow. This is not very probable, because there is always horizontal and vertical mixing going on. The improvement of gas transfer due to the improvement of the plug flow is negligible when the stream is divided into more than 20 completely mixed barrels.

Graphs

The block 'Graphical output iron filter' will give an output screen with three graphs (see Figure 3.x).

Image:Stimela-FiltrationIronOutput.png
Figure 3.x - Graphical output for a dual media filter

3.5 Nitrification

3.5.1 Process

Nitrite is toxic to human at low concentrations. It causes oxidation of haemoglobin, which diminishes the oxygen transport capacity of blood. According to the Dutch drinking water standards nitrite concentrations are not allowed to exceed 0.1 mg NO₂⁻ per litre. Nitrite is an intermittent product of the nitrification process. Nitrification is a series of two microbial processes. These processes are described by the Equations displayed below.



When ammonia is present in drinking water nitroso-bacteria can develop in the distribution system and nitrite can be formed. Nitro-bacteria only will develop after this nitrite is produced. In the mean time nitrite concentrations might exceed drinking water standards. Therefore the presence of ammonia in drinking water is considered to be a potential health risk. According to the Dutch drinking water standards ammonium concentrations are not allowed to exceed 0.21 mg NH₄⁺ per litre (= 0.16 mg NH₄⁺-N per litre).

3.5.2 Theory

3.5.3 Model

3.5.3.1 Options for Usage

The model for biological filtration can be used for the calculation of removal efficiencies of ammonia and nitrate and the oxygen demand.

3.5.3.2 Model Equations

To predict nitrification in RSF a dynamic simulation model has been developed according to Rittmann and McCarty (1981). The RSF is modelled as a series of completely mixed layers of filter material. The number of layers determines the amount of dispersion in the filters. The nitrifying bacteria are supposed to be immobilized in a biofilm attached to the filter material. The sizes of the nitrifying populations depend on the history of the filter. Substrate conversion can be described theoretically by the Michaelis-Menten equation:

$$r_S^{spec} = \frac{[S]}{K_m + [S]} r_S^{max}$$

In a substrate-rich environment the substrate conversion is not limited by the substrate concentration; the term S/(K_m+S) will almost be equal to 1. The substrate conversion is proportional to the amount of active enzymes. This is incorporated in r_s max. When the substrate concentration is low (magnitude of the affinity-value) the term S/(K_m+S) will be smaller than 1 and substrate: conversion will be limited by the substrate concentration.

If substrate conversion for maintenance of the bacteria is neglected, all substrate is used for growth. In that case the growth rate of the bacteria can be described by a Michaelis- Menten-like equation. Monod discovered this empirically:

$$r_S^{pot} = \frac{[S]}{K_s + [S]} \mu^{max}$$

In fact the Michaelis-Menten constant and the Monod constant are equal; they are both indicated by the term affinity-value.

Bacteria need different substrates for growth. They will take up specific substrates in a more or less fixed ratio. When the conversion of substrate S₁ is relatively large compared to the conversion of substrate S₂, substrate S₂ will be completely converted and substrate S₁ will accumulate inside the cell. This accumulation will cause a reduction of the conversion of S₁ (in fact the conversion is an equilibrium reaction, the reaction will start to run "backwards") until the uptake of S₁ is in balance with the uptake of S₂.

Usually only one substrate will be converted "completely": this is the limiting substrate. To determine which substrate is limiting for bacteria growth, for each relevant substrate the potential growth rates based on that substrate are calculated. The real growth rate is equal to the smallest potential growth rate:

$$\mu^{spec} = min(\mu_{S_1}^{pot}, \mu_{S_2}^{pot}, \dots)$$

The real conversions are calculated by:

$$r_s = -\mu^{spec} \frac{[X]}{Y_S}$$

Of course substrate conversion never is unlimited. In case of complete nitrification the ammonium, respectively nitrite concentration is the limiting substrates for the nitroso, respectively nitro-bacteria.

The nitrification rate is described by Michaelis-Menten- or Monod-like equations based on substrate concentrations inside the biofilm. The substrate concentrations inside the biofilm depend on substrate concentrations in the bulk solution and diffusion rates in the laminent layer and biofilm. Diffusion rates through the laminent layer depend on the thickness of the layer and the diffusion coefficient. The layer thickness is calculated with Sherwood, Reynolds and Schmidt numbers (equations not shown).

For each layer in the model mass balances for all relevant substrates are set up: ammonium, nitrite, oxygen, phosphate, carbon dioxide and hydrogen carbonate. Because the concentrations influence the growth rate and the substrate conversion, and the substrate conversion influences the concentrations, both concentrations and growth rates are calculated implicit from the mass balances.

$$\frac{d[S]_b}{dt} = \frac{v_{real}}{dL} ([S]_{b,infl} - [S]_b) + r_S$$

The conversion rates r_S cannot be solved analytically; they are approximated by (Loosdrecht, 1993):

$$r_S^{Monod} = \left(\frac{|S_b|}{|S_b| + K_S} r_S^{0th} + \left(1 - \frac{|S_b|}{|S_b| + K_S} \right) r_S^{1st} \right) \cdot \frac{1}{2}$$

All factors can be calculated by the following equations:

$$\begin{aligned} r_S^{0th} &= -q_S^{max} \cdot X_{bf} \cdot \delta_{bf} \cdot A_{spec} = -q_S^{max} \cdot X \\ r_S^{1st} &= -q_S^{max} \cdot X \cdot \epsilon \frac{D_{x,S,vf} \cdot |S_b| \cdot A_{spec}}{D_{x,S,vf} \cdot K_S \cdot A_{spec} + q_S^{max} \cdot X \delta_{bf} \cdot \epsilon} \\ q_S^{max} &= \frac{\mu_{max} \cdot \alpha_T \cdot \alpha_{pH}}{Y_S} \end{aligned}$$

The influence of the diffusion from the bulk liquid into the biofilm is incorporated by the effectivity factor:

$$\begin{aligned} \epsilon &= \frac{\tanh \theta}{\theta} \\ \theta &= \sqrt{\frac{q_S^{max} \cdot X_{bf} \cdot \delta_{bf}}{K_S \cdot D_{x,S,bf}}} = \sqrt{\frac{q_S^{max} \cdot X}{K_S \cdot D_{x,S,bf} \cdot A_{spec}}} \end{aligned}$$

With the calculated growth rates mass balances for nitroso- and nitro-bacteria are determined. Convective transport of bacteria is neglected:

$$\frac{d[X]}{dt} = \mu^{spec} \cdot [X] - b \cdot [X]$$

3.5.3.3 Model Calibration

All relevant model parameters were collected from literature, measurements in the production plant and pilot experiments (Table 3.x).

	minimum	most likely	maximum	calibration
Occ. [%]	1	10	100	10
$\mu_{15^\circ\text{C},\text{Nitroso}}^{\max} [\text{s}^{-1}]$	1.7×10^{-5}	3.7×10^{-5}	7.9×10^{-5}	12×10^{-5}
$\alpha_{\text{T},\text{Nitroso}}$ [-]	1.08	1.10	1.12	1.10
$K_{\text{PO}_4,\text{Nitroso}} [\text{mg PO}_4^{3-}\text{-P.l}^{-1}]$	0.001	0.02	0.11	0.005
$Y_{\text{NH}_4,\text{Nitroso}}^{\max} [\text{g dw.g}^{-1} \text{PO}_4^{3-}\text{-P}]$	0.04	0.12	0.17	0.10
$b_{\text{Nitroso}} [\text{s}^{-1}]$	0.46×10^{-6}	1×10^{-6}	4×10^{-6}	0.5×10^{-6}

Table 3.x - Calibration parameters

The model was calibrated on ammonium conversion by nitroso-bacteria only. Nitrite conversion is almost always complete. Only during start-up of filters nitrite temporary may break through. For calibration the run from the pilot RSF after dynamic sand filtration was used. Except for the maximum growth rate at 15°C all calibration parameters are between maximum and minimum values. After calibration the model was validated on the run from the pilot RSF after ultrafiltration. The results of the validation are shown in Figure 3.x (left figure).

A tool has been developed to display the potential growth rates of the nitrifying bacteria. The graph immediately shows which substrate is limiting nitrification. As an example Figure 3.x (right figure) shows the potential growth rates in the top layer of the RSF after dynamic sand filtration. During the first 130 days nitrification is not complete. Nitrification is limited by the phosphate concentration. On day 130 the dosing of 10 µg PO₄³⁻-P per litre was started.

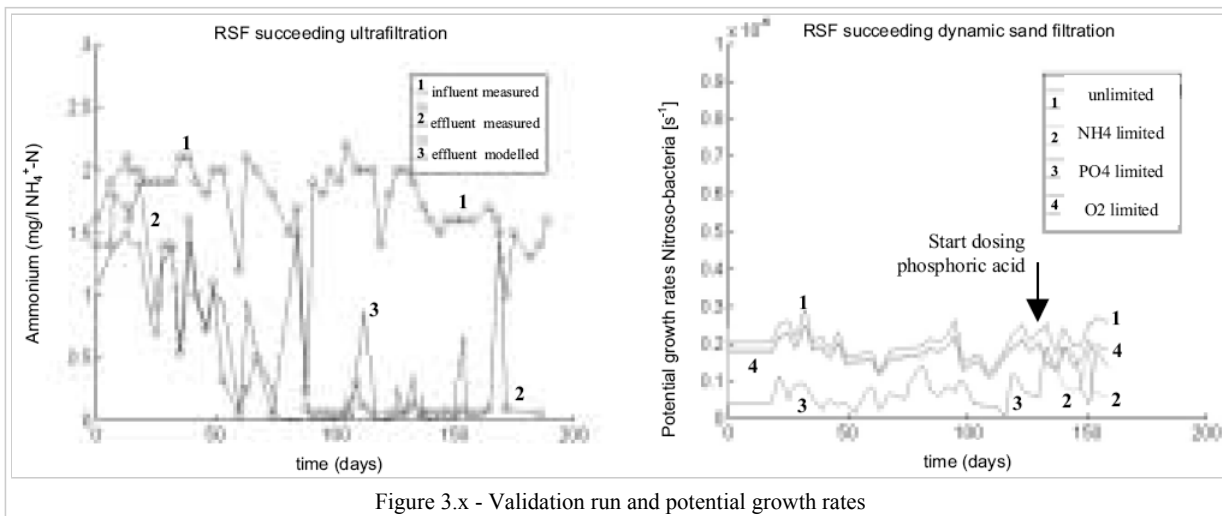


Figure 3.x - Validation run and potential growth rates

Figure 3.x shows indeed that the first 130 days the potential growth rate based on phosphate is limiting (= smallest) potential growth rate. After the dosing started the potential growth rated based on phosphate increases. At day 140 nitrification is complete and ammonium becomes the limiting substrate.

3.5.3.4 Input and Output

The input of the model can be water quality data from a previous model/treatment step or the raw water input block. On top of that the model parameters have to be entered into the filtration model blocks. The output are the new water quality parameters that have been calculated by the model, which can be displayed as time series in graphs.

Model Parameters

When in Stimela a new project including a biological filter is created, the model displayed in Figure 3.x will pop up. In the window are included: a raw water input block, a graphical output block, a nitrification filter block and a backwash block. For the latter two, the model parameters have to be changed for each different situation. In Figure 3.x and 3.x the model parameters for the two blocks are shown. The model parameter windows pop up when each block is double clicked.

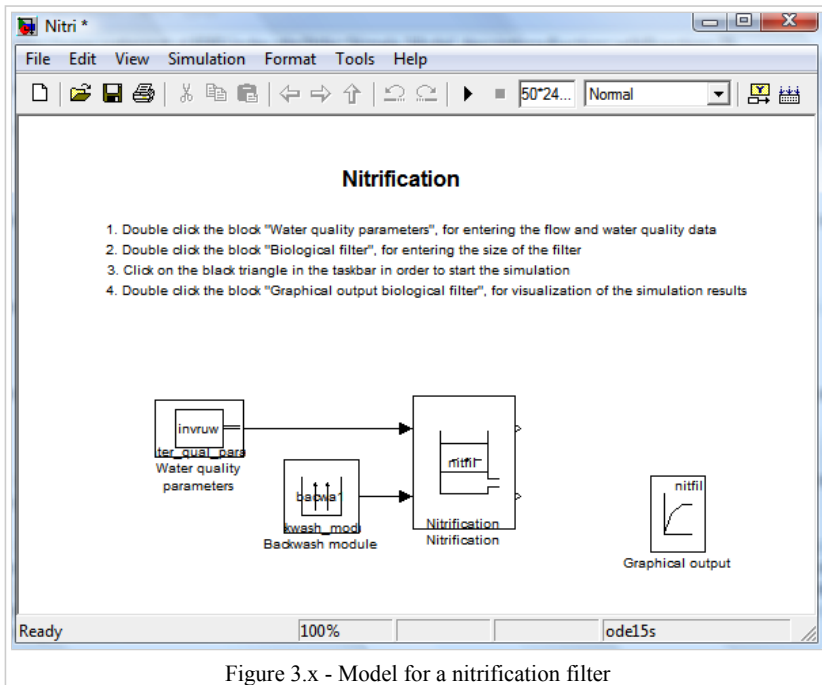


Figure 3.x - Model for a nitrification filter

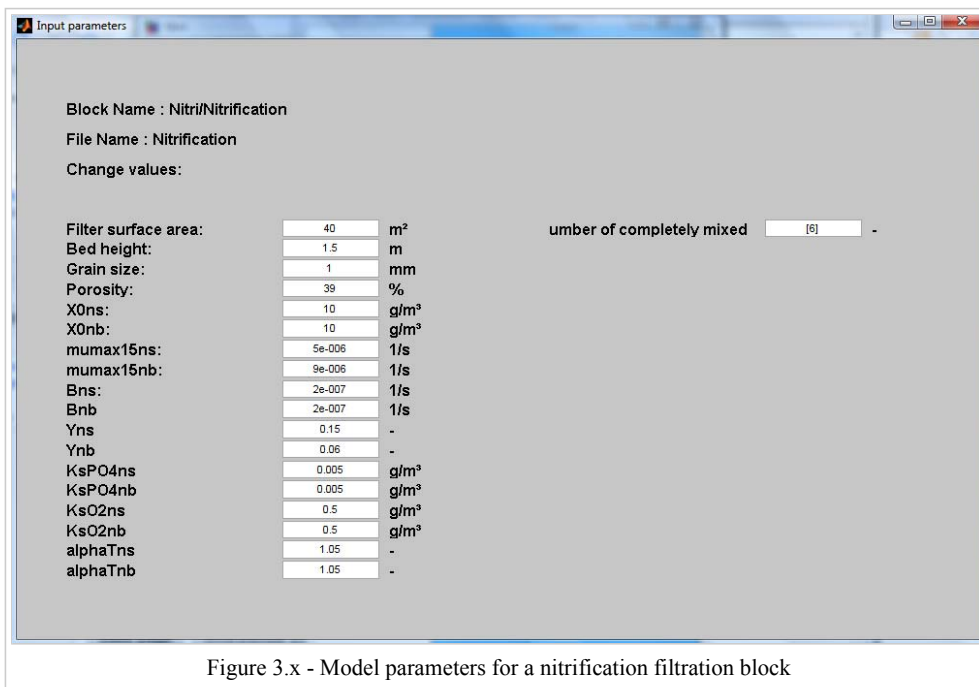


Figure 3.x - Model parameters for a nitrification filtration block

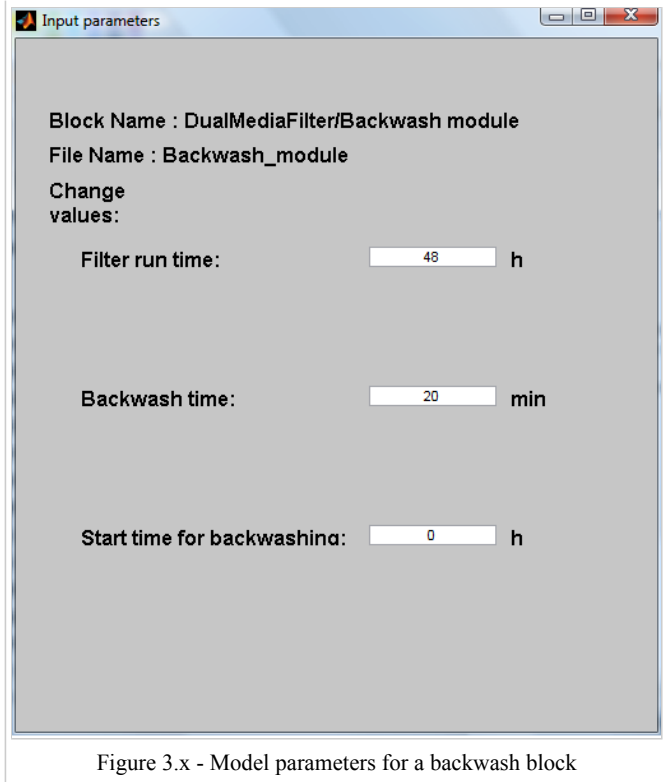


Figure 3.x - Model parameters for a backwash block

For an explanation of most of the input parameters needs to be referred to the previous section on the model equations. The one that hasn't been discussed yet is:

Number of CSTRs between sampling: The number of CSTRs determines the rate of plug flow through the nitrification filter. In the most extreme case, a flow of water could be completely mixed, or divided into an infinite amount of mixing barrels (CSTRs). When a number like 100 is filled in here, the flow will be almost perfect plug flow. This is not very probable, because there is always horizontal and vertical mixing going on. The improvement of gas transfer due to the improvement of the plug flow is negligible when the stream is divided into more than 20 completely mixed barrels.

Graphs

The block 'Graphical output NitFil' will give an output screen with three graphs (see Figure 3.x). On the upper left the graph for the influent and effluent ammonia and nitrate concentration is shown over time, with underneath it the concentration of bacteria in the first filter layer (this model doesn't do anything with this graph) and on the upper right the concentration of the influent and effluent. On the bottom right the input parameters are displayed.

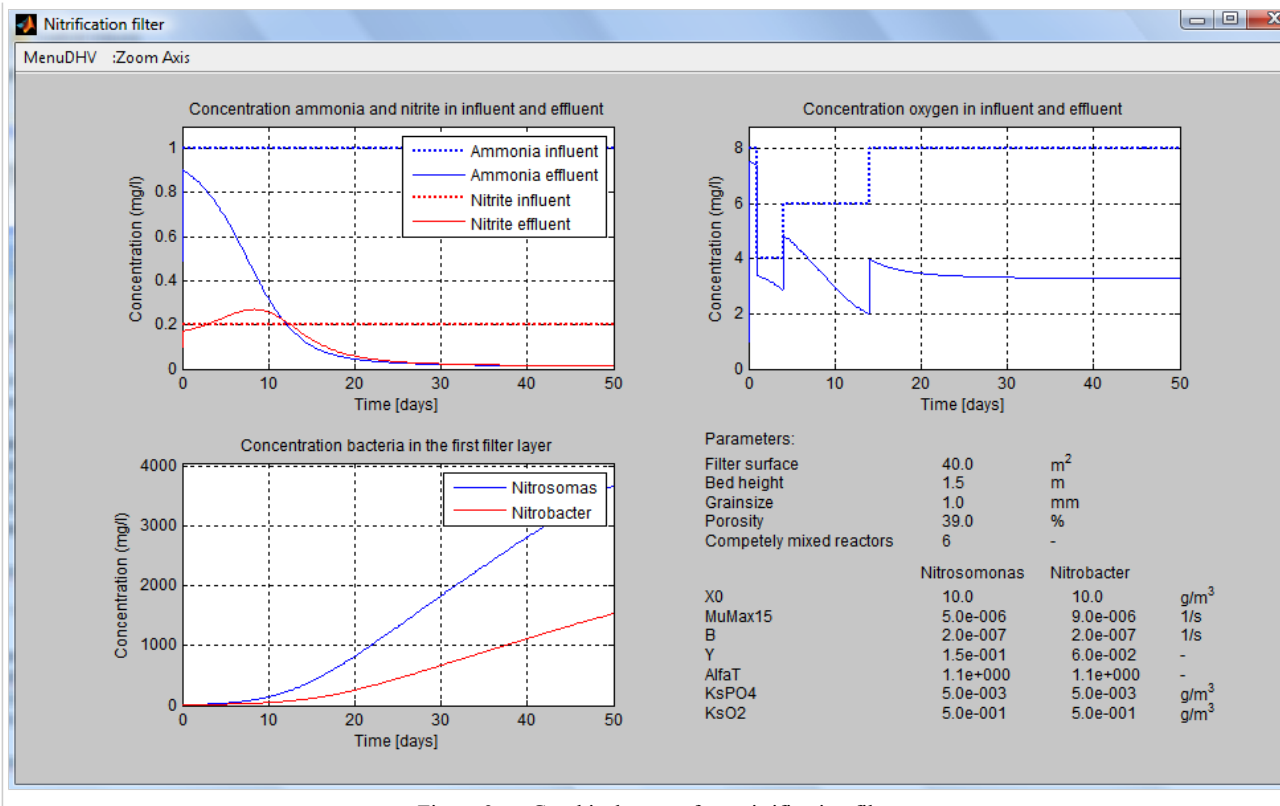


Figure 3.x - Graphical output for a nitrification filter

3.6 Activated Carbon Filter

Activated carbon filters are applied for the removal of constituents in water, that cannot be removed with rapid sand filtration. These substances are organic substances like:

- Odour and taste
- Colour
- Pesticides (like atrazine, diuron)

Activated carbon removes (part of) the present organic substances. Among these are humic acids that give the water colour and a fusty taste. After activated carbon filtration the water is more suitable for consumption. Organic micro pollutants like pesticides can have toxic effect and therefore have to be removed for obvious reasons. Adsorption by activated carbon is therefore an important step in the treatment process.

3.6.1 Process

Activated carbon is a substance with a high carbon content (like charcoal). When exposed to high temperatures, the material will partly be converted to carbon monoxide and water, therefore giving the carbon a more open structure. The internal surface of the activated carbon is much bigger than the external surface, so that the majority of the adsorbed substances are within the granular carbon itself. Not always does the carbon need to be granular. It can be found in powdered form as well (PAD).

Organic substances diffuse from the water phase onto the surface of the carbon grains, after which the organic substances are transported deeper into the carbon structure, to eventually settle in the pores. The adsorption of organics is not infinite. An equilibrium between the constituents present in the water and the amount of dissolved substances adsorbed by the carbon is found after a certain run time. When there are multiple organic substances in the water, competition between them will occur. Well adsorbed substances will take places inside the pores that will not be available for other substances after that. Larger organic molecules can block micro pores as well, therefore leaving less place for smaller molecules. After a while the activated carbon will be saturated and needs to be cleaned out. This happens by getting the carbon out of the installation and heating it up to a 1000 °C. This regeneration process has to be performed about once a year.

Activated carbon filtration is mainly applied in the treatment of surface water. In the early days, drinking water made from surface water, went through the following treatment: flocculation, sedimentation, disinfection with chlorine. The hygienic

reliability of the surface water was achieved by the addition of the chlorine. In 1974 in Rotterdam the chief of laboratory Rook discovered that by adding chlorine, carcinogenic side products (trihalomethanes) were formed. In 1987 the water piping company of Amsterdam discovered that pesticides (bentazon) were present in the drinking water supply. Because of these two discoveries, traditional surface water treatment was no longer sufficient. Adding activated carbon filtration to the process was necessary.

In the treatment of groundwater, activated carbon can be applied when the groundwater has a high colour or pesticides concentration.

3.6.2 Theory

Equilibrium

As mentioned before, an equilibrium can be found in the adsorption process. With a certain loading, as much substance will adsorbed as desorbed. The maximum loading (loading capacity q) depends on the concentration of adsorbable substance in the water. The higher this concentration, the larger the loading capacity. The relation between the loading capacity and the concentration in the water is called the adsorption isotherm. The most common form in adsorption process is the Freundlich isotherm:

$$q_{max} = \frac{x}{M} = Kc_s^x$$

Where:

q = loading capacity [g/kg]

c_s = equilibrium concentration [g/m³]

x = adsorbed mass of substance [g]

M = mass activated carbon [kg]

K = Freundlich constant [(g/kg)•(m³/g) n]

n = Freundlich constant [-]

The Freundlich constants K and n are not real constants, because they are situation specific. They are influenced by the temperature of the water, pH, the type of carbon and the concentration of other present organic substances.

From laboratory measurements the values of the Freundlich isotherms K and n can be determined for each substance for a certain type of activated carbon. The values of K and n for a couple of substances are shown in section 3.6.3.3. The higher the K value, the better the adsorption.

Kinetics

The kinetics or continuity equation for activated carbon filtration is:

$$\frac{dc}{dt} = -u \frac{dc}{dt} - k_2(c_0 - c_s)$$

Where:

k_2 = mass transfer coefficient [d⁻¹]

c_0 = starting concentration of organic substance [mg/l]

c_s = saturation concentration of organic substance [mg/l]

The speed at which the mass transfer occurs is (just like with aeration) proportional to the difference between the actual concentration and the saturation concentration. The saturation concentration depends on the degree of saturation and the relation is determined by the Freundlich isotherm. The lower the degree of saturation of the carbon, the lower the saturation

concentration and therefore, the higher the mass transfer speed. The mass transfer speed is depending on the substance that needs to be adsorbed and the type of carbon (including grain size). On top of that, can the mass transfer coefficient get influenced by the velocity of the water through the grains. The higher the water velocity, the better the mass transfer from liquid to carbon.

Mass balance

In Figure 3.x, the activated carbon filter is simplified as a square, in which:

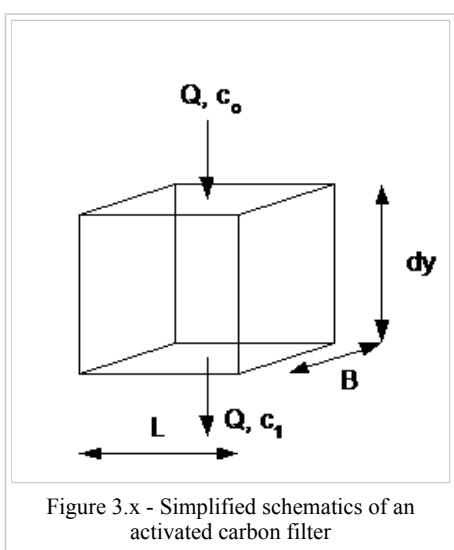
Q = discharge [m^3/h]

B = width of the filter [m]

L = length of the filter [m]

dy = height of the filter [m]

c = concentration organic substance [g/m^3]



Organic substances with a concentration c_0 go through the system with a discharge Q and will leave the system with a concentration c_1 . The difference in concentration between the in and outgoing water is adsorbed onto the activated carbon en thereby increases the loading of the carbon. The continuity equation is:

$$\frac{dq}{dt} = -\frac{v}{\rho} \frac{dc}{dy}$$

Where:

v = filtration velocity [m/h]

q = loading [g/g]

ρ = density of activated carbon [g/m^3]

3.6.3 Model

The GAC model uses the fundamental mass balance of adsorption to predict the removal of pesticides and organic compounds from the water. The model simulates the performance of a bank of adsorbers (maximum 8). The regeneration of the adsorbers in the bank can be staggered and each adsorber can have a different period between regenerations.

3.6.3.1 Options for Usage

The model for biological filtration can be used for the calculation of breakthrough curves, DOC removal efficiencies and the DOC concentration over the bed height at a certain moment in time.

3.6.3.2 Model Equations

The liquid phase material balance is:

$$U \frac{\partial C}{\partial z} + \epsilon \frac{\partial C}{\partial t} + \rho \frac{\partial q}{\partial t} = 0$$

Where:

C = liquid phase concentration of material of interest (kg/m^3)

U = flow velocity (m/s)

ϵ = bed voidage (-)

ρ = bulk density of GAC (kg/m^3)

q = kg of material adsorbed per kg of GAC (kg/kg)

z = distance down bed (m)

t = time (s)

The rate of adsorption is given by:

$$\frac{\partial q}{\partial t} = k_s(q^* - q)$$

Where:

q^* = equilibrium amount adsorbed (kg/kg)

k_s = rate adsorption coefficient (h^{-1})

The equilibrium amount adsorbed can be calculated from the Freundlich isotherm, which is expressed by the following equation:

$$q^* = KC^n$$

Where:

K = Freundlich capacity constant (mg/g)

n = Freundlich exponential constant (-)

The Freundlich constants are used to describe the relationship between the pesticide concentration and the maximum amount of pesticide that can be adsorbed by the GAC for that concentration (GAC capacity). In practice, the GAC capacity given by the Freundlich isotherm is not achieved, because the adsorption process is controlled by mass transfer processes. The rate of mass transfer is governed by the rate constant (α), i.e. the greater the value of α , the faster the material is adsorbed and the closer it gets to the Freundlich isotherm capacity.

The rate adsorption coefficient is given by:

$$k_s = \frac{60D_n}{d_p^2}$$

Where:

D_s = surface diffusion constant (m^2/h)

d_p = diameter of GAC particles (m)

The surface diffusion coefficient is calculated from:

$$D_S = \frac{\alpha D_t C_i}{\rho q_e^b}$$

Where:

α = model term (-)

D_t = liquid diffusivity of compound (m^2/h)

C_i = inlet concentration of compound (kg/m^3)

q_e^* = equilibrium solids concentration, based on the inlet concentration (kg/kg)

The equilibrium solids concentration can be calculated from the Freundlich isotherm equation for the inlet solids concentration:

$$q_e^* = K C_i^n$$

The model enables the user to enter a non-adsorbable fraction. This is to account for material that passes straight through the bed. It is similar to the non-settleable fraction in the clarification models. There is also a biodegradable fraction, also entered by the user. These two values are constant once set by the user, and are independent of the water quality and temperature. This fraction defines the maximum concentration of material in the effluent water, such that

Maximum Outlet Concentration = (1 - Biodegradable fraction) * Inlet Concentration

The model assumes that the regeneration process completely refreshes the GAC to its original state. At the end of the regeneration period, the bed is immediately refreshed and put back into service. In reality, the bed would be out of service while the regeneration takes place.

3.6.3.3 Model Calibration

The objective of the calibration procedure is to determine the calibration constants for a single pesticide/GAC/water combination, to enable the mathematical model to be run. For any pesticide/GAC/water combination, three calibration constants are required. These are:

- the Freundlich capacity constant (K),
- the Freundlich exponential constant (n), and
- the rate constant (α).

The Freundlich constants are used to describe the relationship between the pesticide concentration and the maximum amount of pesticide that can be adsorbed by the GAC for that concentration (GAC capacity). The relationship between the concentration and the capacity is termed the Freundlich isotherm (see section 3.6.3.1).

In practice the GAC capacity given by the Freundlich isotherm is not achieved, because the adsorption process is controlled by mass transfer processes. The rate of mass transfer is governed by the rate constant (α), i.e. the greater the value of α , the faster the pesticide is adsorbed and the closer it gets to the Freundlich isotherm capacity.

The calibration constants can either be determined from full scale, pilot plant or laboratory test data. Laboratory tests usually take the form of rapid column tests, where different types of water, pesticide and GAC can be quickly tested and the results used for calibrating the model.

The data required for the calibration procedure is the experimental breakthrough profile from a single filter. This consists of the influent and effluent pesticide concentrations, and the flow data. Before the data is used for calibration the breakthrough profile should be examined to assess whether any data are spurious. Any spurious data has to be removed from the data set as they can have a detrimental effect on the calibration.

The GAC capacity is determined from the experimental results (the concentration breakthrough curve) by first determining the GAC loading (i.e. pesticide removed during the experiment) using the following equation:

$$q(t) = q(t - \Delta T) + \frac{Q(t)[C_i(t) - C_e(t)]}{M} \Delta t$$

Where:

$q(t)$ = cumulative pesticides removed ($\mu\text{g/g}$)

$Q(t)$ = flowrate at time t (1/time)

$C_i(t)$ = influent pesticide concentration at time t ($\mu\text{g/l}$)

$C_e(t)$ = effluent pesticide concentration at time t ($\mu\text{g/l}$)

M = mass of GAC bed (g)

t = time

Δt = time between samples

By summation this equation, from time zero over the duration of the test, it is possible to determine the total amount of pesticide adsorbed.

For modelling purposes, the equilibrium capacity is required, i.e. when 100% breakthrough is achieved. This is never achieved in practice, so manipulation of the data is required. Experience has shown that the following procedure can be used to determine the equilibrium capacity:

$$q(t) = A + B \frac{C_e(t)}{C_i(t)}$$

Where:

A,B = constants

By plotting $q(t)$ against $C_e(t)/C_i(t)$, and performing linear regression it is possible to determine the equilibrium capacity, by extrapolation.

For situations where the influent pesticide concentration varies significantly, e.g. because of seasonal variations, it can be difficult to obtain reasonable regression data (i.e. the regression correlation coefficient could deviate from 1 or be negative). Under such circumstances the GAC capacity can only be estimated from the experimental data (a good starting point is the final loading achieved by the GAC for the experimental data of interest).

One experiment will provide one data set (i.e. concentration, GAC capacity) for the isotherm determination. Ideally, the results of more than one experiment are required to obtain accurate Freundlich constants. Although this can be achieved by undertaking controlled laboratory scale experiments, it can be difficult to obtain suitable data from pilot or full scale tests. Two slightly different procedures are used for the different cases.

Case 1 - More than one data set

If experimental results are available for several tests performed with different pesticide concentrations it is possible to

determine the two Freundlich constants, by regression analysis.

$$\ln q = \ln K + n * \ln C$$

Hint: Groups of pesticides can be similarly adsorbed, e.g. atrazine and simazine. It may, therefore, be possible to combine data for more than one pesticide to obtain a data set.

Case 2 - Only one data set

If only one test result is available it is not possible to determine the two Freundlich constants. In this case, the Freundlich exponential constant (n) is assumed and the Freundlich capacity constant (K) is calculated by rearranging the last equation. As a guide, for high TOC surface waters n is usually between 0.6 and 0.8. For ground waters, n is between 0.5 and 0.7. To obtain the appropriate value of n , several calibration runs may have to be performed to obtain the most accurate value.

Once the Freundlich isotherm constants have been found the third calibration constant α can be determined. To do this the mathematical model is used to simulate the experimental data. Accurate simulations will only be achieved with the correct value of α .

3.6.3.4 Input and Output

The input of the model can be water quality data from a previous model/treatment step or the raw water input block. On top of that the model parameters have to be entered into the filtration model blocks. The output are the new water quality parameters that have been calculated by the model, which can be displayed as time series in graphs.

Model Parameters

When in Stimela a new project including an activated carbon filter is created, the model displayed in Figure 3.x will pop up. In the window are included: a raw water input block, a graphical output block, an activated carbon filter block and a regeneration block (which acts in the same fashion as a backwash module). For the latter two, the model parameters have to be changed for each different situation. In Figure 3.x and 3.x the model parameters for the two blocks are shown. The model parameter windows pop up when the blocks are double clicked.

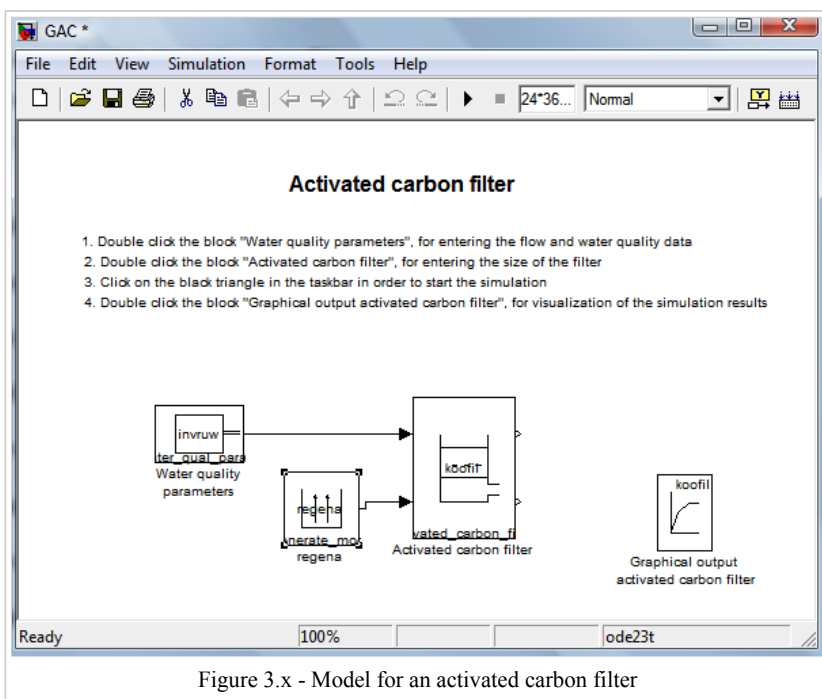


Figure 3.x - Model for an activated carbon filter

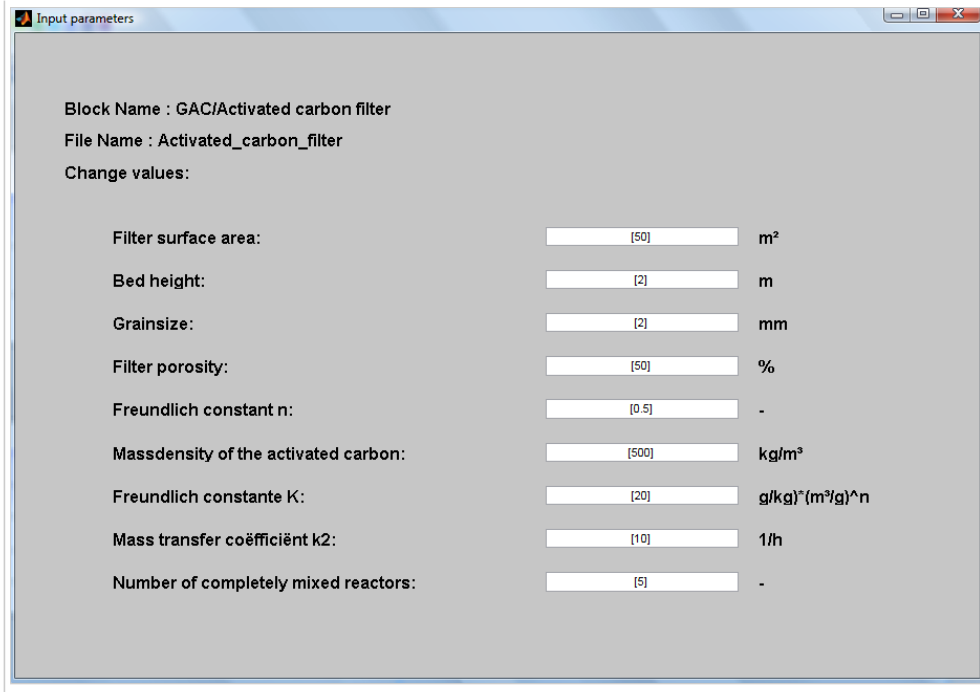


Figure 3.x - Model parameters for an activated carbon filtration block

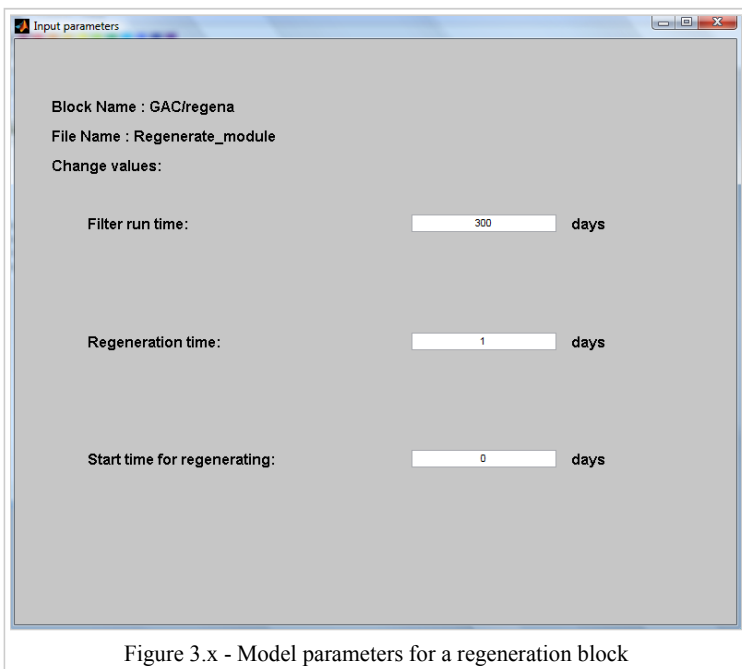


Figure 3.x - Model parameters for a regeneration block

For an explanation of most of the input parameters needs to be referred to the previous section on the model equations. The one that hasn't been discussed yet is:

Number of CSTRs between sampling: The number of CSTRs determines the rate of plug flow through the activated carbon filter. In the most extreme case, a flow of water could be completely mixed, or divided into an infinite amount of mixing barrels (CSTRs). When a number like 100 is filled in here, the flow will be almost perfect plug flow. This is not very probable, because there is always horizontal and vertical mixing going on. The improvement of mass transfer due to the improvement of the plug flow is negligible when the stream is divided into more than 20 completely mixed barrels.

Graphs

The block 'Graphical output biological filter' will give an output screen with three graphs (see Figure 3.x). On the upper left the breakthrough curve is shown over time, with underneath it the DOC effluent concentration and on the upper right the

concentration over the height of the bed for the first filter run. On the bottom right the input parameters are displayed. The graphs are acquired with the default parameters (see above). In this example it can be clearly seen that the filter breaks through way too soon. Either it should be regenerated more often or the dimensions need to be changed.

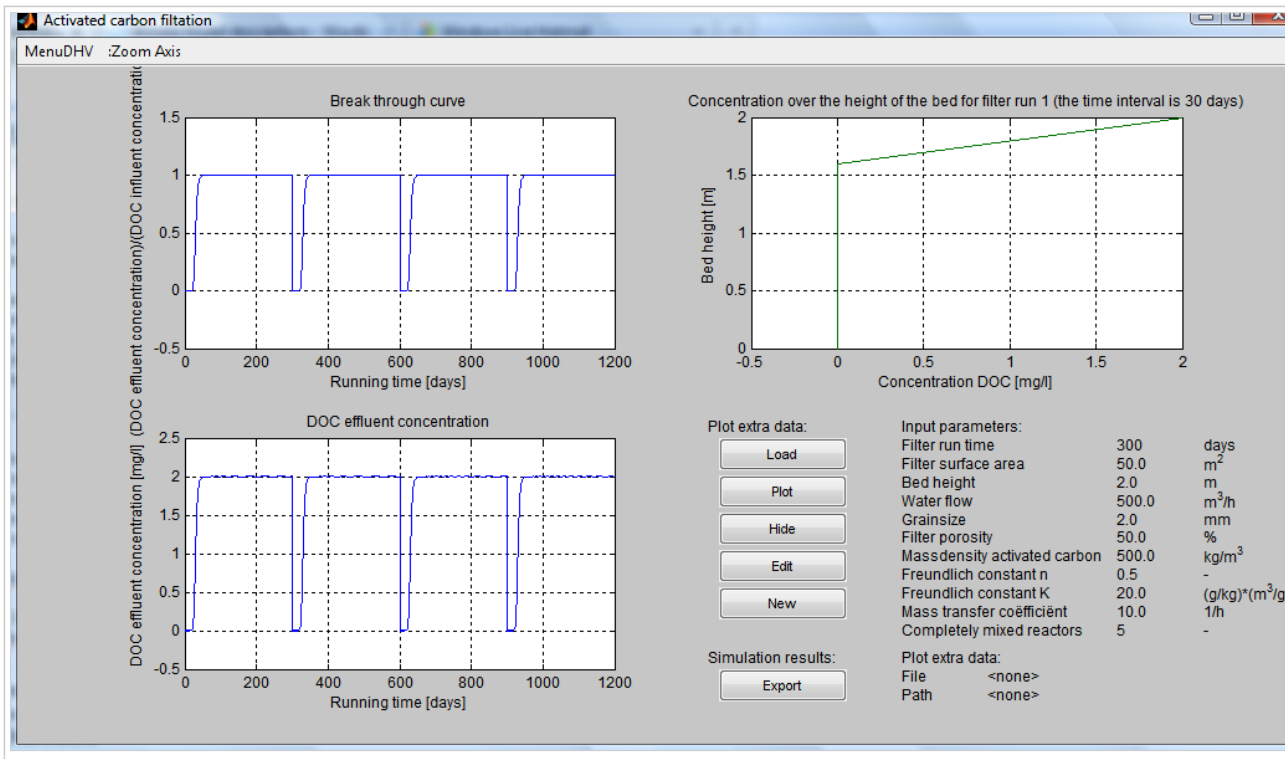


Figure 3.x - Graphical output for an activated carbon filter

3.7 References

Aa, L.T.J. van der, Magic-Knezev, A., Rietveld, L.C., van Dijk, J.C., 2006, Biomass development in biological activated carbon filters, Waternet, TU Delft

Armirtharajah, A., Some theoretical and conceptual views of filtration, Journal of the American Water Works Association, Vol.80, No.12, pp 36-46, 1988.

Billen, G., Servais, P., Bouillot, P., Ventresque, C., 1992, Functioning of biological filters used in drinking-water treatment - the Chabrol model, J. WATER SUPPLY RESEARCH & TECHNOLOGY-AQUA 41 (4), pp. 231-241

Hozalski, R.M., Bouwer, E.J., 1996, Deposition and retention of bacteria in backwashed filters: Biomass accumulation in laboratory-scale filters is not impaired by backwash with water alone, Journal / American Water Works Association 90 (1), pp. 71-85

Hunik, J. ,1993, Engineering Aspects of Nitrification with Immobilized Cells. PhD-thesis Wageningen University, The Netherlands

Ives, K.J., Mathematical models of deep bed filtration, In: The scientific basis of filtration, Ives, K.J. ed. , Noordhoff-Leyden, 1975

Ives, K.J., 1968, The Physical and mathematical basis of deep bed filtration, University College London

Van Der Kooij, D., Hijnen, W.A.M., 1984, Substrate utilization by an oxalate-consuming Spirillum species in relation to its growth in ozonated water, Applied and Environmental Microbiology 47 (3), pp. 551-559

Kors, L., Moorman, J., Wind, A. and Hoek, J. van der ,1998, Nitrification and low temperature in a raw water reservoir and rapid sand filters. Wat. Sci. Tech. 37(2), 169–176

Lerk C F, Enkele aspecten van de ontijzering van grondwater, 1965, Dissertatie TH Delft

Loosdrecht, M. van ,1993, Diffusive transport in biofilms and flocs. Syllabus Department of Biochemical Engineering, Delft

University of Technology, The Netherlands

Rittmann, B. and McCarty ,1981, Substrate Flux into Biofilms of Any thickness. Jour. Environ. Engrg. 107(EE4), 831

Rittmann, B.E., Stilwell, D., 2002, Modelling biological processes in water treatment: The integrated biofiltration model, Journal of Water Supply: Research and Technology - AQUA 51 (1), pp. 1-14

Schlegel, S., 1992, Operational results of waste water treatment plants with biological N and P elimination, Water Science and Technology 25 (4-5), pp. 241-247

Sontheimer, H., Volker, E., 1988, Characterization and estimation of wastewater treatment plant effluents from the point of view of drinking water supply, GWF, das Gas- und Wasserfach: Wasser/Abwasser 129 (3), pp. 216-230

Uhl, W., Gimbel, R., 2000, Dynamic modeling of ammonia removal at low temperatures in drinking water rapid filters, Water Science and Technology 41 (4-5), pp. 199-206

Yoshizaki, T. and Ozaki, M., 1993, On removal of ammonium by addition of phosphoric acid in ozon-granulated active carbon treatment. Water Supply 11(3/4), 321–330

4 Oxidation and Disinfection

4.1 Disinfection in General

With oxidation and disinfection organic micro-pollutants, such as pesticides, are converted into decomposable organic material (Dissolved Organic Carbon), while pathogenic micro-organisms like bacteria, viruses and protozoa are eliminated. There are a couple treatment techniques that can be applied for oxidation and disinfection: ozone (O_3) dosing, chlorine (Cl_2) dosing, chlorinedioxide (ClO_2) dosing or irradiating the water with UV.

Because as of now only treatment with ozone is included in Stimela, this is the technique that will be discussed in more detail. Ozone has both oxidizing and disinfecting properties. Ozone takes care of the decomposition of micro-pollutants into organic material (which then has to be filtered out by i.e. activated carbon filters). Because of this ozone has disinfecting properties. Ozone dosing also has a downside, because the harmful substance bromate (BrO_3^-) is created. This is an important aspect of the process. Ozone dosing is usually applied to the treatment of surface water.

4.2 Disinfection with Ozone

4.2.1 Process

An ozone reactor is usually a column through which water flows up or down. At the bottom of the reactor air saturated with ozone is being added in bubble form (see Figure 4.1, left side). Another layout for the reactor is a maze of multiple contact spaces, in which some spaces have dosing points. This can be seen on the right side of Figure 4.1.

The gas transfer of ozone from air to water happens on the contact surface area of the bubbles. Therefore the gas transfer is more efficient with smaller bubbles. Because this is basically an aeration process with air, there is not just exchange of ozone taking place, but oxygen and nitrogen as well.

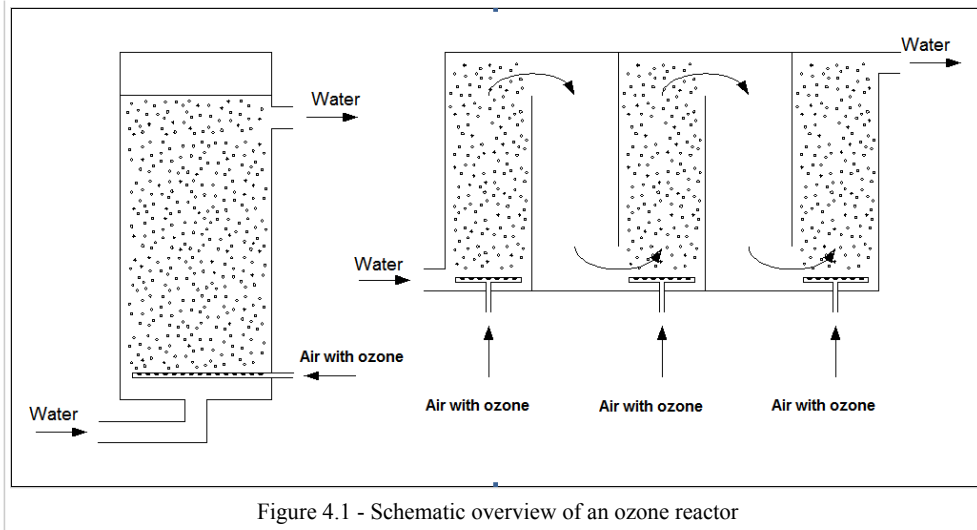


Figure 4.1 - Schematic overview of an ozone reactor

4.2.2 Theory

Ozone reactor are made for the transfer of ozone from air to water. For the complete theory of gas transfer, please refer to Chapter 2 (Aeration). In this section additions to this theory are made, necessary for the ozone reactor.

In Chapter 2 it is stated that the air used for the dosing, is fully saturated with water vapour, which causes a pressure p_w on the air. On top of that bubbles of ozone are created and added at the bottom of the reactor. This causes the air pressure in the bubbles to be increase with the static pressure of the water. The static pressure will decrease as the bubble gains height in the reactor. The partial pressure of a gas corrected with the water vapour saturation concentration of the air en static pressure will then be:

$$p = V_f(P + (h_{react} \rho_w g) - p_w)$$

In which:

p = Partial pressure [Pa]

V_f = Volume fraction of a gas in dry air [-]

P = Total pressure [Pa], which is under atmospheric circumstances equal to atmospheric pressure

h_{react} = The distance from the water surface to the point in which the pressure is calculated [m]

ρ = The density of water ($= 1000 \text{ kg/m}^3$)

g = Gravitation constant ($= 9,81 \text{ m/s}^2$)

p_w = Water vapour pressure [Pa]

Adjusting the k_2 value

In the kinetics equations in Chapter 1, the gas transfer coefficient k_2 is being used. The k_2 can be written as:

$$k_2 = k_L a$$

In which:

k_L = partial gas transfer coefficient

a = specific surface area

The specific surface area is the contact surface area between the bubbles and the water in a volume of water.

$$a = \frac{A_b}{V_l}$$

In which:

A_b = Surface area of air bubbles

V_l = Volume of water of the intended part

The surface area of a bubble can be determined by:

$$A_b = V_b \frac{6}{d}$$

The volume of the air bubbles can be calculated by:

$$V_b = \frac{Q_g/c_g \cdot \Delta x}{Q_l/c_l \cdot \Delta x} * V_l = RQ * \frac{v_l}{v_g} * V_l$$

In which:

Q_g = Air discharge [m³/h]

Q_l = Water discharge [m³/h]

v_g = Air velocity [m/s]

v_l = Water velocity [m/s]

Δx = Height of the intended water layer [m]

The kinetics for gasses in water can now be written as:

$$\frac{dc_l}{dt} = k_L * RQ * \frac{v_l}{v_g} * \frac{6}{d} (k_D * c_g - c_l)$$

And the kinetics for gasses in air are now described by:

$$\frac{dc_g}{dt} = -k_L * \frac{6}{d} (k_D * c_g - c_l)$$

Initial ozone usage

When ozone is transferred from air to water, an instant reaction of ozone with DOC takes place, thereby using up some initial ozone. This reaction lowers the ozone concentration in the water, causing the driving force between air and water to remain large.

Velocity of an air bubble

The velocity of an air bubble rising through the water column and the diameter of the bubble are assumed to be constant in this model. This is a simplification that, causes the calculated ozone transfer to be a little smaller than it is in reality. For the velocity of the air bubble, a value of 0.3 m/s is taken, while the bubble diameter can be entered into the model as an input parameter (see section 4.2.3.2).

4.2.3 Model

An integrated model containing the water quality parameters Escherichia coli (E. coli), bromate, assimilable organic carbon (AOC), dissolved organic carbon (DOC) and UV absorbance at 254 nm (UVA254) has been developed for dissolved ozone dosing in a plug flow reactor (van der Helm et al., 2007a,b). Use of the integrated ozone model for the operational support

and control of existing ozone bubble column installations requires that the model be extended to account for gas transfer for ozone transport from the gas phase to the liquid phase. Gas transfer in bubble columns is incorporated in the integrated ozone model, to determine relationships between model parameters of different treatment plants so the same model can be applied to different locations, and to use the model for the evaluation of control strategies for operational support and process control of ozonation.

4.2.3.1 Options for Usage

The model of the ozone reactor can be used to calculate the input of ozone and the transfer of oxygen and nitrogen into water.

4.2.3.2 Model Equations

The model used by van der Helm et al. (2007a) to describe ozone decay in a plug flow reactor where dissolved ozone was dosed was extended with gas exchange according to the model of Rietveld (2005) for application in ozone bubble columns. In the model rapid ozone consumption was determined by the decrease in UVA₂₅₄:

$$\frac{\partial c_{O_3}}{\partial t} = -u \frac{\partial c_{O_3}}{\partial x} + k_L R Q \frac{u}{u_g d} (\alpha k_D c_{O_3g} - C_{O_3}) - k_{UVA}(UVA - UV A_0) Y - k_{O_3} c_{O_3}$$

In which:

u = the water velocity (m/s)

x = the length of the reactor (m)

k_L = the gas transfer coefficient (m/s)

RQ = the gas to water flow ratio (Q_g/Q) (Nm³/m³)

Q and Q_g = the water flow (m³/h) and gas flow (Nm³/h) respectively

u_g = the gas velocity (m/s)

d_b = the bubble diameter (m)

α = the temperature and pressure correction factor $\alpha = (P_g/P_o)(T_o/T_g)$

P_o and P_g = the standard pressure (101325 Pa) and the gas pressure in the reactor (Pa), respectively

T_o and T_g = the standard temperature (273.15 K) and the gas temperature in the reactor (K), respectively

k_D = the distribution coefficient (-)

c_{O_3g} = the ozone in gas concentration (g-O₃/Nm³)

k_{UVA} = UVA₂₅₄ decay rate (1/s)

UVA = UVA₂₅₄ in water (1/m)

UVA_0 = the stable UVA₂₅₄ after completion of the ozonation process (1/m)

Y = the yield for ozone consumed per UVA₂₅₄ decrease ((mg-O₃/l)/(1/m))

k_{O_3} = the slow ozone decay rate (1/s)

The α is determined by the gas temperature and the water height in the bubble columns, and thus changes over the height of the bubble column. u_g was calculated using the equation for the rising velocity of a bubble in stagnant water derived by Wallis (1969):

$$u_b = 0.0135 \left(\frac{2000\sigma}{\rho_w d_b} \right)^{0.5}$$

In which:

σ = the surface tension (N/m)

ρ_w = the water density (kg/m^3)

For co-current bubble columns, $u_g = u_b + u$, and for counter current bubble columns $u_g = u_b - u$.

The ozone concentration in the gas phase was described by the following equation (Rietveld, 2005):

$$\frac{\partial c_{O3g}}{\partial t} = -u_g \frac{\partial c_{O3g}}{\partial x} + k_L \frac{6}{d_b} (\alpha k_D c_{O3g} - e_{O3})$$

For the gas transfer coefficient, k_L , the expression by Hughmark (1967) was used:

$$k_L = \frac{D_{O3}}{d_b} \left(2 + a \left(\left(\frac{u_b d_b}{\nu} \right)^{0.484} \left(\frac{\nu}{D_{O3}} \right)^{0.339} \left(\frac{d_b g^{1/3}}{D_{O3}^{2/3}} \right)^{0.072} \right)^b \right)$$

In which:

D_{O3} = the diffusion coefficient of ozone (m^2/s)

a and b = empirical constants (for single gas bubbles a = 0.061 and b = 1.61, and for swarms of gas bubbles a = 0.0187 and b = 1.61)

u_b = the bubble rising velocity (m/s)

ν = the kinematic viscosity (m^2/s)

g = the specific gravity (m/s^2)

The equations used for UVA_{254} decrease, bromate formation, E. coli inactivation with the Hom model, the CT and AOC formation were from van der Helm et al. (2007a):

$$\frac{\partial(UVA)}{\partial t} = -u \frac{\partial(UVA)}{\partial x} - k_{UVA}(UVA - UVA_0)$$

$$\frac{\partial c_{BrO3}}{\partial t} = -u \frac{\partial c_{BrO3}}{\partial x} + k_{BrO3} e_{O3}$$

$$c_{BrO3,ini} = F_{BrO3,ini} c_{O3,DOS} + c_{BrO3,in}$$

$$\frac{\partial N}{\partial t} = -u \frac{\partial N}{\partial t} \frac{k}{60} m N e_{O3}^n t^{m-1}$$

$$\frac{\partial CT}{\partial t} = -u \frac{\partial CT}{\partial t} + e_{O3}$$

$$c_{AOC} = F_{AOC} c_{O3,DOS} c_{DOC,in} + c_{AOC,in}$$

In which:

c_{BrO3} = the bromate concentration ($\mu\text{g-BrO}_3/\text{l}$)

k_{BrO3} = the bromate formation rate constant ($(\mu\text{g-BrO}_3/\text{l})/((\text{mg-O}_3/\text{l}) * \text{min})$)

$c_{BrO3,ini}$ = the initial bromate formation ($\mu\text{g-BrO}_3/\text{l}$)

$F_{BrO_3,ini}$ = the constant for initial bromate formation ($(\mu g-BrO_3/l)/(mg-O_3/l)$)

$c_{O_3,DOS}$ = the ozone dosage ($mg-O_3/l$)

$c_{BrO_3,in}$ = the influent bromate concentration ($\mu g-BrO_3/l$)

N = the number concentration of organisms (CFU/100 ml)

k = the inactivation rate coefficient ($l/(mg-O_3 * min)$) for $n=1$ and $m=1$ n and m are empirical constants (-)

c_{AOC} = the AOC concentration ($\mu g-C/l$)

F_{AOC} = the constant for AOC formation per DOC ($(\mu g-C/l)/(mg-O_3/l * mg-C/l)$)

$c_{DOC,in}$ = the influent dissolved organic carbon concentration ($mg-C/l$)

$c_{AOC,in}$ = the influent AOC concentration ($\mu g-C/l$)

A possibility exists to simulate short-circuiting in the bubble column. As a result, part of the water flow through the bubble column has no contact with ozone and mixes at the bottom of the bubble column. The short-circuit flow in the bubble column relative to the total flow is given by:

$$SC_{BC} = \frac{Q_{SC,BC}}{Q}$$

In which:

SC_{BC} = the factor for short-circuiting in the bubble column (-)

$Q_{SC,BC}$ = the short-circuiting flow in the bubble column (m^3/h)

4.2.3.3 Model Calibration

In the PhD thesis by Alex van der Helm (2007), the model had been calibrated for the hydraulic properties of the DOPFR (Dissolved Ozone Plug Flow Reactor), ozone decay and UVA254, bromate formation and AOC formation which were all separately discussed. The results for the hydraulic properties are presented below. For a full overview of the conducted experiments and calibration results, please refer to the thesis itself.

Calibration of the hydraulic properties of the DOPFR

In Figure 4.x the results of three tracer experiments for three different sampling points with their respective calibrated hydraulic properties are presented, demonstrating a CSTR in series model can be applied for the DOPFR. In Table 4.x the number of CSTRs and the hydraulic residence time for all sampling points of the plug flow reactor are given. Linear regression shows that the static mixer represents 10 CSTRs and that the number of CSTRs in the plug flow reactor is linear with the increase of the hydraulic residence time, so the hydraulic properties are the same over the total length of the plug flow reactor. However, the tracer experiment at sampling point 1 resulted in an unlikely high number of CSTRs, higher than at the second sampling point which is physically not possible. On basis of the 37 linear regressions, the number of CSTRs on sampling point 1 was estimated equal to 19. The calculated number of CSTRs was used in the model to describe the hydraulic properties. The high number of CSTRs demonstrates the tube has good plug flow characteristics.

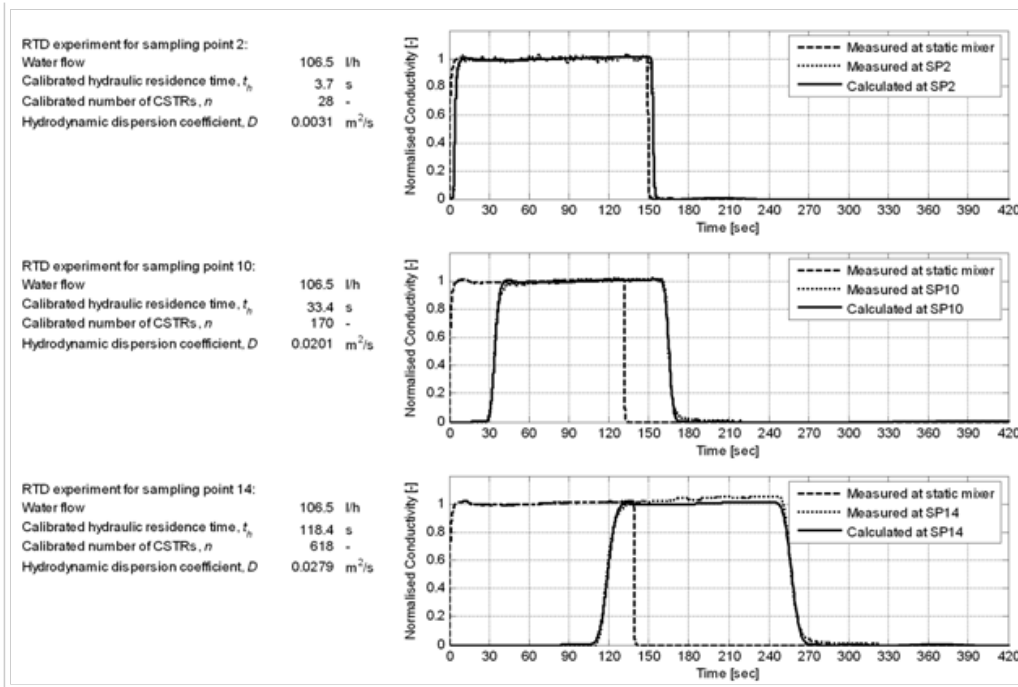


Figure 4.x - Calibration results for the number of CSTRs and the hydraulic residence time at three different sampling points for a water flow of 106.5 l/h through the DOPFR

Sampling point	1	2	3	4	5	6	7
CSTRs (-)	30	28	40	51	57	70	104
t_h (s)	1.9	3.7	5.9	8.3	10.5	12.9	17.9
Sampling point	8	9	10	11	12	13	14
CSTRs (-)	121	141	170	243	323	460	618
t_h (s)	23.2	28.4	33.4	47.9	62.2	90.7	118.4

Table 4.x - Number of CSTRs and the hydraulic residence time determined from tracer experiments for a flow of 106.5 l/h through the DOPFR

4.2.3.4 Input and Output

The input of the model can be water quality data from a previous model/treatment step or the raw water input block. On top of that the model parameters have to be entered into the ozonation model blocks. The output are the new water quality parameters that have been calculated by the model, which can be displayed as time series in graphs.

Model Parameters

When in Stimela a new project including an ozone reactor is created, the model displayed in Figure 4.2 will pop up. In the window are included: a raw water input block, a graphical output block, an ozone dosage block, an ozone bubble column block and an ozone contact column block. For the latter three, the model parameters have to be changed for each different situation. In Figure 4.3, 4.4 and 4.5 the model parameters for the three blocks are shown. The model parameter windows pop up when each block is double clicked.

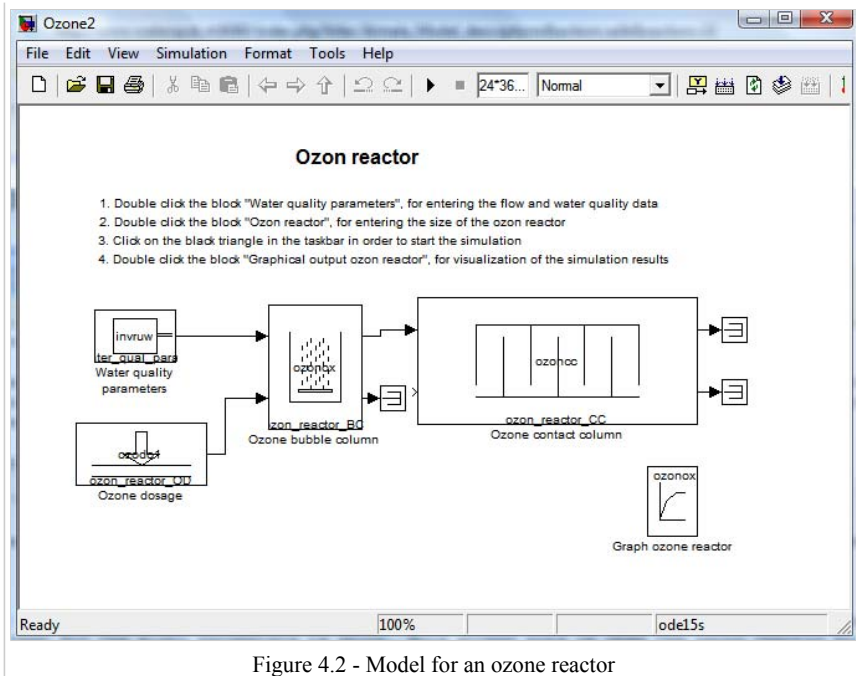


Figure 4.2 - Model for an ozone reactor

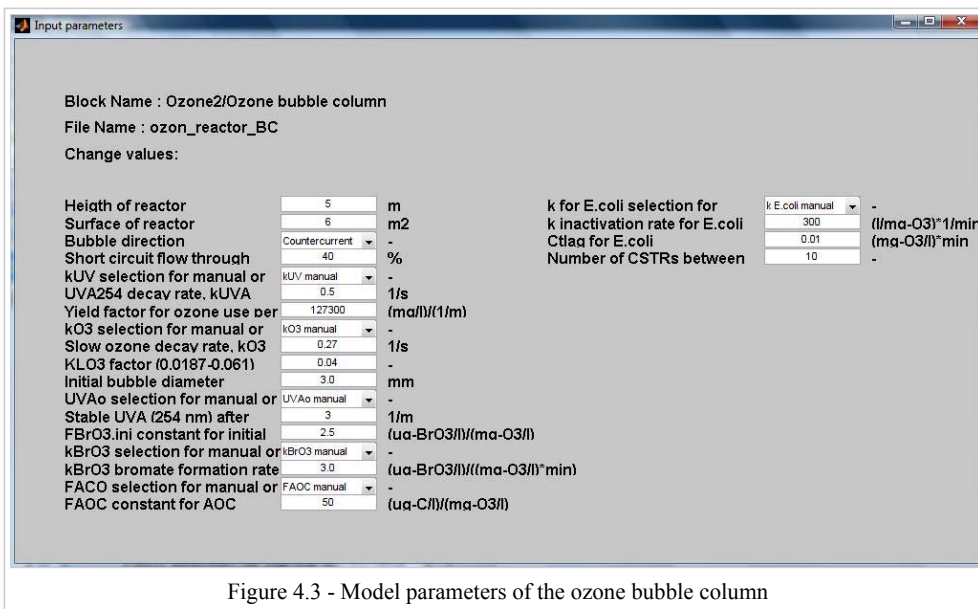


Figure 4.3 - Model parameters of the ozone bubble column

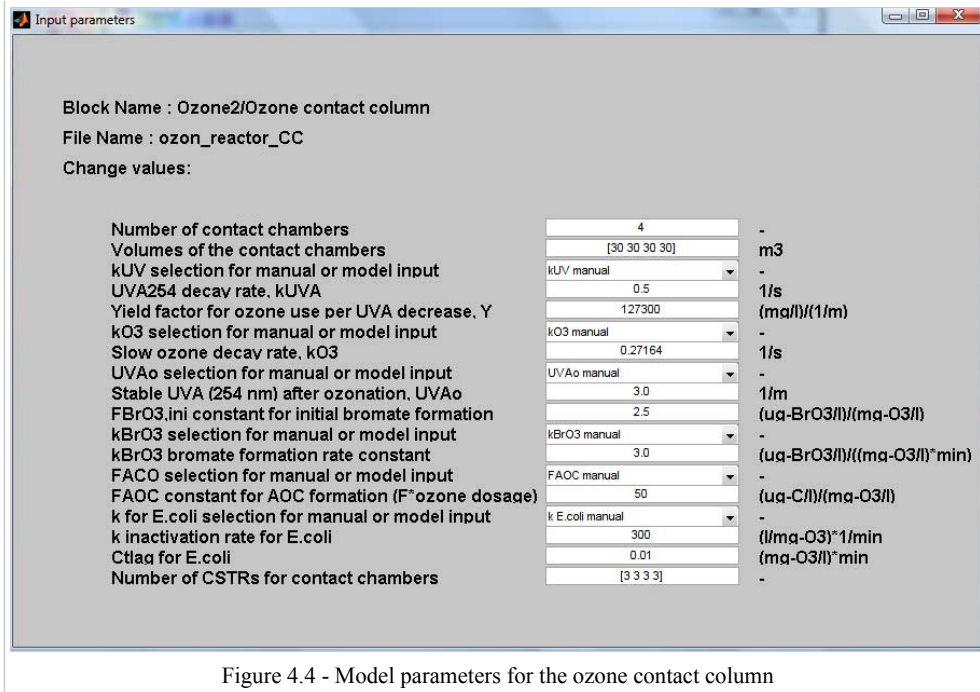


Figure 4.4 - Model parameters for the ozone contact column

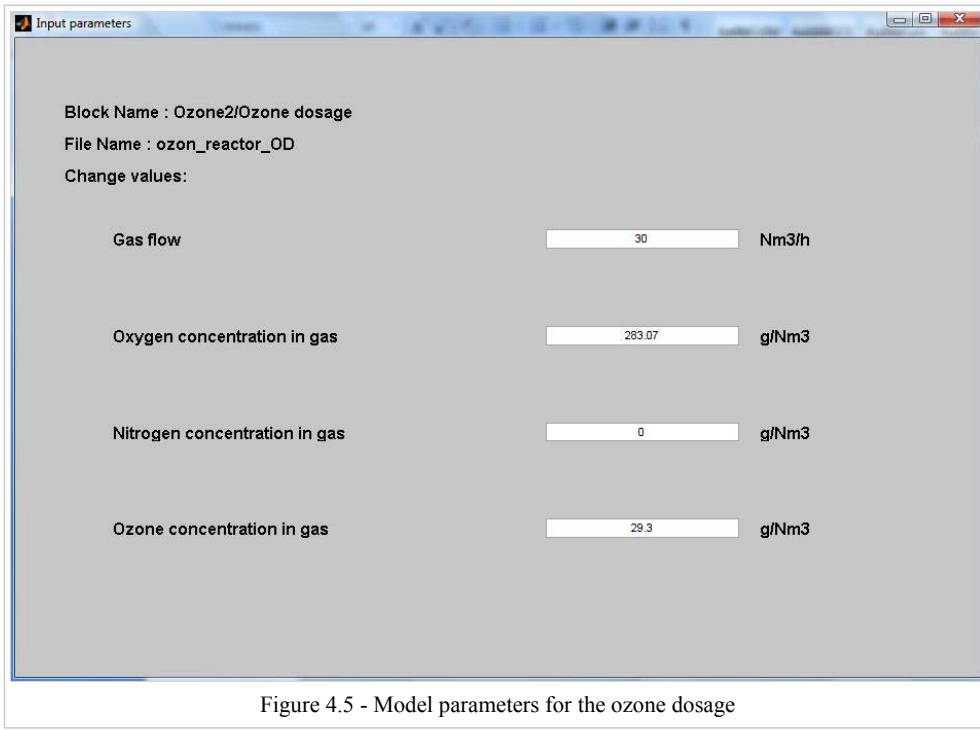


Figure 4.5 - Model parameters for the ozone dosage

For an explanation of most of the input parameters needs to be referred to the previous section. The ones that haven't been discussed yet are:

Bubble direction: This can be set to co-current or counter-current, indicating whether the bubbles of the modelled treatment process go with the flow or against the flow of the water.

Number of CSTRs between sampling: The number of CSTRs determines the rate of plug flow through the tower aerator. In the most extreme case, a flow of water could be completely mixed, or divided into an infinite amount of mixing barrels (CSTRs). When a number like 100 is filled in here, the flow will be almost perfect plug flow. This is not very probable, because there is always horizontal and vertical mixing going on. The improvement of gas transfer due to the improvement of the plug flow is negligible when the stream is divided into more than 20 completely mixed barrels.

Graphs

The graphical output block gives in 3 different graphs for ozone, oxygen and nitrogen the gas concentration curve in the water across the height of the reactor. The changing of the gas saturation concentration is given as well for each gas. The gas saturation concentration is equal to the gas concentration in the air multiplied by the distribution factor kD.

Apart from the 3 graphs, the input parameters for the ozone reactor are given. The results from Figure 4.6 are obtained with the default parameters.

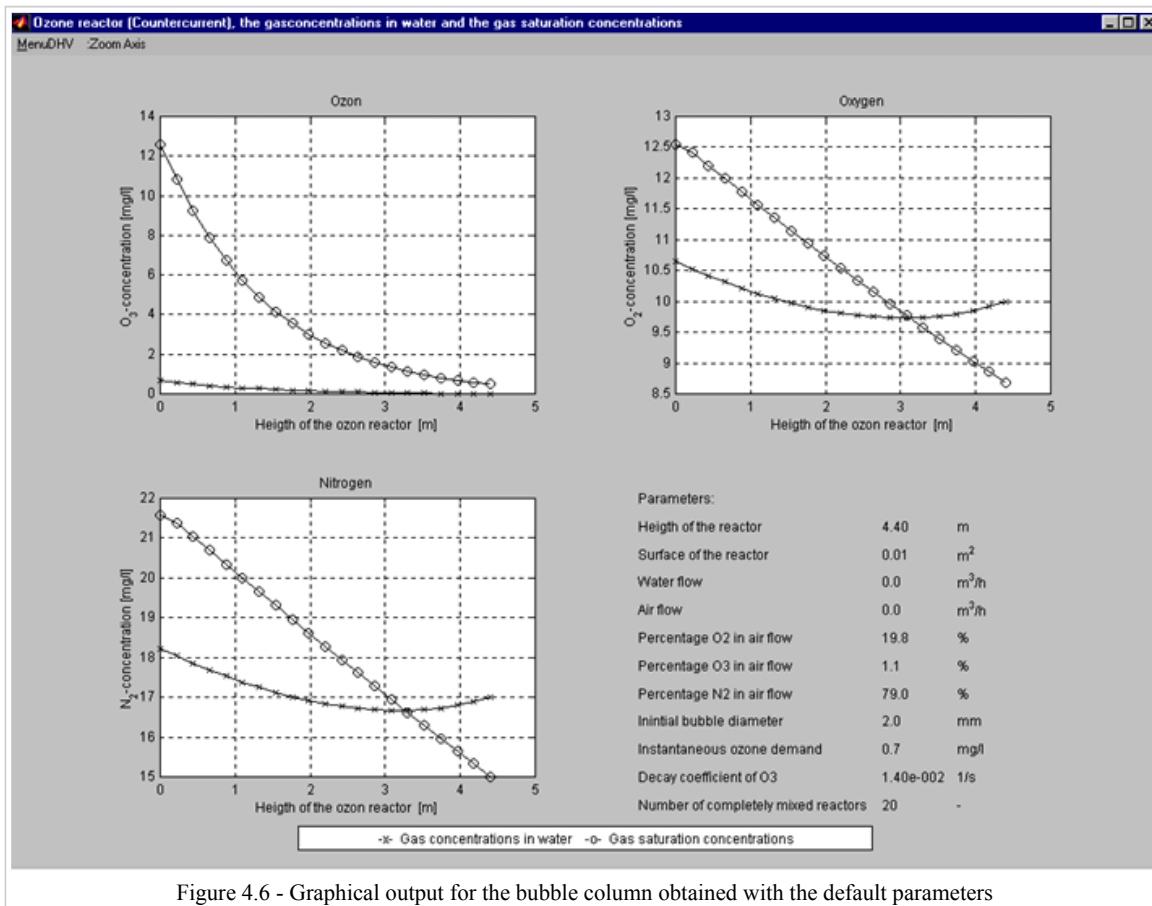


Figure 4.6 - Graphical output for the bubble column obtained with the default parameters

4.3 References

Hughmark, G.A. (1967). Holdup and mass transfer in bubble columns. Ind. Eng. Chem. Process Des. Dev., 6(2), 218-220.

Rietveld, L.C. (2005). Improving operation of drinking water treatment

van der Helm, A.W.C., Rietveld, L.C., Baars, E.T. and van Dijk, J.C. (2007a). Disinfection and by-product formation during ozonation in a pilot-scale plug flow reactor and CSTR. J. Water Supply Res. Technol. AQUA, submitted for publication, September 2007.

Wallis, G.B. (1969). One-dimensional two-phase flow, McGraw-Hill, New York, USA.

5 Softening

Some sources of water are located near places with a lot of minerals, or rock. Especially when it concerns limestone, this produces a water source with a very high calcium concentration. High calcium content in drinking water can have nasty consequences for domestic appliances (such as washing machines or water boilers), detergent usage, the water distribution network and for the taste of the water itself. Getting rid of this excess calcium is vital for meeting drinking water standards.

5.1 Pellet Softening Reactor

5.1.1 Process

In the Netherlands, central softening of drinking water is mainly carried out with fluidised pellet reactors. The pellet reactor consists of a cylindrical vessel that is partly filled with seeding material. The diameter of the seeding grain is small, between 0.2 and 0.4 mm, and consequently the crystallisation surface is large. The water is pumped through the reactor in an upward direction at high velocities, maintaining the seeding material in a fluidised condition. In the bottom of the reactor, chemicals are dosed (caustic soda, soda ash or lime). Calcium carbonate then becomes supersaturated and crystallises on the seeding material, resulting in the formation of pellets. At regular intervals, pellets at the bottom of the reactor are removed. These pellets can be re-used in industry.

Softening in a reactor is normally in excess of the required levels. Therefore, a part of the water can be bypassed and mixed with the effluent of the reactors. In general several identical parallel reactors are installed to increase the reliability of the system and the flexibility in operation. Reactors can be switched on and off in case of flow changes, maintaining water velocities between 60 and 100 m h^{-1} .

The mixture of the effluent of the reactors and the bypass water must be chemically stable to avoid crystallisation in the filters after the softening step. To optimise the operation of pellet softening reactors using caustic soda (NaOH), a mathematical model has been developed. The purpose of modelling is to simulate the softening process, in order to make decisions on operation, leading finally to model predictive control of the process. During operation, water quality and flow change frequently and manipulation of the process has influence on the behaviour of the softening process. The dynamics of the process are therefore taken into account.

5.1.2 Theory

WELLICHT REEDS BEHANDELT IN VORIGE EN VOLGENDE SECTIE

5.1.3 Model

The softening process consists of a number of fluidised bed reactors with one bypass. The chemical reactions in the water take place in the reactor. The mixing process of reactor effluents and bypass water is modelled as instantaneous mixing (taking the calcium carbonic equilibrium into account) without any reaction kinetics.

Various models have been developed (Dijk & Wilms 1991, Bogt et al. 1992). These models are steady-state, used for design purposes. Van Schagen et al. (2008) developed a new, dynamic, model of the pellet softening process, which has been implemented first in Stimela and now in SimEau. This model takes diffusion in the fluidised bed and new insights in the fluidised bed behaviour of pellet softening reactors into account.

The model is defined in the following three sections. In the first section, the calcium carbonic equilibrium, which determines the crystallisation in the reactor, is explained. The second section describes the fluidisation of the bed, which determines the available crystallisation surface in the reactor. Finally the crystallisation rate is modelled based on the crystallisation surface and the calcium carbonic equilibrium.

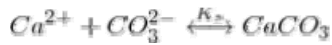
5.1.3.1 Options for Usage

The model for softening can be used for the calculation of calcium removal, the pH of the mixed effluent with a certain NaOH dose, the headloss, pellet diameter, bed height and pressure difference over time and the pellet diameters at different heights of the reactor. By using the block "graphical output pels25" the previously mentioned parameters are plotted in time.

5.1.3.2 Model Equations

Modelling the Calcium Carbonic Equilibrium

The crystallisation of calcium carbonate is a shift in the equilibrium between the solid and soluble state of calcium carbonate (Wiechers et al. 1975):

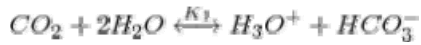


$$K_s = f^8 [Ca^{2+}] [CO_3^{2-}]$$

where the equilibrium constant K_s is an experimentally determined constant depending on the water temperature. The activity factor f is based on the ionic strength (IS) of the water and is given by (Schock 1984):

$$\log(f) = \frac{-0.5\sqrt{IS}}{\sqrt{1000 + \text{sqrt}IS}} + 0.00015IS$$

To determine the carbonate concentration, the carbonic equilibrium must be taken into account. This is the balance between three carbonic fractions (CO_2 , HCO_3^- and CO_3^{2-}). The ratio between the concentrations of these fractions has a strong relation with the pH. The following reactions describe the equilibrium:



The reaction rates of these equilibria are high, and it is therefore assumed that the carbonic fractions are always in equilibrium. The conservative parameters m-alkalinity (M) and the p-alkalinity (P) are used to describe the equilibrium. The actual concentrations of the equilibrium can now be found by solving the following set of algebraic equations:

$$M = 2[CO_3^{2-}] + [HCO_3^-] + [OH^-][H_3O^+]$$

$$P = [CO_3^{2-}] - [CO_2] + [OH^-] - [H_3O^+]$$

$$K_1 = f^2 [HCO_3^-][H_3O^+][CO_2]^{-1}$$

$$K_2 = f^4 [CO_3^{2-}][H_3O^+][HCO_3^-]^{-1}$$

$$K_w = f^2 [H_3O^+][OH^-]$$

where K_1 , K_2 and K_w are experimentally well determined constants depending on the water temperature (Jacobsen & Langmuir 1974, Plummer & Busenberg 1982). The equation is a set of five equations with seven unknown concentrations (M, P, CO_2 , HCO_3^- , CO_3^{2-} , H_3O^+ and OH^-). Two concentrations must be known to determine the remaining ones. The H_3O^+ and the HCO_3^- are known concentrations in the raw water of the softening reactors. The H_3O^+ concentration is normally measured as pH:

$$pH = -\log(f[H_3O^+])$$

It is now possible to determine the carbonate concentration throughout the crystallisation process. Based on the measured pH and HCO_3^- concentration, the m-alkalinity and the p-alkalinity are determined using the set of 5 equations and the equation for the pH. The dosing of caustic soda causes an increase of the m-alkalinity and alkalinity due to the feed of OH^- . With the new m-alkalinity and p-alkalinity, the CO_3^{2-} concentration is determined. As soon as crystallisation takes place, carbonate (CO_3^{2-}) is removed from the water and m-alkalinity and p-alkalinity are accordingly lowered. Based on the lowered m-alkalinity and p-alkalinity the new carbonate concentration is determined.

Two parameters describe the super-saturation of calcium carbonate in water. The Saturation Index (SI) is defined as the pH offset at which the actual calcium concentration is in equilibrium with the carbonate:

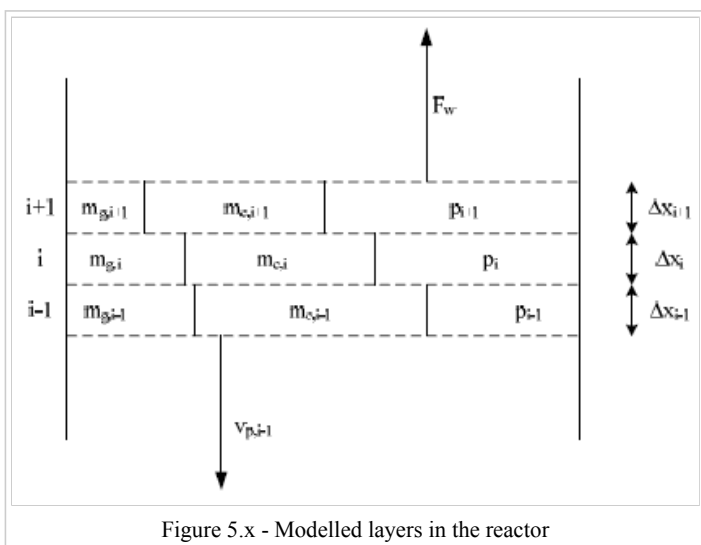
$$SI = \log \left(\frac{f^8 [Ca^{2+}] [CO_3^{2-}]}{K_s} \right)$$

and is a measure for the driving force in the crystallisation process. The TCCP (theoretical calcium carbonate crystallisation potential) is the amount of calcium in (mol/m^3) that should crystallise to obtain water in chemical equilibrium. The TCCP is a measure for the amount of calcium carbonate that can be formed in consecutive process steps. The two indices are strongly related, but are both used separately to quantify the performance of the crystallisation process.

Modelling the fluidised bed

The aim of the fluidised bed model is to describe the fluidisation of the bed and the transportation of the pellets through the bed. The fluidisation model is necessary to determine bed properties such as bed height, pressure drop and porosity depending on pellet size, water flow, pellet discharge speed and temperature. The porosity is used to model the crystallisation rate in the next paragraph.

The model is deduced by dividing the reactor in layers as shown in Figure 5.x. The water flow is schematised as a one-dimensional flow in upward direction, keeping the bed of pellets fluidised. In the case of a pellet discharge the pellets are transported in downward direction. The state variables of the fluidised bed model are the mass of the calcium carbonate m_c and the mass of the grains m_g .



Each layer is divided into 3 sections: the volume of grains, the volume of calcium carbonate and the water volume determined by the porosity. The height of each layer is given by the porosity of the bed and the mass of pellets, consisting of grains and calcium carbonate:

$$\Delta x_i = \left(\frac{m_{g,i}}{\rho_g} + \frac{m_{c,i}}{\rho_c} \right) (1 - p_i)^{-1} A^{-1}$$

The porosity p_i in the i^{th} layer is based on temperature, pellet diameter and water velocity and is accurately described by the Richardson-Zaki expansion formula (Richardson & Zaki 1954) (the indices i are dropped for readability):

$$p = \left(\frac{F_w}{Av_0} \right)^{\frac{1}{n}}$$

The terminal settling velocity v_0 and the exponent n are experimentally determined properties of a single particle. Richardson and Zaki found the following empirical relationship for the exponent n :

$$n = 4.6 \quad \text{for } Re_0 < 0.2$$

$$n = 4.4 Re_0^{-0.03} \quad \text{for } 0.2 < Re_0 < 1$$

$$n = 4.4 Re_0^{-0.1} \quad \text{for } 1 < Re_0 < 500$$

$$n = 2.4 \quad \text{for } Re_0 > 500$$

For perfectly round, smooth and uniform particles, v_0 can be determined using the Newton-Stokes equation (Bird et al. 1960):

$$v_0^2 = \frac{3}{4} \frac{d_p (\rho_p - \rho_w) g}{C_{w2} \rho_w}$$

The drag coefficient C_{w2} is experimentally determined. The following drag coefficient for calcium carbonate pellets with a garnet seeding material was found (Schagen et al. 2006):

$$C_{w2} = \frac{24}{Re_0} (1 + 0.79 Re_0^{0.87})$$

where the terminal settling Reynolds number is given by:

$$Re_0 = \frac{v_0 d_p}{\nu}$$

The average pellet diameter is determined using the mass of crystallised material. Assuming an even distribution of the mass over the grains, in the layer under consideration, the pellet diameter is calculated as follows:

$$d_p = d_g \sqrt[3]{1 + \frac{m_c \rho_g}{m_g \rho_c}}$$

The pressure drop over each layer is given by the submerged weight of the fluidised pellets:

$$\Delta P = (\rho_p - \rho_w)(1 - p)g\Delta z$$

where the density of the pellets is a function of the accumulated mass of the crystallised material and the mass of the grains:

$$\rho_p = (m_c + m_g) \left(\frac{m_{g,i}}{\rho_g} + \frac{m_{c,i}}{\rho_c} \right)^{-1}$$

The transportation of pellets is modelled as a transportation of grain material with the calcium carbonate attached. The velocity of transportation $v_{p,i}$ is given in kilograms of grain material per second. The transportation of the calcium carbonate part of the pellet is given by the ratio of calcium carbonate mass and grain mass. Since grain material can be accumulated in the reactor, the transportation of grains into the layer is different from the transportation of grains out of the layer. The accumulation of calcium carbonate caused by pellet transportation through the reactor is given by:

$$\frac{dm_{c,i}}{dt} = v_{p,i+1} \frac{m_{c,i+1}}{m_{g,i+1}} - v_{p,i} \frac{m_{c,i}}{m_{g,i}}$$

The increase of calcium carbonate, due to the crystallisation process, is determined by the crystallisation reaction and is given at the end of the next paragraph.

Modelling crystallisation

The aim of the crystallisation model is to describe the crystallisation of calcium carbonate in the bed and the transportation of the dissolved components through the bed.

The crystallisation model is deduced using layers of the reactor as given in Figure 5.x. The m-alkalinity, p-alkalinity and ionic strength in a layer determine carbonic equilibrium as described by the equations in the section "Modelling the Calcium Carbonic Equilibrium". The crystallisation rate of the equilibrium is determined by the crystallisation kinetics K, the available crystallisation surface S and the supersaturation of calcium carbonate (Wiechers et al. 1975):

$$C = \kappa S \left([Ca^{2+}][CO_3^{2-}] - \frac{K_s}{f^8} \right)$$

The specific surface of the pellets is determined by the porosity p of the layer and the diameter of the pellet in the layer.

$$S = \left(\frac{6(1-p)}{d_p} \right)$$

The crystallisation kinetics is modelled as a two-stage crystallisation process (Karpinski 1980). The first stage is the transportation of supersaturated water to the pellet surface (k_f), which depends on water flow and temperature. The second stage is the crystallisation of the supersaturated water on the pellet (k_T), which only depends on temperature.

$$\kappa = \frac{k_T k_f}{k_T + k_f}$$

The transportation of the supersaturated water to the surface of the pellets depends on the flow pattern of the water between the pellets (Budz et al. 1984). Based on the Reynolds number of the water flow in the bed Re_h and the Schmidt number Sc the Sherwood number Sh is given by the Froessling equation:

$$Re_h = \frac{2}{3} \frac{vd_p}{(1-p)\nu}$$

$$Sc = \frac{D_f}{\nu}$$

$$Sh = 0.66 Re_h^{0.5} Sc^{0.33}$$

The transportation coefficient k_f is given by:

$$k_f = \frac{Sh \cdot D_f}{d_p}$$

The temperature dependency of k_T is found by Wiechers et al. (1975) as:

$$k_T = 1.053(T - 20)k_{T_{20}}$$

The change of m-alkalinity, p-alkalinity and ionic strength and calcium over time in one layer is now given by the combination of water flow through the reactor and crystallisation of calcium carbonate. Based on the mass balance over the layer, this is given by:

$$p_i A \Delta x_i \frac{d[Ca^{2+}]_i}{dt} = F_w ([Ca^{2+}]_{i-1} - [Ca^{2+}]_i) - A \Delta x_i C$$

$$p_i A \Delta x_i \frac{dM_i}{dt} = F_w(M_{i-1} - M_i) - 2A \Delta x_i C$$

$$p_i A \Delta x_i \frac{dP_i}{dt} = F_w(P_{i-1} - P_i) - 2 \Delta x_i C$$

$$p_i A \Delta x_i \frac{dIS_i}{dt} = F_w(IS_{i-1} - IS_i) - 2A \Delta x_i C$$

At the bottom of the reactor, where caustic soda is dosed, the concentration of the water flowing into the first section is given as:

$$M_0 = \frac{(M_{raw}F_w + [OH^-]F_l)}{F_w + F_l}$$

$$P_0 = \frac{(P_{raw}F_w + [OH^-]F_l)}{F_w + F_l}$$

$$IS_0 = \frac{(IS_{raw}F_w + 0.5[OH^-]F_l)}{F_w + F_l}$$

Finally the increase of crystallised material in the layer is equal to the crystallised mass of calcium in mol times the molecular weight of calcium carbonate (M_c):

$$\frac{dm_{c,i}}{dt} = Adx_i M_c C$$

5.1.3.3 Model Calibration

To determine the parameters of the model, the model was calibrated at the pilot plant installation of the Weesperkarspel Treatment Plant of Waternet, the water cycle company of Amsterdam and surroundings. The calibrated model was validated using data from the full-scale installation of Weesperkarspel.

Calibration at Weesperkarspel pilot plant

The aim was to calibrate the crystallisation constant k_T and diffusion constant D_f in the model. The model with the calibrated constants minimise the Mean Squared Error (MSE) based on the measurements of total hardness, pH and m-alkalinity.

The model was calibrated with data from the Weesperkarspel pilot plant. The softening process in the pilot plant consists of two columns with a diameter of 31 cm and a height of 4.5 m. A regulated valve controls the flow between 4 m³/h and 7 m³/h. Caustic soda dosage is controlled between 0 and 2 l/h. To determine the fluidised bed status, the reactors are equipped with on-line measurements of water flow, water temperature, bed height, pressure drop over the total fluidised bed and pressure drop between 20 and 60 cm from the bottom of the reactor. To follow the crystallisation process, the turbidity, pH, total hardness, m-alkalinity and the conductivity are automatically measured using an online titration unit (Applikon ADI 2040) every 15 minutes.

Before calibration one reactor was operated at constant flow (6 m³/h) and caustic soda dosage (1 l/h) for one month (February 2005). In this period the discharge of pellets was controlled using the pressure drop measurement at the bottom of the reactor (with a set point of 3.5 kPa), resulting in a constant pellet size at the bottom of the reactor. The bed height was kept constant at a height of 4 m by dosing garnet sand as seeding material.

The composition of the bed was constant after this run-in period. The state of the bed (described by $m_{c,i}$ and $m_{g,i}$) is identified using manual pressure drop measurements at 5 heights in the bed and the online bed height measurement at 3 different flows. The identification was performed with a different number of layers, to determine the influence on the prediction of the pressure drop and level measurements. The best estimate minimises the MSE using a nonlinear optimisation technique. The MSE is used for all calibration and validation experiments and is generically given by:

$$MSE = \frac{1}{N} \sum_{j=1}^N \sqrt{\frac{1}{N_j} \sum_{i=1}^{N_j} \left(\frac{y_{model,j,i} - y_{data,j,i}}{y_{data,j,i}} \right)^2}$$

where y are the N outputs from the model and the measurement data and N_j are the number of samples for the j^{th} output.

In the calibration experiment the water flow through the reactor and caustic soda flow were changed every 20 minutes. The water flow was varied between $4 \text{ m}^3/\text{h}$ and $7 \text{ m}^3/\text{h}$ and the caustic soda was varied between 0.5 and 1.5 l/h. After 20 minutes the water quality parameters were measured automatically. In this manner 40 different combinations of water flow and caustic soda dosage settings were performed in a random order. This procedure was repeated three times.

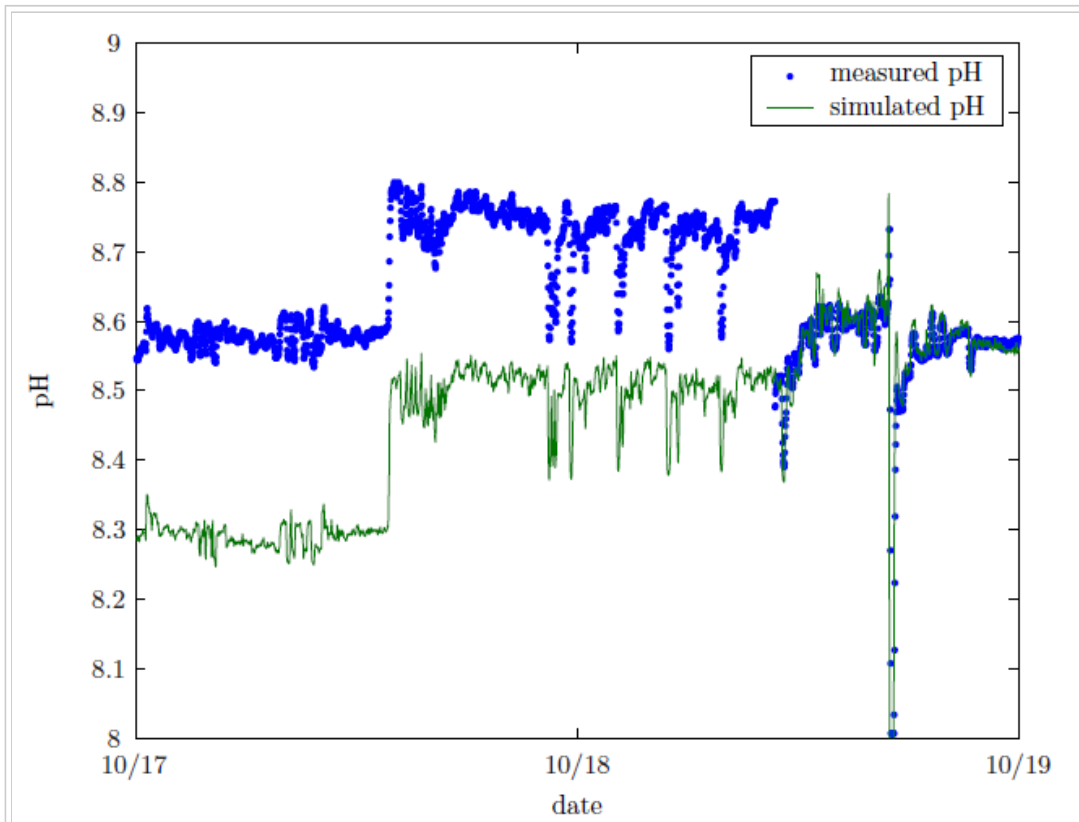
Validation at Weespervarspel full-scale plant

The model for the pellet softening process was first validated with data from the eight softening reactors of WTP Weespervarspel of Waternet. The Weespervarspel treatment plant uses lake water with relatively high organic concentrations as source water. Before softening the water is treated with ozone.

The reactors operate at a variable flow velocity of $60\text{-}100 \text{ mh}^{-1}$ to keep the ratio between bypass and reactor flow constant for different total flows. The reactor height is 4.5 meter, the seeding material is garnet sand and the dosage is caustic soda. The pellet discharge is based on the total pressure drop and the garnet sand dosage is based on the amount of discharged pellets.

The aim was to validate the dynamic output of the model. Therefore data from the full-scale plant was selected with relatively large variations in flow and caustic soda. For a five day period (15-20 October 2005) the dynamic simulation was performed for all 8 reactors. The inputs for the simulation model were the on-line measured temperature, water flow and caustic soda flow. The quality data (pH, bicarbonate and conductivity) were assumed constant based on laboratory values from that particular week. The state of the bed was deduced from the sieve analyses from the corresponding day.

The outputs of the model were compared to the on-line measured pH of the full-scale plant. The laboratory measurement of calcium was only performed once a day. This measurement was also compared to the simulated value. The on-line pH measurement suffered from static offset due to drift of the measurement device. For Reactor 6, the pH measurement was recalibrated on October 18th, after which the pH measurement was close to the simulated value (see Figure 5.x)

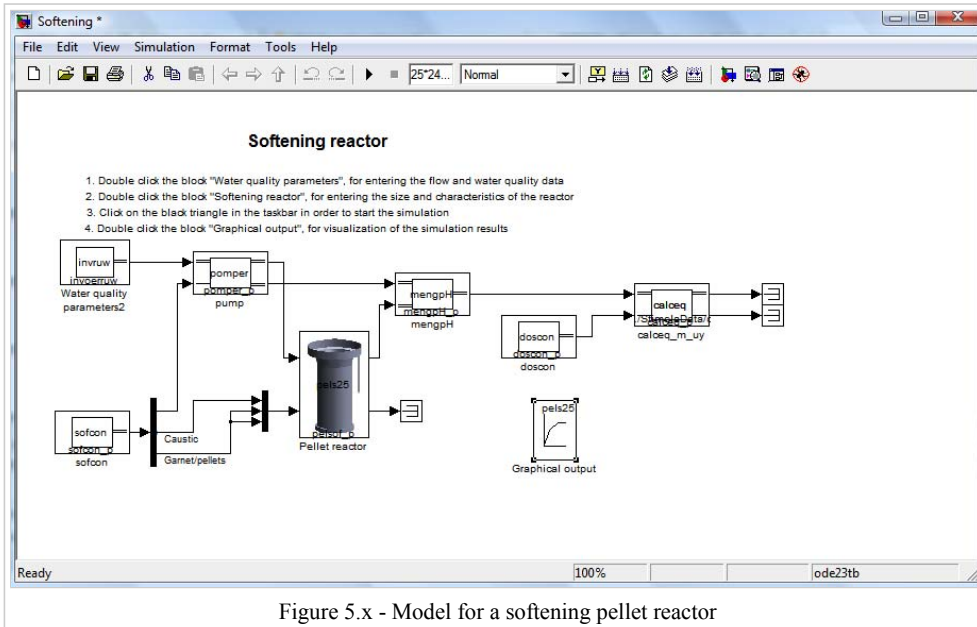


5.1.3.4 Input and Output

The input of the model can be water quality data from a previous model/treatment step or the raw water input block. On top of that the model parameters have to be entered into the pellet reactor model block. The output are the new water quality parameters that have been calculated by the model, which can be displayed as time series in graphs.

Model Parameters

When in Stimela a new project including a softening reactor is created, the model displayed in Figure 5.x will pop up. In the window are included: a raw water input block, a graphical output block, a pump block, a 'mengpH' block (see "Building a Treatment Train"), a dosing block, a 'sofcon' block and a pellet reactor block. For the latter three, the model parameters have to be changed for each different situation. In Figure 5.x, 5.x and 5.x the model parameters for each block are shown. The model parameter windows pop up when each block is double clicked.



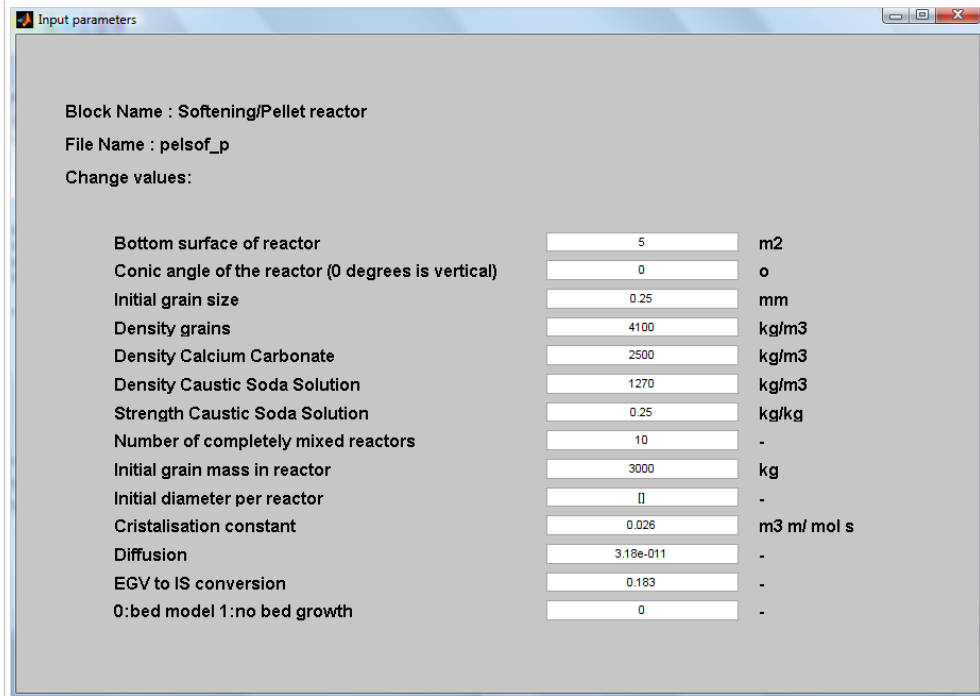


Figure 5.x - Model parameters for a softening pellet reactor

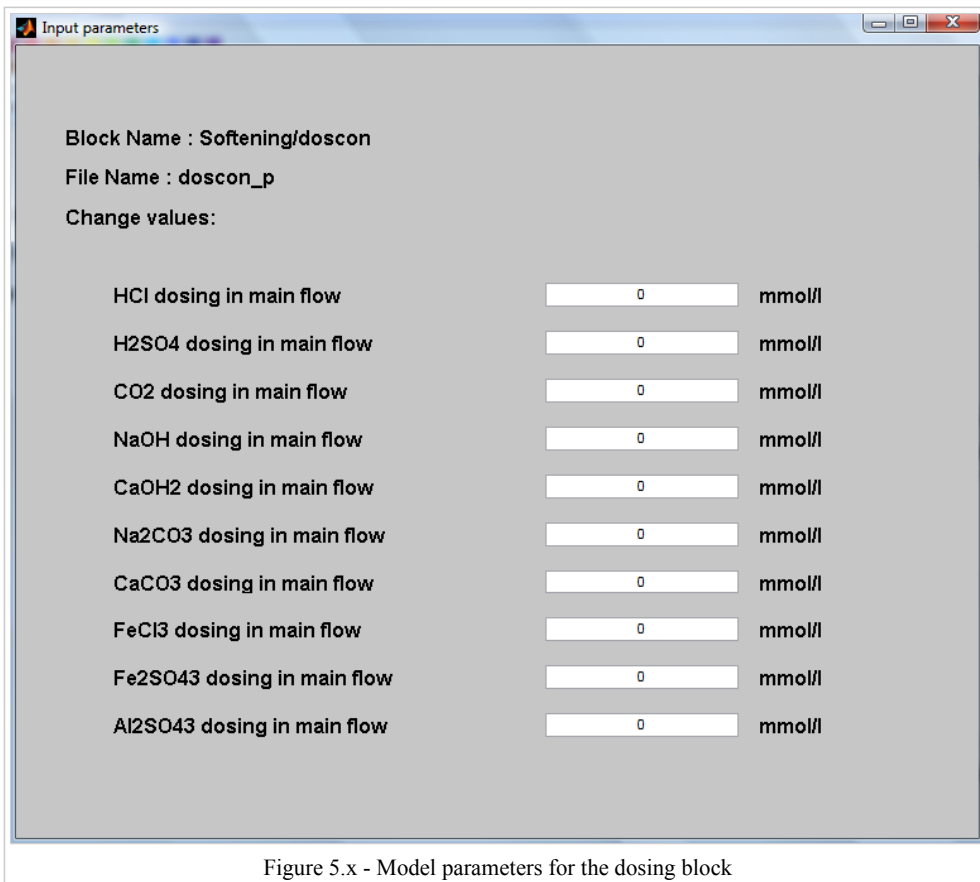


Figure 5.x - Model parameters for the dosing block

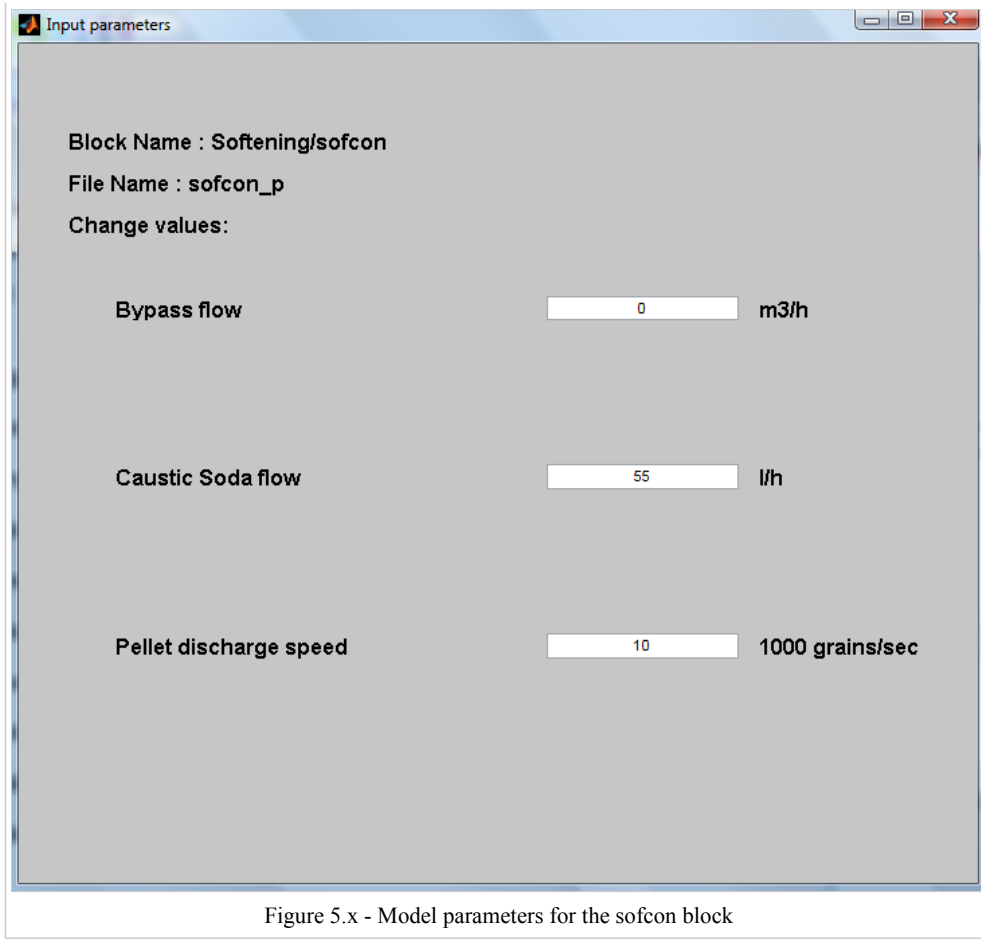


Figure 5.x - Model parameters for the sofcon block

For an explanation of most of the input parameters needs to be referred to the previous section on model equations. The ones that haven't been discussed yet are:

Number of CSTRs between sampling: The number of CSTRs determines the rate of plug flow through softening reactor. In the most extreme case, a flow of water could be completely mixed, or divided into an infinite amount of mixing barrels (CSTRs). When a number like 100 is filled in here, the flow will be almost perfect plug flow. This is not very probable, because there is always horizontal and vertical mixing going on. The improvement of gas transfer due to the improvement of the plug flow is negligible when the stream is divided into more than 20 completely mixed barrels.

INSERT MORE PARAMETER EXPLANATIONS

Graphs

When double clicked, the block "Graphical output pels25" will produce 4 graphs for the calcium concentration, the pH of the mixed effluent with a certain (NaOH) dose, the headloss, pellet diameter, bed height and pressure difference over time and the pellet diameters at different heights of the reactor (see Figure 5.x).

The graph on the top left shows the influent and effluent calcium concentration and the TCCP, which is the theoretical calcium carbonate crystallisation potential or in other words the amount of calcium in mol m⁻³ that should crystallise to obtain water in chemical equilibrium. Naturally the influent concentration is constant, but as the effluent concentration becomes closer to the equilibrium, the TCCP drops.

On the top right the pH of the influent and effluent is shown. Of course the influent pH is constant again, while the effluent pH drops over time in the same fashion as the calcium concentration does. Underneath the pH the Dosing of NaOH and pellets is shown. These parameters are defined with the input and therefore constant as well.

The graph on the bottom left represents four different calculated parameters: the headloss (m), pellet diameter (mm), bed height (m) and pressure difference (kPa) over time. The bed height increases due to the forming of larger lighter pellets. The bed doesn't infinitely increase, it will go to an equilibrium around 4 meters. Because of this increase, the headloss increases in the same fashion. The pellet diameter increases from 0.25 mm (which is the initial grain size) to 0.78 mm.

On the bottom right a graph is displayed which represents the pellet diameter over the height of the reactor after 6 different run times.

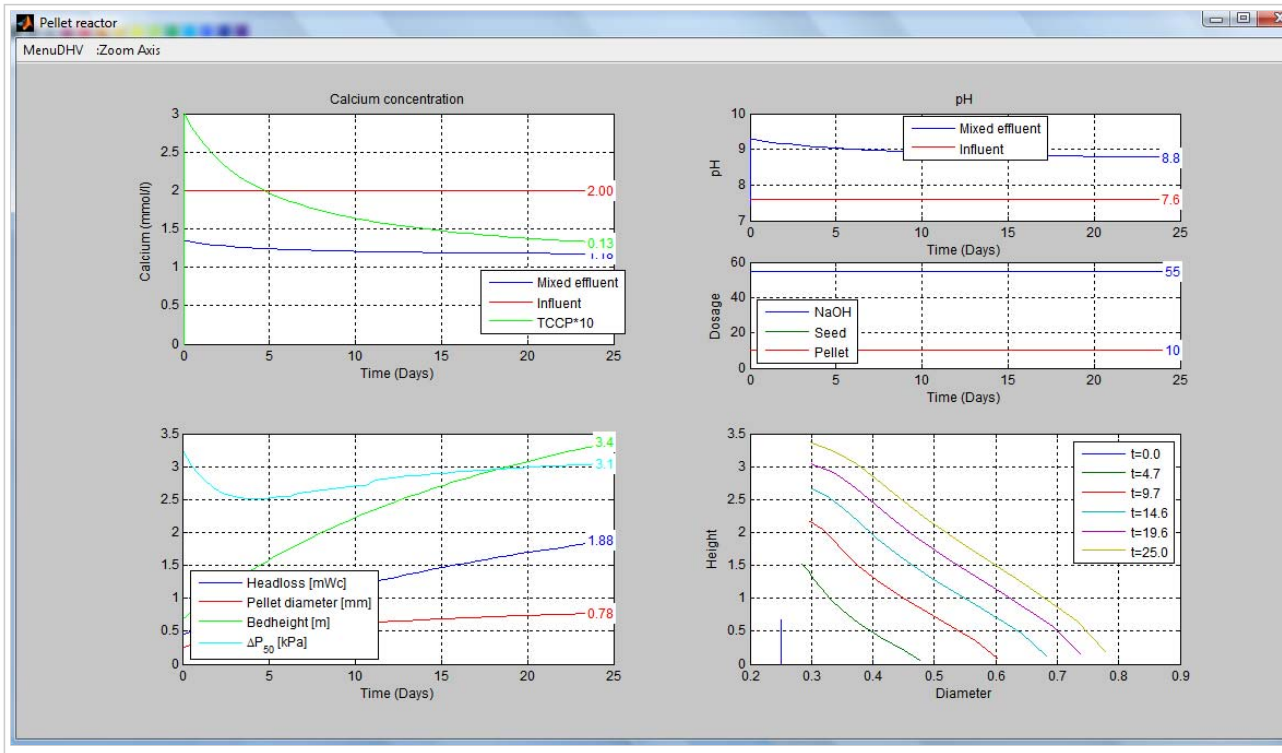


Figure 5.x - Graphical output for a pellet softening reactor

5.2 References

- D5.4.1, L Rietveld and J Dudley, 2006. "Models for drinking water: State of the art", available at www.techneau.eu
- D5.4.2, L Rietveld and J Dudley, 2006. "Models for drinking water: Methodology for integration", available at www.techneau.eu
- D5.4.3, L Rietveld, P Ross, G Dillon and J Dudley, 2007. "Conceptual design modelling framework", available at www.techneau.eu
- Bird, R., Stewart, W. & Lightfoot, E., 1960. Transport Phenomena. Wiley, New York
- ter Bogt, L., Roos, P., Rosens, E., van Veen, A. & Veenendaal, M., 1992. Modellering ontharding in korrelreactoren. Technical report, TU Twente, Enschede, The Netherlands. CR II-verslag
- Budz, J., Karpinski, P. & Nuruc, Z., 1984. Influence of hydrodynamics on crystal growth and dissolution in a fluidized bed. AIChE J. 30(5), 710–717
- van Dijk, J. & Wilms, D., 1991. Water treatment without waste material - fundamentals and state of the art of pellet softening. J. Wat. Suppl.: Res. Technol.-AQUA 40(5), 263–280
- Jacobsen, R. & Langmuir, D., 1974. Dissociation constants of calcite and CaHCO₃ from 0 to 50 °C. Geochim. Cosmochim. Acta 38, 301–308
- Karpinski, P., 1980. Crystallization as a mass transfer phenomenon. Chem. Eng. Sci. 35, 2321–2324
- Plummer, L. & Busenberg, E., 1982. The solubilities of calcite, aragonite and vaterite in CO₂-H₂O solutions between 0 and 90 °C, and an evaluation of the aqueous model for the system CaCO₃-CO₂-H₂O. Geochim. Cosmochim. Acta 46, 1011–1040
- Richardson, J. F. & Zaki, W. N., 1954. Sedimentation and fluidisation: Part I. Trans. Inst. Chem. Eng. 32, 35–53

van Schagen, K., Rietveld, L., Babuska, R. & Kramer, O., 2007. Model-based operational constraints for fluidised bed crystallisation. *Wat. Res.* doi:10.1016/j.watres.2007.07.019

Schock, M., 1984. Temperature and ionic strength correction to the Langelier Index-revisited. *J. Am. Wat. Wks. Assoc.* 76, 72–76

Wiechers, H., Sturrock, P. & Marais, G., 1975. Calcium carbonate crystallization kinetics. *Wat. Res.* 9, 835–845D

6 Coagulation and Flocculation

In surface water different compounds are present that must be removed if drinking water is to be produced.

The compounds can be subdivided into:

- Suspended solids
- Colloidal solids
- Dissolved solids

Suspended solids have a diameter larger than 10^{-6} m, colloidal solids between 10^{-9} and 10^{-6} m and dissolved solids smaller than 10^{-9} m. Particles with a diameter larger than 10^{-5} m, and a specific density larger than 2,000 kg/m³ will settle in water. Smaller particles will also settle, but more slowly. To be removed, particles that are smaller than 10^{-5} m must be made larger or heavier. The latter is impossible and, therefore, removal is only possible by increasing the particle size. During the coagulation process, coagulants are added to the water to aid in floc formation. These flocs are precipitates in water in which small particles are incorporated. Turbidity is caused by colloidal particles (order of magnitude 0.1 - 10 µm). Colloidal particles are negatively charged and repulse each other. Colour is caused by humic substances (order of magnitude 0.01 µm). The charge of humic substances (and thus the removal) is dependent upon the pH of the water.

6.1 Coagulation

Coagulation is a unit process of fundamental importance for drinking water treatment as initial measure for water purification in many water utilities and its practice can affect noticeably water quality characteristics and performance of subsequent treatment steps. Nowadays one of the coagulation roles in water treatment that has arisen with more emphasis is the removal of natural organic matter (NOM: complex of heterogeneous mixture of organic substances produced from vegetative decay process) by enhanced coagulation due to a number of reasons including that dissolved organic carbon (DOC) influences greatly on coagulant demand, may control coagulation conditions and coagulation efficiency.

6.1.1 Process

The coagulation process is the dosing of a coagulant in water, resulting in the destabilization of negatively charged particles. To remove particles present in water, the particles must be incorporated into flocs. These flocs will be formed after dosing coagulant. In the Netherlands iron chloride (FeCl_3) is frequently used as the coagulant. Alternatively, aluminium sulphate ($\text{Al}_2(\text{SO}_4)_3$) can be applied. In a water treatment plant the coagulant is dosed, after which some mixing needs to occur. The mixing has to be sufficient to maintain an efficient coagulation and flocculation process. In case mixing is poor, local under and overdosing might occur.

6.1.2 Theory

When the pH of the surface water is known, the concentration of iron (Fe^{3+}) ions can be calculated using the solubility product of iron hydroxide and the ion product of water:



Rewriting the water equilibrium results in the following equation:

$$K_w = 10^{-14} = [H_3O^+] \cdot [OH^-] \implies [OH^-] = \frac{10^{-14}}{[H_3O^+]}$$

Combining the equation mentioned above with the solubility product of iron hydroxide gives:

$$[Fe^{3+}] \cdot [OH^-]^3 = 10^{-38} \implies$$

$$[Fe^{3+}] = 10^{-38} \frac{[H_3O^+]^3}{(10^{-14})^3} = 10^4 \cdot [H_3O^+]^3$$

$$\log[Fe^{3+}] = \log(10^4) + 3\log[H_3O^+] = 4 - 3 \cdot pH$$

In addition to iron hydroxide the following hydrolysis products of Fe^{3+} are also formed:



When the pH of water is known, the amount of hydrolysis product in a volume of water can be determined. With a pH of 4.6, 10^{-7} mol/m³ Fe^{3+} , 10^{-4} mol/m³ $FeOH^{2+}$ and 10^{-4} mol/m³ $FeOH_2^+$ are present. The pH and the predominant hydrolysis product influence the predominant coagulation mechanisms.

Coagulation mechanisms

Destabilization of turbidity and color-causing substances can be induced by different mechanisms. The following subdivisions can be made:

- electrostatic coagulation
- adsorptive coagulation
- precipitation coagulation

For more information on coagulation, please refer to the drinking water 1 lecture notes by J.C. van Dijk

6.1.3 Model

Mathematical models that relate the nature and concentration of DOC in the raw water to inorganic coagulant dosing that maximize the removal of DOC have been developed as a systematic attempt to translate conceptual understanding of coagulation process into mathematical terms that allow prediction of the behaviour of this process under changing conditions (Rietveld, 2005; Eikebrokk et al, 2006).

6.1.3.1 Options for Usage

6.1.3.2 Model Equations

The Langmuir isotherm model was developed by Edwards (Eikebrokk et al, 2006) for predicting the DOC concentration remaining after enhanced coagulation. This model considers only adsorption mechanisms described by Langmuir isotherm assuming that DOC is adsorbed onto the surface of metal hydroxide floc having been generated by the addition of aluminium or iron based coagulant. In this way equilibrium exists between DOC in solution and DOC adsorbed that can be described by the isotherm.

The fraction of non-adsorbable DOC that is not removed by coagulation is related to UV254 according to the following equations:

$$F_{NDOC} = K_1 (SUVA_{raw}) + K_2$$

$$SUVA_{raw} = UV_{raw} / DOC_{raw}$$

Where:

F_{NDOC} = fraction of non-adsorbable DOC

K_1, K_2 = empirical fitting constants

$SUVA_{raw}$ = Specific absorbance UV254 of raw water [$L (m mg)^{-1}$]

UV_{raw} = UV254 absorbance of raw water (m^{-1})

DOC_{raw} = DOC of raw water (mg/L)

The next equation allows calculation of the concentration of adsorbable DOC (DOC_{ads}):

$$DOC_{ads} = [1 - F_{NDOC}] DOC_{raw}$$

The model has its bases in the equilibrium distribution of DOC between hydroxides flocs and water. It is governed by a Langmuir relationship:

$$\frac{x}{M} = \frac{abC_{eq}}{1 + bC_{eq}}$$

$$x = DOC_{ads} - C_{eq}$$

Where:

x = DOC removed (mg/L)

M = coagulant added (Al^{3+} or Fe^{3+} in mmol/L)

C_{eq} = adsorbable DOC remaining in solution at equilibrium (mg/L)

a = maximum specific DOC adsorption (mg DOC/mM Me $^{3+}$, Me=Al or Fe)

b = adsorption constant for DOC on metal hydroxide (L/mg DOC)

The “ a ” constant is determined by:

$$a = x_1 pH + x_2 pH^2 + x_3 pH^3$$

Where: pH = coagulation pH

x_1, x_2, x_3 = fitting constants

From the operational and chemical perspective the maximum specific DOC adsorption (“ a ”) is a clue factor that relates the amount of DOC capable to be adsorbed by metallic coagulants to the amount of coagulant applied to the raw water. Edwards based the prediction of this capacity on pH and empirical constants “ x ”. Further research to determine a mathematical relationship that describes “ a ” in function of pH and other parameters that influence coagulation (temperature, alkalinity, applied G values, etc) could help to avoid the use of the empirical constants “ x ”, maximising coagulation efficiency and providing a better understanding and control of the process.

From previous equations a formula for C_{eq} is derived which can be solved knowing the raw water DOC, UV₂₅₄ absorbance, coagulant dose, coagulation pH and the six constants:

$$\frac{[1 - K_1(SUVA_{raw}) - K_2]DOC_{raw} - C_{eq}}{M} = \frac{(x_1pH + x_2pH^2 + x_3pH^3)bC_{eq}}{1 + bC_{eq}}$$

The amount of dissolved organic carbon still present in solution after coagulation (DOC_{coag}) is:

$$DOC_{coag} = C_{eq} + F_{NDOC} DOC_{raw}$$

Edwards has calculated the values for the empirical constants by an extensive revision of experimental database excluding any data where the applied pH promoted a significant dissolution of the coagulant (for Aluminium coagulants: pH < 5 or pH > 8; for Iron coagulants: pH < 4).

The general values for the empirical constants are listed in table 6.x.

Constant	Case				
	¹ Fe coagulant	² Al coagulant	³ General	⁴ General Low DOC (< 10 mg/L)	⁵ Site specific
K ₁	- 0.028	- 0.075	- 0.054	- 0.053	- 0.059
K ₂	0.23	0.56	0.54	0.54	0.45
x ₁	280	284	383	387	223
x ₂	- 73.9	- 74.2	- 98.6	- 99.2	- 57.3
x ₃	4.96	4.91	6.42	6.44	3.76
b	0.068	0.147	0.145 (Al) 0.092 (Fe)	0.107	Calibrate
1) From data where coagulant was ferric sulphate or ferric chloride. 2) From data where coagulant was aluminium sulphate. 3) All data. The type of coagulant was found to have a significant effect on the constant b. 4) In this case the type of coagulant was found not to have a significant effect on the constant b. 5) The constant b was dependent on water type and coagulant type and was used to calibrate the model, the other constants being fixed.					

Table 6.x - Model constants suggested by Edwards for predicting DOC removal (WRc, 2003; Eikebrokk et al., 2006) Case

The values determined by Edwards (1997) keep the standard error below 10% and according with Tseng and Edwards (1999) the accuracy of the Langmuir adsorption model is higher than other proposed models predicting DOC or TOC removal.

6.1.3.3 Model Calibration

6.1.3.4 Input and Output

Model Parameters

Graphs

6.2 Flocculation

6.2.1 Process

6.2.2 Theory

6.2.3 Model

6.2.3.1 Options for Usage

6.2.3.2 Model Equations

6.2.3.3 Model Calibration

6.2.3.4 Input and Output

Model Parameters

Graphs

6.3 References

Eikebrokk, B., Juhna, T. and Østerhus, S.W. Water treatment by enhanced coagulation – Operational status and optimization issues. TECHNEAU, pp 1 – 107, 2006.

Rietveld, L.C. Improving operation of Drinking water treatment through modelling. PhD Thesis. Delft University of Technology, pp 6, 2005.

WRc. Process Model Description Manual. WRc OTTER 2.1.3, pp 3 – 11, 2003.

J.C. van Dijk, Drinking water treatment 1, lecture notes, Delft University of Technology, 2006

7 pH adjustment

A model for the simulation of changes in pH throughout a treatment plant has been defined by van Schagen (2009). To monitor the integral treatment plant, with respect to the pH, a grey-box model is used. The considered model describes the effect of chemical dosing and reactions through the so called M and P-alkalinity, related to the pH. The M-and P alkalinity can be measured semi-online using a titration device, but are normally only determined in the laboratory. However, the pH is measured online at multiple treatment steps in the plant. The goal of this monitoring scheme is to validate the pH measurements online, using an estimate of the M and P alkalinity, based on flow and dosage measurements.

7.1 Model description

The advantage of using the M-alkalinity and P-alkalinity is that they have a linear relationship with respect to dosing of chemicals, in contrast to the pH. It is, therefore, possible to model M and P alkalinity throughout the plant with a grey-box model. In Figure 7.x a snapshot is taken, with respect to M and P throughout the Weespervarspel treatment plant of Waternet. The bold line describes the M and P changes in the different treatment steps. Starting with lake water as source water, the dosage of acid causes a drop of M and P alkalinity equal to the amount of dosed acid, as can be deduced from the definition of M and P in Equation (1) and (2). The process of CO₂ exchange with air raises P, depending on the reaction rate of this process. The dosage of caustic soda at the softening treatment step increases both M and P equally, but the process of CO₃²⁻ crystallisation lowers the M-alkalinity twice as much as the P alkalinity. After the acid dosage after softening, the CO₂ formation in BAC filtration and the caustic soda dosage after BAC filtration, the treated water has the given M en P alkalinity.

$$M = 2[CO_3^{2-}] + [HCO_3^-] + [OH^-] - [H_3O^+]$$

$$P = [CO_3^{2-}] - [CO_2] + [OH^-] - [H_3O^+]$$

The pH which corresponds to the M and P alkalinity is plotted in Figure 7.x as thin lines, with corresponding pH values. The

relation between pH, M and P alkalinity is known as the carbonic equilibrium and depends mainly on water temperature and slightly on ionic strength.

To determine the dynamic grey-box model of the complete treatment plant each treatment step is divided into n sections with a total volume V ($V_1 \dots V_n$), as shown in Figure 7.x. The dosage takes always place at the beginning of the treatment step before the first volume, possibly changing the M-alkalinity and P-alkalinity of the previous treatment step ($[MP]_{prev}$) instantaneously. To model generic processes taking place in the treatment step, also a so called reactant is modelled. The dosage and reactant differs for each treatment step, but the model structure is the same for all treatment steps. In the consecutive compartments the reactions of M, P and reactant r take place, changing the M-alkalinity and P-alkalinity based on a given reaction rate. The final alkalinities ($[MP]_n$) are the input to the next treatment step.

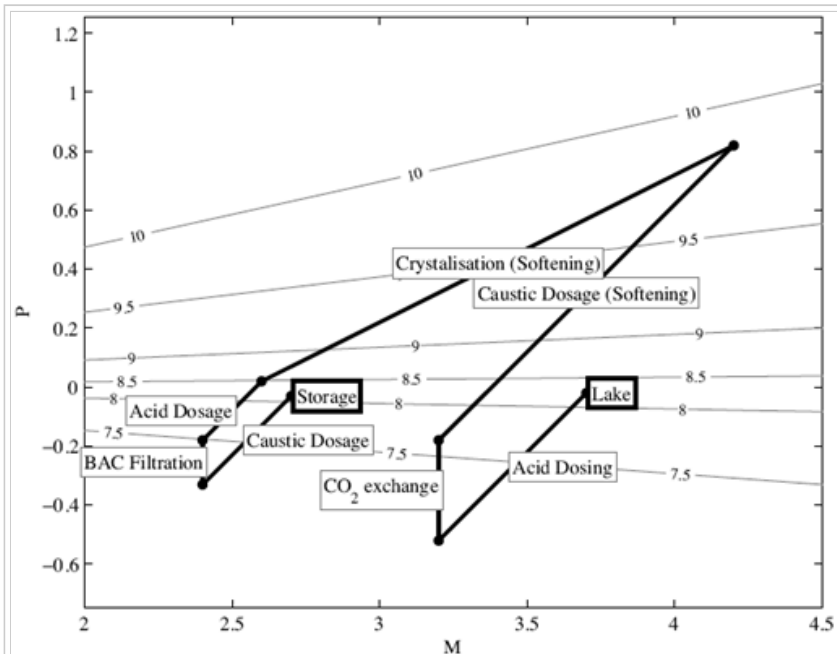


Figure 7.x - Dependency of pH on M-alkalinity and P-alkalinity for the Weespervarspel treatment plant at 15°C and a snapshot of the changes in M-alkalinity and P-alkalinity at the different treatment steps.

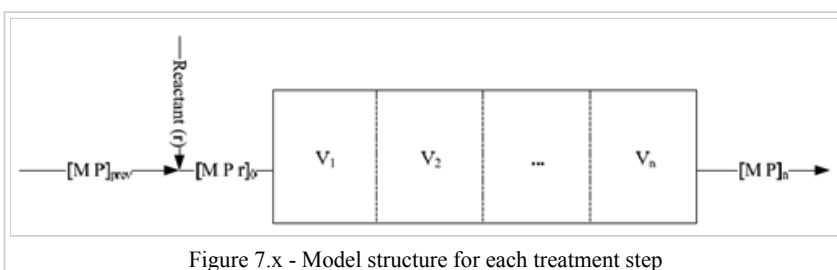


Figure 7.x - Model structure for each treatment step

Each treatment step is now modelled with the general model $k = 1..n$:

$$\frac{dM_k}{dt} = \frac{F}{V_k} (M_{k-1} - M_k) - R_M(M_k, P_k, r_k, Temperature)$$

$$\frac{dP_k}{dt} = \frac{F}{V_k} (P_{k-1} - P_k) - R_P(M_k, P_k, r_k, Temperature)$$

$$\frac{dr_k}{dt} = \frac{F}{V_k} (r_{k-1} - r_k) - R_r(M_k, P_k, r_k, Temperature)$$

$$M_0 = M_{prev} + f_M(r_{in})$$

$$P_0 = P_{prev} + f_P(r_{in})$$

Where:

F = the flow

V = the water volume in the corresponding treatment step

r = the reactant in the water

R_M, R_P, R_r = description of the reactions in the treatment step depending on the temperature.

The functions f_M and f_P are the instantaneous changes in M and P due to the dosage of chemicals and M_{prev} and P_{prev} are the M and P alkalinities from the previous treatment step.

The pH module that can be found in Stimela has an input, an output and mixing in between. The input can be two different flows of water, or a dosing of a certain chemical into the flow of treated water. Using the calcium carbonic equilibrium the pH of the output is calculated, after mixing. The equations used to calculate the new output are:

$$IB_1 = IB_0 + 0.5*HCl + 2*H_2SO_4 + 0.5*NaOH + 2*CaOH_2 + Na_2CO_3 + 2*CaCO_3 + 6*FeCl_3 + 15*Fe_2(SO_4)_3 + 15*Al_2(SO_4)_3$$

$$Ca_{Tot} = Ca_{Tot} + CaOH_2 + CaCO_3$$

$$Pn = Pn - HCl - 2*H_2SO_4 - DosCO_2 + NaOH + 2*CaOH_2 + Na_2CO_3 + CaCO_3 - 3*FeCl_3 - 3*Fe_2(SO_4)_3 - 3*Al_2(SO_4)_3$$

$$Mn = Mn - HCl - 2*H_2SO_4 + NaOH + 2*CaOH_2 + 2*Na_2CO_3 + 2*CaCO_3 - 3*FeCl_3 - 3*Fe_2(SO_4)_3 - 3*Al_2(SO_4)_3$$

$$SO_4 = SO_4 + H_2SO_4 + 3*Fe_2(SO_4)_3 + 3*Al_2(SO_4)_3$$

Knowing that:

$$H_3O = 10^{(3-pH)/f}$$

$$OH = K_w / (f^2 * H_3O)$$

$$IB_0 = IS_0 - (HCO_3/2 + 2*CO_3 + H_3O/2 + OH/2)$$

With these new values for the P-number, M-number, calcium and sulphate, a new pH and calcium carbonic equilibrium can be calculated.

7.2 Model Calibration

In the PhD thesis by van Schagen (2009) a comparison is made between the pH measurements at Loenderveen-Weesperkarspel and the results of a simulation with the plants input parameters. The results are summarized in Figure 6.x. For a detailed description of the simulation results and validation of the model, see the full thesis.

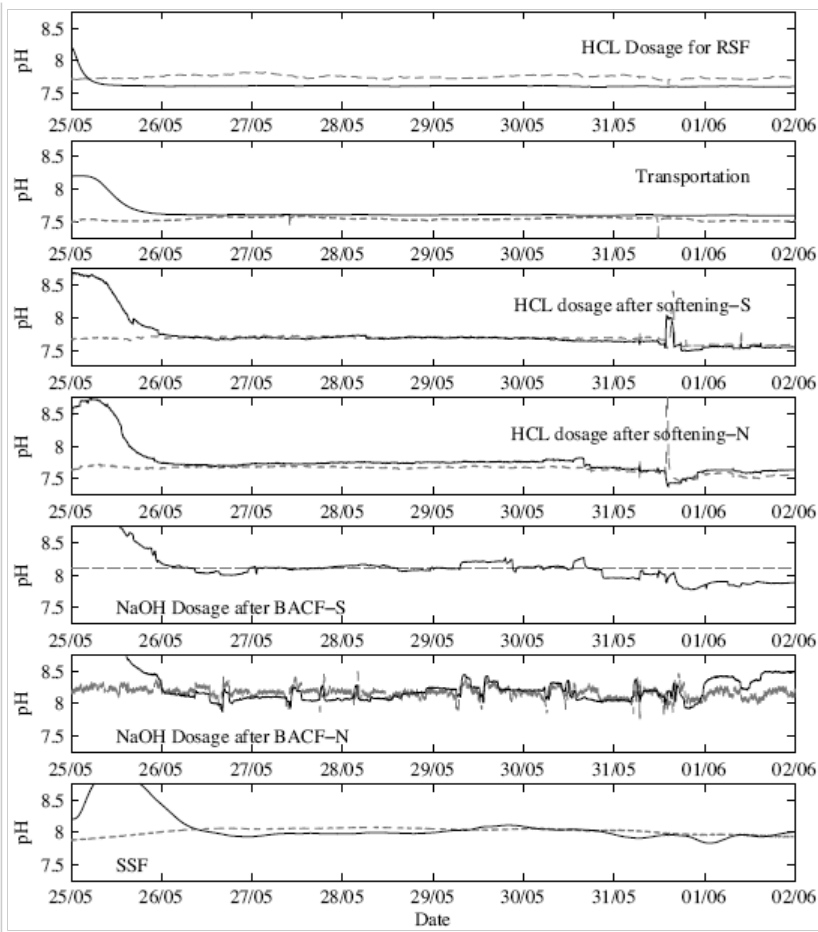


Figure 7.x - Simulated and actual (dashed) pH measurements using constant reaction coefficients and the measured flows and dosages for the treatment plant of Loenderveen-Weespervarspel.

7.3 References

Schagen, K.M. van, 2009, Model-based control of drinking-water treatment plants, TU Delft

Retrieved from "http://www.waterspot.nl:8080/index.php/Stimela_Model_descriptions"

- This page was last modified on 9 December 2009, at 13:45.